



LUND UNIVERSITY

Brain injury after cardiac arrest - the predictive information of computed tomography

Lang, Margareta

2025

Document Version:

Publisher's PDF, also known as Version of record

[Link to publication](#)

Citation for published version (APA):

Lang, M. (2025). *Brain injury after cardiac arrest - the predictive information of computed tomography*. [Doctoral Thesis (compilation), Department of Clinical Sciences, Lund]. Lund University, Faculty of Medicine.

Total number of authors:

1

Creative Commons License:

Unspecified

General rights

Unless other specific re-use rights are stated the following general rights apply:

Copyright and moral rights for the publications made accessible in the public portal are retained by the authors and/or other copyright owners and it is a condition of accessing publications that users recognise and abide by the legal requirements associated with these rights.

- Users may download and print one copy of any publication from the public portal for the purpose of private study or research.
- You may not further distribute the material or use it for any profit-making activity or commercial gain
- You may freely distribute the URL identifying the publication in the public portal

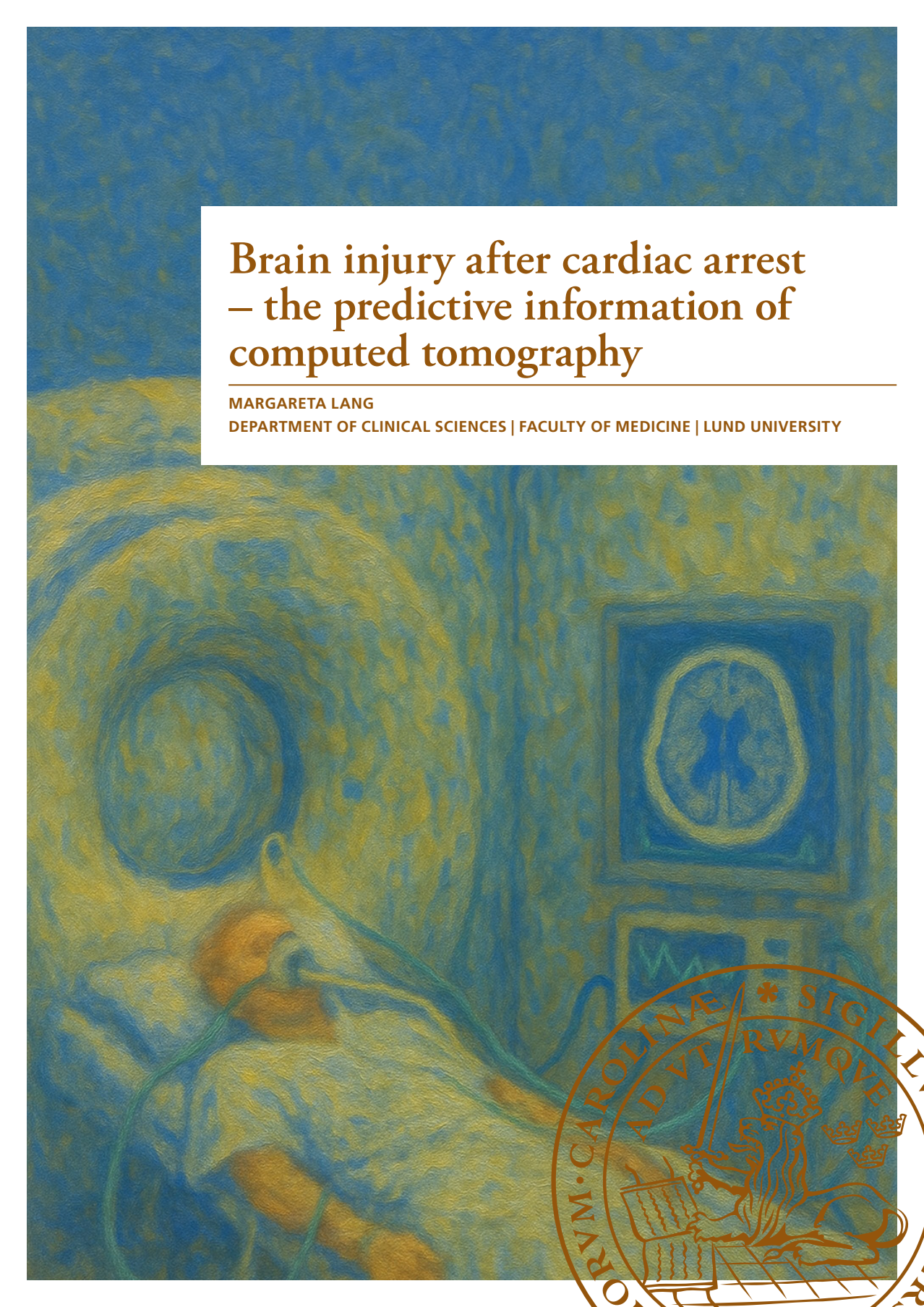
Read more about Creative commons licenses: <https://creativecommons.org/licenses/>

Take down policy

If you believe that this document breaches copyright please contact us providing details, and we will remove access to the work immediately and investigate your claim.

LUND UNIVERSITY

PO Box 117
221 00 Lund
+46 46-222 00 00



Brain injury after cardiac arrest – the predictive information of computed tomography

MARGARETA LANG

DEPARTMENT OF CLINICAL SCIENCES | FACULTY OF MEDICINE | LUND UNIVERSITY





MARGARETA LANG works as a radiologist within the Department of Radiology at Helsingborg Hospital



Brain injury after cardiac arrest –
the predictive information of computed tomography

Brain injury after cardiac arrest – the predictive information of computed tomography

Margareta Lang



LUND
UNIVERSITY

DOCTORAL DISSERTATION

by due permission at the Faculty of Medicine at Lund University, Sweden.

To be defended on September 12th, 2025, at 9.00 a.m.

at Medicinhistoriska Museet, Bergaliden 20, 252 23 Helsingborg

Faculty opponent

Daniel Strbian, Associate Professor, University of Helsinki,
Helsinki, Finland

Organisation: LUND UNIVERSITY

Document name: Doctoral dissertation

Date of issue: September 12th, 2025

Author: Margareta Lang

Title: Brain injury after cardiac arrest – the predictive information of computed tomography

Background: Hypoxic-ischaemic encephalopathy (HIE) is a leading cause of morbidity and mortality in unconscious patients resuscitated after out-of-hospital cardiac arrest. Many patients die after withdrawal of life-sustaining treatments (WLST), often based on a presumed poor prognosis. The evidence for head computed tomography (CT) as a reliable predictor of poor outcome after cardiac arrest is low. Aim: To evaluate qualitative and quantitative CT indicators of HIE to strengthen the evidence for CT as a prognostic tool in unconscious cardiac arrest patients.

Methods: I) Post-hoc analysis of a prospective multicentre study, the Target Temperature Management at 33 °C versus 36 °C after Cardiac Arrest (TTM) trial. Adult patients from Swedish sites with CTs were included. Two blinded radiologists assessed early (<24 hours) and late (≥24 hours) CTs with various qualitative and quantitative (grey-white matter ratio (GWR)) methods to predict poor outcome, defined as a modified Rankin scale (mRS) score of 4-6 at six months. (II) Protocol to establish pre-specified radiological criteria for identifying signs indicative of HIE on CT, aimed at predicting poor functional outcomes after cardiac arrest. (III) Prospective international multicentre sub-study of the Hypothermia versus Normothermia after Out-of-hospital Cardiac Arrest (TTM2) trial. CTs performed >48 hours ≤7 days after cardiac arrest were assessed using manual (standardised qualitative and basal ganglia GWR) and automated atlas-based GWR. Prognostic performance for poor outcome prediction (mRS 4-6 at six months) for the qualitative assessment and for the pre-defined GWR cut-off <1.10 was calculated. Inter- and intrarater agreement were analysed. IV) In-depth analysis of prognostic performance and interrater agreement for individual CT items included in the standardised qualitative assessment in Paper III. V) Retrospective single-centre study. GWR at the basal ganglia level was calculated using two different-sized Regions Of Interests (ROIs) by three raters on CTs in an age- and sex-matched cohort to a cardiac arrest population.

Results: I) N=106. All tested CT assessment methods had better predictive performance for poor outcome on late compared to early CTs. A GWR cut-off <1.10 showed 100% specificity across all methods and raters. The highest sensitivity at this cut-off, 50-63%, was achieved with the GWR using 8 ROIs at the basal ganglia level. III) N=140. Standardised qualitative CT assessment and all GWR methods at cut-off <1.10 predicted poor outcome with 100% specificity. Median sensitivity for the seven raters was: 37% (qualitative), 39% (GWR <1.10 8 ROIs), 30% (GWR <1.10 4 ROIs), and 41% (automated GWR <1.10). The highest interrater agreement was achieved with the GWR <1.15 8 ROIs method, kappa 0.83. IV) Loss of grey-white matter distinction predicted poor outcome with 100% specificity and 45-50% sensitivity. The specificity for sulcal effacement was 93-99% and the sensitivity 29-49%. The highest interrater agreement was achieved with loss of grey-white matter distinction at the high convexity level, kappa 0.74. V) N=155. No participant had GWR <1.10, regardless of ROI size. Variability between raters and ROI sizes was ± 0.1.

Conclusion: CT is a highly specific tool for predicting poor functional outcomes after cardiac arrest and should be considered in patients who remain unconscious >48 hours post-arrest, as part of a multimodal neuroprognostication strategy. Combining a structured qualitative assessment of definite severe HIE with a GWR <1.10, assessed manually or via an automated method at the basal ganglia level, enables prediction of poor functional outcome with high specificity and moderate sensitivity. Improving interrater agreement will require further refinement of standardised qualitative assessment, with focus on the robust predictive marker of loss of grey-white matter distinction.

Key words: Computed tomography, cardiac arrest, hypoxic ischaemic encephalopathy, prognosis.

Language English

Number of pages:

ISSN: 1652-8220

ISBN: 978-91-8021-740-8

I, the undersigned, being the copyright owner of the abstract of the above-mentioned dissertation, hereby grant to all reference sources permission to publish and disseminate the abstract of the above-mentioned dissertation.

Signature

Date 2025-09-12

Brain injury after cardiac arrest – the predictive information of computed tomography

Margareta Lang



LUND
UNIVERSITY

Coverphoto by OpenAI, 2025. ChatGPT, <http://chat.openai.com>. [Downloaded: June 28th 2025].

Copyright pp 1 - 117 Margareta Lang

Paper 1 © The authors 2022 (Open access in Resuscitation).

Paper 2 © The authors 2022 (Open access in Resuscitation Plus).

Paper 3 © The authors 2024 (Open access in Intensive Care Medicine).

Paper 4 © The authors 2025 (Open access in Resuscitation).

Paper 5 © The authors 2025 (Open access in Resuscitation).

Faculty of Medicine

Department of Clinical Sciences, Lund University

ISBN 978-91-8021-740-8

ISSN 1652-8220

Printed in Sweden by Media-Tryck, Lund University

Lund 2025



Media-Tryck is a Nordic Swan Ecolabel
certified provider of printed material.
Read more about our environmental
work at www.mediatryck.lu.se

MADE IN SWEDEN 

“There’s more to the picture than meets the eye”
Neil Young

Table of Contents

Abbreviations	10
Declaration of generative artificial intelligence usage	13
List of Papers.....	14
Abstract	17
Populärvetenskaplig sammanfattning.....	19
Thesis at a glance	22
Background.....	24
Cardiac arrest	24
Hypoxic ischaemic encephalopathy	26
Intensive care	27
Neurological prognostication	29
Guidelines ERC/ESICM.....	29
Clinical neurological examination.....	30
Neurophysiology	32
Blood based biomarkers	33
Neuroimaging.....	33
Outcome	36
Computed tomography	38
Methodology.....	38
Non-contrast head CT.....	39
Artefacts	40
Signs indicating hypoxic ischaemic encephalopathy on CT	41
Qualitative CT assessment methods.....	44
Quantitative CT assessment methods.....	45
Other CT methods	48
Knowledge gap.....	49
Aims of the thesis	50
Materials and methods.....	51
TTM trial.....	52
Paper I	53

TTM2 trial	55
Paper II-III.....	57
Paper IV	61
Paper V	62
Statistical analyses.....	64
Self-fulfilling prophecy bias.....	68
Ethics.....	69
Radiation exposure	69
Research on unconscious patients	70
Results.....	72
Paper I	72
Paper III-IV	75
Paper III.....	77
Paper IV	81
Paper V	84
Discussion	88
Timing of CT.....	88
Assessment methods	89
Qualitative CT assessment methods.....	89
Quantitative CT assessment methods.....	90
Raters.....	92
Strengths.....	93
Limitations	94
Conclusions	95
Future perspectives	96
Acknowledgements	98
References	101

Abbreviations

ADC	Apparent diffusion coefficient
AI	Artificial intelligence
ALARA	As low as reasonably achievable
ASPECT	Alberta stroke program early computed tomography
AUROC	Area under the receiver operating characteristic curve
AV	Average
BG	Basal ganglia
CA	Cardiac arrest
CBC	Cerebellar cortex
CBW	Cerebellar white matter
CC	Genu corpus callosum
CE	Cerebrum
CI	Confidence interval
CN	Head of the caudate nucleus
CPC	Cerebral performance category
COSCA	Core outcome set for cardiac arrest
CPR	Cardiopulmonary resuscitation
CSF	Cerebrospinal fluid
CT	Computed tomography
CTDI _{vol}	Computed tomography dose index (volumetric)
CTP	Computed tomography perfusion
DLP	Dose length product
DNA	Deoxyribonucleic acid
DTI	Diffusion tensor imaging
DWI	Diffusion-weighted imaging
ECMO	Extracorporeal membrane oxygenation
EEG	Electroencephalography
ESCIM	European Society of Intensive Care Medicine

ERC	European Resuscitation Council
FA	Fractional anisotropy
FLAIR	Fluid-attenuated inversion recovery
FN	False negative
FP	False positive
FOUR	Full Outline of Unresponsiveness (scale)
GCS	Glasgow Coma Scale
GOS-E	Glasgow Outcome Scale Extended
GRADE Evaluation	Grading of Recommendations Assessment, Development, and Evaluation
GWR	Grey-white matter ratio
HACA	Hypothermia after cardiac arrest
HIE	Hypoxic-ischaemic encephalopathy
HMEP	Highly malignant EEG patterns
HRQoL	Health-Related Quality of Life
HU	Hounsfield unit
ICP	Intracranial pressure
ICU	Intensive care unit
ILCOR	International Liaison Committee on Resuscitation
IHCA	In-hospital cardiac arrest
IQR	Interquartile Range
LUSEC	Lund University Secure Environment for Computing
LV	Lateral ventricle
MC	Medial cortex
MC1	Medial cortex at the level of centrum semiovale
MC2	Medial cortex at the high convexity level
MCA	Middle cerebral artery
mRS	Modified Rankin Scale
MRI	Magnetic resonance imaging
mGy	Milligray

N	Number of patients
NCS	Neurocritical Care Society
NfL	Neurofilament light chain protein
NSE	Neuron-specific enolase
NWU	Regional brain Net Water Uptake
OHCA	Out-of-hospital cardiac arrest
ONSD	Optic nerve sheath diameter
PCD-CT	Photon counting detector computed tomography
PACS	Picture archiving and communication system
PCAS	Post-cardiac arrest syndrome
P-SAH	Pseudo-subarachnoid haemorrhage
pCSFV	Proportion cerebrospinal fluid volume
PIC	Posterior limb of the internal capsule
PLR	Pupillary light reflex
PU	Putamen
RB	Robust
ROC	Receiver Operating Characteristic
ROI	Region of Interest
ROSC	Return of spontaneous circulation
SE	Sulcal effacement
SEBES	Subarachnoid haemorrhage Early Brain Edema Score
SI	Simple
SOP	Standardised Operating Procedures
SSEP	Somatosensory evoked potentials
SSDE	Size specific dose estimate
T2 FLAIR	T2-weighted Fluid-Attenuated Inversion Recovery
TH	Thalamus
TIA	Transient ischaemic attack
TN	True negative

TNF	True negative fraction
TP	True positive
TPF	True positive fraction
TTM	Targeted Temperature Management
TTM1	Targeted Temperature Management trial 1
TTM2	Targeted Temperature Management trial 2
VF	Ventricular fibrillation
WL	Window Level
WLST	Withdrawal of Life-Sustaining Therapy
WM1	White matter at the level of the centrum semiovale
WM2	White matter at the high convexity level
WW	Window Width

Declaration of generative artificial intelligence usage

To improve language and readability in this thesis, a generative artificial intelligence (AI) model (GPT-4o-mini) was used. I, the author, have reviewed and processed the generated text and take full responsibility for its content.

List of Papers

This thesis is based on the following Papers, which are referred to by their Roman numerals in the text. All Papers are appended at the end of the thesis.

- I. **A pilot study of methods for prediction of poor outcome by head computed tomography after cardiac arrest**
Lang M, Nielsen N, Ullén S, Abul-Kasim K, Johnsson M, Helbok R, Leithner C, Cronberg T, Moseby-Knappe M
Resuscitation. 2022 Oct; 179:61-70.

- II. **Prognostic accuracy of head computed tomography for prediction of functional outcome after out-of-hospital cardiac arrest: Rationale and design of the prospective TTM2-CT-substudy**
Lang M, Leithner C, Scheel M, Kenda M, Cronberg T, Düring J, Rylander C, Annborn M, Dankiewicz J, Deye N, Halliday T, Lascarrou JB, Matthew T, McGuigan P, Morgan M, Thomas M, Ullén S, Undén J, Nielsen N, Moseby-Knappe M
Resuscitation Plus. 2022 Oct 12; 12:100316.

- III. **Standardised and automated assessment of head computed tomography reliably predicts poor functional outcome after cardiac arrest: a prospective multicentre study**
Lang M, Kenda M, Scheel M, Martola J, Wheeler M, Owen S, Johnsson M, Annborn M, Dankiewicz J, Deye N, Düring J, Friberg H, Halliday T, Jakobsen JC, Lascarrou JB, Levin H, Lilja G, Lybeck A, McGuigan P, Rylander C, Sem V, Thomas M, Ullén S, Undén J, Wise MP, Cronberg T, Wassélius J, Nielsen N, Leithner C, Moseby-Knappe M
Intensive Care Medicine. 2024 Jul;50(7):1096-1107.

IV. **Radiological signs of hypoxic-ischaemic encephalopathy on head computed tomography for prediction of poor functional outcome after cardiac arrest: a prospective observational cohort study**

Lang M, Kenda M, Scheel M, Martola J, Wheeler M, Owen S, Johnsson M, Annborn M, Dankiewicz J, Deye N, Düring J, Halliday T, Jakobsen JC, Lascarrou JB, Levin H, Lilja G, Lybeck A, McGuigan PJ, Rylander C, Sem V, Thomas M, Ullén S, Undén J, Wise MP, Cronberg T, Wassélius J, Nielsen N, Leithner C, Moseby-Knappe M
Resuscitation. 2025 Sep; 214:110675.

V. **Computed tomography grey-white matter ratio at the basal ganglia level in a reference population for hypoxic ischaemic encephalopathy after cardiac arrest: a cross-sectional observational study**

Lang M, Kenda M, Johnsson M, Ullén S, Cronberg T, Leithner C, Moseby-Knappe M, Nielsen N, Wassélius J
Resuscitation. Published online July 4, 2025.

All five Papers were published with open access.

Author's contributions to Papers I-V

- I. I was the primary contributor to the study design, and I wrote the final project plan. I organised the collection of CTs in our PACS, was one of the raters assessing the CTs, and I did most of the statistical analyses. I authored and revised the manuscript as the main and corresponding author.
- II. I contributed to the study design and the methodology. I authored the manuscript as the main author.
- III. The final Paper was originally two separate manuscripts, leading to an equally shared co-authorship where I worked alongside Martin Kenda. We both took part in the manual CT assessment. I was the primary contributor to the analyses of the manual CT assessments, and Dr. Kenda to the automated CT assessment method. We took equal part in writing and revising the manuscript.
- IV. I was the primary contributor to the study design and the data analyses. I authored and revised the manuscript as the main and corresponding author.
- V. I was the primary contributor to the idea, I wrote the project plan, and I obtained ethical approval. I organised the collection of CTs in our PACS, and I was one of the raters assessing the CTs. I analysed the data and authored and revised the manuscript as the main and corresponding author.

Related Papers not included in this thesis

Brain injury markers in blood predict signs of hypoxic ischaemic encephalopathy on head computed tomography after cardiac arrest

Lagebrant A, Lang M, Nielsen N, Blennow K, Dankiewicz J, Friberg H, Hassager C, Horn J, Kjaergaard J, Kuiper MA, Mattsson-Carlsson N, Pellis T, Rylander C, Sigmund R, Stammet P, Undén J, Zetterberg H, Wise MP, Cronberg T, Moseby-Knappe M

Resuscitation. 2023 Mar; 184:109668.

Regional Brain Net Water Uptake in Computed Tomography after Cardiac Arrest - A Novel Biomarker for Neuroprognostication

Kenda M, Lang M, Nee J, Hinrichs C, Dell'Orco A, Salih F, Kemmling A, Nielsen N, Wise M, Thomas M, Düring J, McGuigan P, Cronberg T, Scheel M, Moseby-Knappe M, Leithner C

Resuscitation. 2024 May 23;110243.

Magnetic resonance imaging in comatose adults resuscitated after out-of-hospital cardiac arrest: A post-hoc study of the Targeted Therapeutic Mild Hypercapnia after Resuscitated Cardiac Arrest trial

Eastwood GM, Bailey M, Nichol AD, Dankiewicz J, Nielsen N, Parke R, Cronberg T, Olasveengen T, Grejs AM, Iten M, Haenggi M, McGuigan P, Wagner F, Moseby-Knappe M, Lang M, Bellomo R; TAME trial investigators

Australian Critical Care. 2025 Mar;38(2):101130.

The semi-quantitative Cardiac Arrest Brain Ischemia (CABI) score for magnetic resonance imaging predicts functional outcome after cardiac arrest

Arctadius I, Wassélius J, Lang M, Drake M, Johnsson M, Friberg H, Leithner C, Kenda N, Lybeck A, Moseby-Knappe M

Accepted for publication in Critical Care, July 2025.

Abstract

Background and aim

Hypoxic-ischaemic encephalopathy (HIE) is a leading cause of morbidity and mortality in unconscious patients resuscitated after out-of-hospital cardiac arrest. Many patients die after withdrawal of life-sustaining treatments (WLST), often due to a presumed poor prognosis. To minimise the risk of premature WLST, guidelines recommend using a multimodal prognostication. Head computed tomography (CT) is widely used after cardiac arrest, but the evidence supporting its reliability as a predictor of poor outcome remains limited.

This thesis aims to evaluate qualitative and quantitative CT indicators of HIE to strengthen the evidence for CT as a prognostic tool in unconscious cardiac arrest patients.

Methods

I) Post-hoc analysis of a prospective multicentre study, *the Target Temperature Management at 33 °C versus 36 °C after Cardiac Arrest (TTM) trial*. Adult patients from Swedish sites with CTs were included. Two blinded radiologists assessed *early* (<24 hours) and *late* (\geq 24 hours) CTs with various qualitative- and quantitative (grey- white matter ratio (GWR)) methods to predict poor outcome, defined as a modified Rankin scale (mRS) score of 4-6 (moderate severe disability, severe disability, or death) at six months. (II) Protocol to establish pre-specified radiological criteria for identifying signs indicative of HIE on CT, aimed at predicting poor functional outcomes after cardiac arrest. (III) Prospective international multicentre sub-study of *the Hypothermia versus Normothermia after Out-of-hospital Cardiac Arrest (TTM2) trial*. CTs performed >48 hours \leq 7 days after cardiac arrest were assessed with manual (standardised qualitative and basal ganglia GWR) and automated atlas-based GWR. Prognostic performance for poor outcome prediction (mRS 4-6 at six months) for the qualitative assessment and for the pre-defined GWR cut-off <1.10 was calculated. Inter- and intrarater agreement were analysed. (IV) In-depth analysis of prognostic performance and interrater agreement for individual CT items included in the standardised qualitative assessment in Paper III. (V) Retrospective single-centre study. GWR at the basal ganglia level was calculated using two different-sized Regions of Interests (ROIs) by three raters on CTs without current significant pathology, in an age- and sex-matched cohort to a cardiac arrest population.

Results

I) N=106. All tested CT assessment methods had better predictive performance for poor outcome on *late* compared to *early* CTs. A GWR cut-off <1.10 showed 100% specificity across all methods and raters. The highest sensitivity at this cut-off, 50-63%, was achieved on late CTs with the GWR basal ganglia 8 ROIs. (III) N=140. Standardised qualitative CT assessment and all GWR methods at cut-off <1.10

predicted poor outcome with 100% specificity. Median sensitivity for the seven raters was: 37% (qualitative), 39% (GWR <1.10 8 ROIs), 30% (GWR <1.10 4 ROIs), and 41% (automated GWR <1.10). The highest interrater agreement was achieved with the GWR <1.15 8 ROIs method, kappa 0.83. IV) Loss of grey-white matter distinction predicted poor outcome with 100% specificity and 45-50% sensitivity. The specificity for sulcal effacement was 93-99% and the sensitivity 29-49%. The highest interrater agreement was achieved with loss of grey-white matter distinction at the high convexity level, kappa 0.74. V) N=155. No participant had GWR <1.10, regardless of ROI size. Median GWR ranged from 1.30 to 1.32 (0.1 cm² ROIs) and from 1.27 to 1.32 (0.2 cm² ROIs). Variability between raters and ROI sizes was ± 0.1 .

Conclusions

CT is a highly specific tool for predicting poor functional outcomes after cardiac arrest and should be considered in patients who remain unconscious >48 hours post-arrest, as part of a multimodal neuroprognostication strategy.

Combining a structured qualitative assessment of definite severe HIE with a GWR <1.10, assessed manually or via an automated method at the basal ganglia level, enables prediction of poor functional outcome with high specificity and moderate sensitivity.

Improving interrater agreement will require further refinement of standardised qualitative assessment, with focus on the robust predictive marker of loss of grey-white matter distinction.

Populärvetenskaplig sammanfattning

Hjärtstopp utanför sjukhus är ett globalt folkhälsoproblem som årligen drabbar hundratusentals individer. Ungefär 20% överlever till sjukhusankomst och av dessa cirka hälften till utskrivning. Majoriteten av de som avlider under sjukhusvården gör det efter att livsuppehållande behandling avslutats, oftast på grund av omfattande hjärnskada.

Olika strategier för att begränsa hjärnskada efter hjärtstopp har utvärderats. I djurmodeller har kylbehandling visat skyddande effekt. År 2013 publicerade vår forskargrupp the Target Temperature Management Trial after Out-of-Hospital Cardiac Arrest (TTM-studien) med 939 vuxna hjärtstoppspatienter från europeiska och australiensiska sjukhus (2010–2013). Studien kunde inte visa någon skillnad i överlevnad eller neurologisk funktion sex månader efter hjärtstoppet mellan patienter som kylts till 33 °C versus 36 °C. I efterföljande studie, the Hypothermia versus Normothermia after Out-of-hospital Cardiac Arrest (TTM2) trial (2017–2020), med 1 861 patienter från 61 sjukhus, jämfördes nedkylning till 33 °C med aktiv feberbehandling (<37,8 °C). Inte heller i denna studie observerades någon skillnad i överlevnad eller neurologisk funktion sex månader efter insjuknandet.

För att undvika felaktiga prognosbedömningar rekommenderar internationella riktlinjer att en neurologisk prognos efter hjärtstopp baseras på en kombination av kliniska neurologiska bedömningar, elektrofysiologiska tester, analyser av biomarkörer för hjärnskada i blodet samt radiologiska undersökningar såsom datortomografi av hjärnan (CT).

Datortomografi av hjärnan är en vanlig undersökning som har många fördelar. Den går snabbt att utföra, är relativt billig och är på de flesta sjukhus tillgänglig dygnet runt. Metoden bygger på röntgenstrålar (fotoner) som roterande röntgenrör avger och som passerar genom skallen i tunna skikt. Dessa fotoner kan spridas, absorberas eller överföras till en rad detektorer placerade motsatt röntgenröret för bildgenerering. Varje bildelement i en CT-bild tilldelas ett värde i Hounsfield-enheter (HU), vilket kvantifierar graden av fotondämpningen i det skannade volymelementet. CT-diagnostik baseras på att olika vävnadstyper har karakteristiska fotondämpande egenskaper. För att visuellt skilja på fotondämpning omvandlas HU-värden till gråskala, där högre värden ger ljusare och lägre värden mörkare områden i bilden. På CT-bilder från en neurologiskt frisk individ kan man därmed skilja den cellkroppstäta grå hjärnsubstansen som har högre täthet (mer fotondämpning och framstår ljusare) jämfört med den mer fetrika vita hjärnsubstansen som har lägre täthet (lägre fotondämpning och framstår mörkare).

Vid ett hjärtstopp upphör cirkulationen och hjärnan får inget syre. Eftersom hjärnan saknar förmåga att lagra syre och glukos uppstår hjärnskada redan efter några minuter. Även efter återkomst av egen hjärtaktivitet med pulserande blodflöde kan sekundära mekanismer förvärra hjärnskadan.

Hjärnskada i samband med hjärtstopp kan leda till ett nettoinflöde av vatten, vilket på CT ger en minskad dämpning av fotoner, särskilt i den grå substansen som är känsligast för syrebrist. På CT framträder detta som en minskad täthetsskillnad mellan grå- och vit hjärnsubstans. Denna skillnad kan, utöver att bedömas kvalitativt, kvantifieras genom att mäta HU-värden med små cirkulära arealer (Regions of Interest, ROIs) i utvalda delar av grå och vit substans. Kvoten mellan medelvärdena av dessa HU-värden, *the grey-white matter ratio (GWR)*, kan kvantifiera graden av hjärnskada. Den generella hjärnsvullnaden kan även påverka hjärnans morfologi med utslätade fåror och en kompression eller distorsion av basala cisterner.

Internationella riktlinjer rekommenderar att tecken som ”diffus och omfattande anoxisk skada” eller en ”kraftigt sänkt GWR” på CT kan användas för att förutsäga dålig prognos efter hjärtstopp. Trots att CT är en av de vanligaste undersökningarna hos medvetslösa hjärtstoppspatienter är evidensen för dess prediktiva värde svag.

Det övergripande syftet med denna avhandling var att utvärdera och optimera CT avseende dess förmåga att påvisa irreversibel hjärnskada efter hjärtstopp.

Delarbete I är en retrospektiv studie baserad på patienter från svenska sjukhus inkluderade i TTM-studien. Delarbete II är en protokollstudie. Delarbete III är en prospektiv observationsmulticenterstudie inom TTM2-studien, där standardiserad kvalitativ- och kvantitativ manuell och automatiserad metod med förutbestämd GWR cut-off validerades. Delarbete IV är en djupanalys av radiologiska tecken på irreversibel hjärnskada ingående i den standardiserade kvalitativa bedömningen från delarbete III. Delarbete V är en retrospektiv singelcenterstudie med kvantitativ CT bedömning av en referensgrupp utan hjärtstopp för att undersöka GWR i en matchad kohort.

De viktigaste fynden från denna avhandling är:

- CT är ett specifikt verktyg för att förutsäga dåligt utfall hos medvetslösa patienter efter hjärtstopp. Sensitiviteten påverkas av metod, bedömare och tidpunkt för undersökningen. CT bör övervägas som del av den multimodala prognosbedömningen av patienter som förblir medvetslösa >48 timmar efter hjärtstoppet.
- En bilateral och generell minskad täthetsskillnad mellan grå och vit substans på CT är ett robust visuellt tecken på HIE.
- GWR <1.10 i basala ganglierna är mycket ovanligt hos äldre utan hjärtstopp, ger i en hjärtstoppskohort i medeltal liknande sensitivitet som kvalitativ metod och erbjuder bättre interbedömarsamstämmighet.
- Automatiserad beräkning av GWR kan underlätta kvantifieringen av CT och göra metoden mer tillgänglig.

Thesis at a glance

Paper	Aim	Methods	Results / Conclusions
I	To explore the prognostic performance and the interrater agreement of both established and novel qualitative and quantitative CT ^A assessment methods for predicting poor outcome on <i>early</i> - (<24 hours) and <i>late</i> (≥24 hours) CTs following cardiac arrest.	<p>Post-hoc analysis of a multicentre study (TTM^B trial). Two blinded radiologists individually assessed 106 CTs.</p> <p>AUROC^C and a contingency table presented the prognostic performances. Percentage agreement and Bland-Altman plots presented the interrater agreement.</p>	<p>All CT methods achieved better prognostic performance on <i>late</i>- compared to <i>early</i> CTs.</p> <p>On <i>late</i> CTs, qualitative assessment achieved 100% specificity and sensitivity of 43-78%.</p> <p>At GWR^D <1.10 all GWR models achieved 100% specificity, and the best sensitivity at this cut-off was achieved with the 8 ROIs BG^E GWR model (50-63%). The novel models offered no additional benefit in terms of predictive performance.</p> <p>On <i>late</i> CTs, quantitative assessment achieved better interrater agreement than qualitative assessment.</p>
II	To establish pre-specified radiological criteria for the assessment of HIE ^F signs on CT for poor outcome prediction after cardiac arrest.*		
III	To validate standardised manual-qualitative and quantitative CT methods, and an automated quantitative CT method to detect signs of HIE for poor outcome prediction after cardiac arrest.	<p>Prospective international multicentre observational sub-study (TTM2-CT-sub-study). 140 CTs performed >48 hours ≤7 days after cardiac arrest were assessed standardised qualitatively and manual quantitatively (GWR at the basal ganglia level) individually by 7 raters.</p> <p>Automated GWR at the basal ganglia level was calculated in the prospective cohort and in a post-hoc analysis of 341 CTs ≤7 days after cardiac arrest.</p> <p>AUROC and a contingency table presented the prognostic performances. Intra- and interrater agreement were presented with Fleiss'- and Cohen's kappa.</p>	<p>Standardised qualitative assessment, manual- and automated GWR at cut-off <1.10, all predicted poor functional outcome with 100% specificity.</p> <p>Sensitivity in median was: 37% (qualitative), 39% (GWR <1.10 8 ROIs^G), 30% (GWR <1.10 4 ROIs).</p> <p>The 8 ROIs BG GWR model demonstrated superior prognostic performance as well as improved intra- and interrater agreement compared to the 4 ROIs BG GWR model.</p> <p>AUROC for automated GWR did not differ significantly from manually obtained GWR.</p>

IV	To investigate the prognostic performance and interrater agreement for individual CT items included in the standardised qualitative assessment in Paper III, with the goal of improving the standardised assessment of HIE signs on CT.	<p>Subanalysis of a prospective multicentre study (n=140) (TTM2-CT-sub-study).</p> <p>Prognostic performance for poor outcome prediction and interrater agreement of single radiological signs of HIE were evaluated and presented in a contingency table respectively with Fleiss' kappa.</p>	<p>"Loss of grey-white matter distinction" predicted poor functional outcome with 100% specificity and 45-50% sensitivity.</p> <p>The specificity for "sulcal effacement" was 93-99% and the sensitivity 29-49%.</p> <p>"The Pseudo Subarachnoid Haemorrhage Sign", "the Reversal Sign", and the "White Cerebellum Sign" predicted poor functional outcome with 99-100% specificity and 8-11% sensitivity.</p> <p>The highest interrater agreement was "moderate" (kappa = 0.74) for the loss of grey-white matter distinction at the high convexity level.</p>
V	To explore the GWR at basal ganglia level in an age- and sex-matched reference population without previous cardiac arrest.	Retrospective single-centre cross-sectional study. 155 CTs from a cardiac arrest matched cohort were assessed quantitatively with (GWR) using ROIs of 0.1 cm ² and 0.2 cm ² size at the basal ganglia level by three independent raters. GWR- and attenuation values were presented. Bland-Altman plots presented the interrater agreement.	<p>Independent of ROI-size, none of the study's participants were assigned a GWR < 1.10.</p> <p>Median GWR ranged from 1.30 to 1.32 (0.1 cm² ROIs) and from 1.27 to 1.32 (0.2 cm²). Variability between raters and ROI sizes was \pm 0.1.</p>

^AComputed Tomography (CT)

^BTargeted Temperature Management (TTM)

^CArea Under the Receiver Operating Characteristic (AUROC)

^DGrey-White matter Ratio (GWR)

^EBasal Ganglia (BG)

^FHypoxic ischaemic encephalopathy (HIE)

^GRegion of Interest (ROI)

Background

Cardiac arrest

Cardiac arrest is defined as the cessation of mechanical cardiac activity accompanied by the absence of systemic circulation.¹ It is commonly categorised according to the first documented rhythm as either shockable or non-shockable, with shockable rhythms generally associated with more favourable outcomes.²⁻⁴ Additionally, cardiac arrests are often classified according to their setting as either out-of-hospital cardiac arrests (OHCA) or in-hospital cardiac arrests (IHCA).⁵⁻⁷ This thesis focuses solely on OHCA patients. The majority of OHCA (approximately 90%) have medical origin, with cardiac causes being the most prevalent, followed by respiratory and neurological causes.⁸⁻¹¹

OHCA constitutes a major global health issue, with an average annual incidence of approximately 82 cases per 100.000 adults.^{8, 9, 12, 13} This incidence corresponds to roughly 300.000 OHCA cases annually in Europe.^{8, 13, 14} Among OHCA patients receiving cardiopulmonary resuscitation (CPR), on average, one-third achieve return of spontaneous circulation (ROSC), one-fifth survive to hospital admission, and one-tenth survive to one year (Figure 1A).¹⁵ However, both incidence and survival rates vary widely across the world. The highest incidence of OHCA is reported in the United States and Japan, whereas the lowest rates are observed in Australia, New Zealand, Singapore, and South Korea.^{16, 17} In comparison to Western countries, Asian countries have lower survival rates after OHCA.¹⁵

In Sweden, approximately 6,000 OHCA cases with initiated CPR are reported annually to the Swedish Cardiopulmonary Resuscitation Registry (SCRR). The median age is 72 years, and 65% are men.¹⁸

Approximately 90% of OHCA patients admitted to hospital in Sweden are unconscious and initially treated in an intensive care unit (ICU). Of these, nearly 45% survive to ICU discharge, and 35% survive at 90 days (Figure 1B).¹⁹

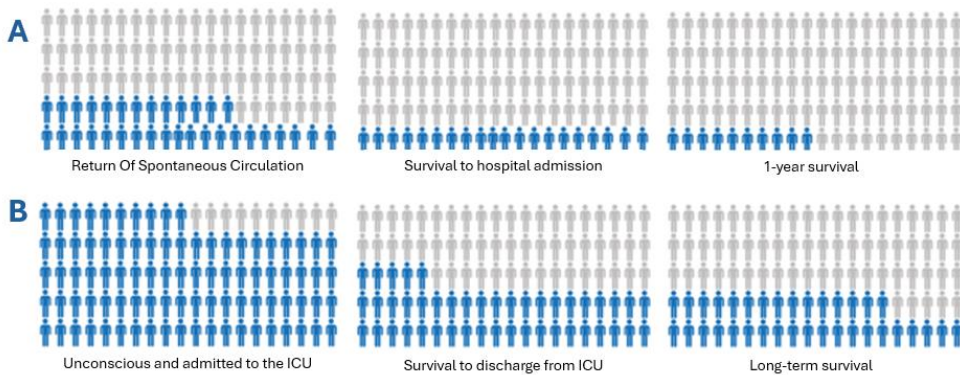


Figure 1A-B.

Symbolic illustration of: A) The proportion (in blue) of out-of-hospital cardiac arrest patients that receive cardiopulmonary resuscitation world-wide that, on average: return to spontaneous circulation, survive to hospital admission, and survive after one year. B) The proportion (in blue) of out-of-hospital cardiac arrest patients in Sweden that achieve return of spontaneous circulation and: are unconscious and admitted to the ICU, survive to discharge from the ICU, and survive long-term.

Image created in biorender.com.

The likelihood of survival after OHCA is affected by interventions within the *chain of survival* (Fig. 2). Originally, this chain comprised four links: 1) recognition and call for help, 2) CPR, 3) defibrillation, and 4) advanced resuscitation.²⁰ In 2010, *post- cardiac arrest care*, was incorporated as the 5th link.²¹ The 6th link, *recovery*, was added in 2020.²²

The 30-day survival rate following OHCA has nearly tripled since year 2000, reaching approximately 12% in Sweden in 2023.¹⁸ This increase in early survival in Sweden and many other Western countries is primarily attributed to higher bystander CPR rates and greater access to public defibrillation, improving the early links in the chain of survival.^{18,20, 21}

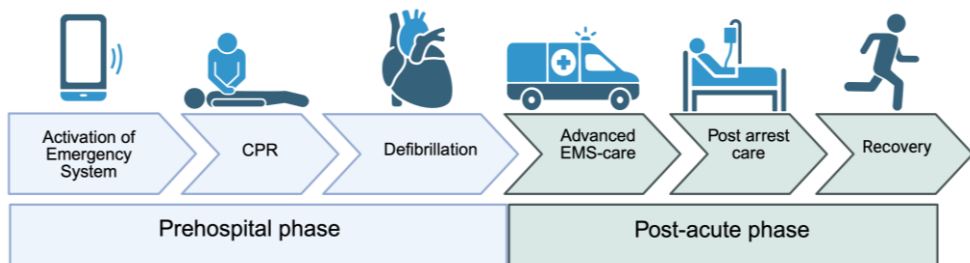


Figure 2.

The chain of survival. CPR; cardiopulmonary resuscitation, EMS; emergency medical services. *Illustration inspired by Thannhauser et al. 2022.²³ Image created in biorender.com.*

Most patients that are discharged alive have a good functional level, meaning that they can lead an independent life.^{11, 24, 25} Nevertheless, almost 50% of OHCA survivors may show some level of cognitive impairment at six months follow-up,²⁶ and five-year survival post-discharge is approximately 80%, highlighting the long-term vulnerability of this population.^{27, 28}

Hypoxic ischaemic encephalopathy

The brain has no internal stores of oxygen or glucose and relies on continuous blood flow, receiving about 15–20% of cardiac output in healthy adults.²⁹ During cardiac arrest, cessation of cerebral perfusion leads to an immediate disruption in neuron functioning.³⁰⁻³² Within minutes, cerebral ischaemia causes failure of energy-dependent plasma membrane ion pumps, resulting in loss of ionic gradients and an influx of osmolytes and water into neurons, which causes cytotoxic oedema.^{30, 33, 34} The consequent reduction in extracellular volume induces a compensatory shift of water from the intravascular compartment into the extracellular space to restore osmotic balance, this net water influx is termed ionic oedema.^{30, 33}

The energy depletion and lactate accumulation within neurons further trigger an excessive release of excitatory neurotransmitters, initiating a cascade of detrimental events including production of free oxygen radicals, destruction of mitochondria and cell membranes, and ultimately neuronal death.^{11, 31}

After ROSC, an imbalance often exists between cerebral energy supply and metabolic demand. Multiple pathophysiological mechanisms may contribute to secondary brain injuries up to days following ROSC. During this period, disruption of the blood-brain barrier may lead to the development of vasogenic (extracellular) oedema, which can increase intracranial pressure and exacerbate neuronal injury (Figure 3).^{31-33, 35}

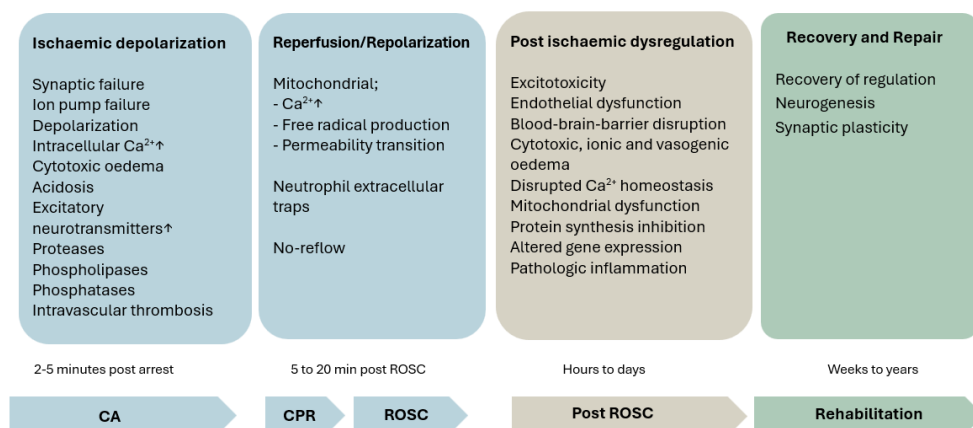


Figure 3.

Theoretical construct for phases of cardiac arrest and post-cardiac arrest brain injuries.

CA; cardiac arrest, Ca; calcium, ROSC; return of spontaneous circulation.

Illustration inspired by Sofia Backman. Reprinted with permission.

The cerebral injury resulting from cardiac arrest is known as hypoxic ischaemic encephalopathy (HIE).³⁶ Neuronal damage in HIE is frequently partial and predominantly involves grey matter, which contain the majority of neurons. Neurons are more vulnerable to ischaemic insult than oligodendroglia and astrocytes, the principal cellular components of the white matter. Blood vessels and microglia demonstrate the highest resistance to ischaemia.³⁶⁻³⁸

The selective vulnerability of grey matter is attributed to its higher basal metabolic rate, a more extensive capillary network, and a greater release of excitatory substances compared to white matter.³⁶ Neocortex and neostriatal structures, such as the caudate nucleus and the putamen, are often more severely affected by HIE than phylogenetically older neurons,^{38, 39} possibly due to lower energy demands of the latter. Brain injury in HIE is typically bilateral, with watershed areas frequently exhibiting relative hypoperfusion and increased susceptibility to ischaemic injury.^{36, 39}

Intensive care

Post-cardiac arrest syndrome

Ischaemic insults during CA, along with subsequent reperfusion injuries, can lead to the development of post cardiac-arrest syndrome (PCAS).^{40, 41} PCAS is a complex multicomponent condition comprising four components: 1) brain injury, 2) myocardial dysfunction, 3) systemic ischaemic/reperfusion response, and 4)

precipitating pathology.⁴¹ Patients with PCAS are generally treated in ICUs, where the goal is to stabilise vital organ functions, particularly to optimise cerebral perfusion and oxygenation by addressing secondary factors that may exacerbate brain injury. However, no specific therapy has yet been shown to modify PCAS sufficiently to improve long-term outcomes.⁴¹⁻⁴⁴

Temperature control

HIE is the leading cause of death and disability following cardiac arrest.⁴⁵⁻⁴⁷ In preclinical models of HIE, induced hypothermia has demonstrated neuroprotective effects, improving neurological outcome and survival.⁴⁸⁻⁵¹ In addition, studies have shown that hyperthermia may worsen outcomes.^{52, 53}

Improved survival and brain function with mild induced hypothermia in humans gained impact in 2002 after particularly two trials: the Bernard trial and the Hypothermia After Cardiac Arrest (HACA) trial.^{54, 55} These trials demonstrated improved neurological outcome⁵⁴ and survival^{54, 55} after hypothermia and resulted in recommendations of hypothermia between 32 °C and 34 °C for unconscious adult patients with ventricular fibrillation (VF) related OHCA by the International Liaison Committee on Resuscitation (ILCOR) in 2003.⁵⁶ Cochrane review supported the new guidelines and over the subsequent decade hypothermia was widely implemented for unconscious cardiac arrest patients.^{57, 58}

Hypothermia after cardiac arrest is, however, not risk-free. To tolerate the treatment of hypothermia, sedation and neuromuscular blockade are given, which may delay awakening, and in worst case, contribute to inappropriate and early withdrawal of life sustaining treatment (WLST).^{59, 60} Hypothermia can also cause arrhythmia.⁶¹ In addition, in patients with inevitable brain death, the hypothermia may cause unnecessary delay of WLST,⁴⁶ with increased health care costs.

A systematic review raised concerns regarding possible bias and random error in the earlier trials, and noted that the sample sizes were insufficient to draw definite conclusions.⁶² In 2013, the Target Temperature Management (TTM) trial, a randomised controlled international multicentre trial enrolling 950 patients to either TTM at 33 °C or 36 °C, could not find any difference in mortality or neurological disability between the two trial groups at six months follow-up.⁶³ The findings from the TTM trial initiated a slow transition from hypothermia, with ILCOR updating recommendations in 2015 to target temperature between 32 and 36 °C.⁶⁴

In 2019, the HYPERION trial, a randomised controlled trial including 581 cardiac arrest patients in French ICUs, reported benefits of hypothermia.⁶⁵ However, this trial investigated non-shockable CA. Furthermore, 25% of included patients were in-hospital cardiac arrests, and the results of the trial were considered fragile.

In 2021 the results from the, to this point, largest trial on the topic, the TTM2 trial were published.²⁴ No difference in mortality or poor outcome at six months was

found between the 1,861 unconscious OHCA patients that had been randomised to moderate hypothermia at 33 °C or normothermia (35.5-37.7 °C) with early fever treatment.

Today there is insufficient evidence regarding general temperature control between 32 °C and 36 °C and early cooling after cardiac arrest. Current guidelines from the European Resuscitation Council (ERC) and the European Society of Intensive Care Medicine (ESICM) recommend temperature control with fever prevention for 72 hours in unconscious patients post-cardiac arrest.⁴³ A large trial is ongoing with the aim to investigate whether fever prevention with treatment with an advanced temperature control system is of benefit, [clinicaltrials.gov](https://clinicaltrials.gov/ct2/show/study/NCT05564754) (NCT05564754, 2022-10-03). Further research is warranted to determine the optimal duration of temperature control, subgroups who may benefit from hypothermia, and assess protocols favouring early and fast cooling.⁶⁶

Neurological prognostication

Most patients with a good outcome regain consciousness within the first days after resuscitation.⁴³ However, a significant proportion of patients who remain comatose during this period may still recover well. Therefore, persistent coma during the first 2–4 weeks alone does not reliably indicate a poor prognosis.⁶⁷⁻⁷⁰

Guidelines ERC/ESICM

Neurological prognostication in unconscious cardiac arrest patients involves a gradual collection of information from several sources, including clinical examination, neuroimaging, neurophysiological testing, and blood biomarkers. Before reliable prognostication can occur, potential confounders (sedation, neuromuscular blockade, hypothermia, severe hypotension, hypoglycaemia, sepsis, and metabolic or respiratory derangements) must be ruled out.

In patients who remain unconscious with a Glasgow Motor Score of ≤ 3 at least 72 hours after ROSC, a multimodal prognostication of neurological function is recommended.⁴³ No single predictor is 100% accurate. Furthermore, they complement one another by evaluating different aspects of the underlying pathophysiology.^{25, 31} Prognostication algorithms for poor outcome in unconscious OHCA patients are provided in the ERC/ESICM guidelines published in 2015⁷¹ and updated in 2021.⁴³ Simplified illustrations of these algorithms are shown in Figure 4. According to the current 2021 guidelines, the presence of at least two unfavourable predictors within a comprehensive multimodal assessment is required to reliably predict poor neurological outcomes following cardiac arrest.

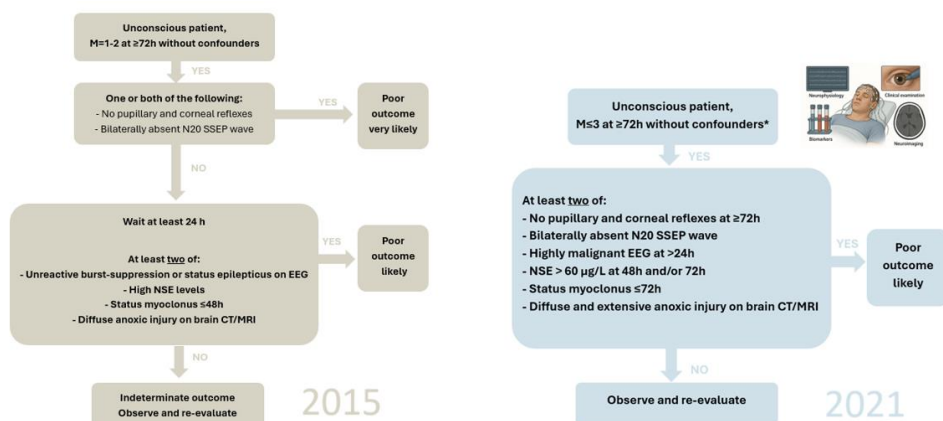


Figure 4.

Simplified illustrations of the ERC/ESICM prognostication strategy algorithms of poor outcome for unconscious OHCA patients in the guidelines from 2015 and 2021.

*Major confounders include analgo-sedation, neuromuscular blockade, hypothermia, severe hypotension, hypoglycaemia, sepsis, and metabolic and respiratory derangements. CT; computed tomography, EEG; electroencephalography, MRI; magnetic resonance imaging, NSE; neuron specific enolase, ROSC; return of spontaneous circulation, SSEP; somatosensory evoked potential.

Illustration created by OpenAI, 2025. ChatGPT, <http://chat.openai.com>. [Downloaded: May 6th 2025].

Clinical neurological examination

The Glasgow Coma Scale

Various instruments are available to assess the level of consciousness, with the Glasgow Coma Scale (GCS) being one of the most widely used. The GCS comprises three tests/subcategories (eye-, verbal-, and motor response) (Table 1).⁷² For each test the best response is added to a total Glasgow Coma Score between 3 (indicating deep unconsciousness) and 15 (fully awake and responsive).

Although the GCS is commonly used in intensive care settings to evaluate unconscious patients, it has notable limitations. Specifically, it cannot reliably assess verbal responses in intubated or aphasic patients, and it provide limited evaluation of brainstem reflexes.

The Full Outline of UnResponsiveness score

The Full Outline of UnResponsiveness (FOUR) score was developed as an alternative to the GCS.^{73, 74} Unlike the GCS, the FOUR score does not include a verbal response, making it particularly useful for assessing intubated patients. Additionally, the FOUR score offers more detailed information on brainstem function and provides clearer definitions of motor responses, including the distinction of a motor score of “4” and awakening, compared to the GCS.

The FOUR score assesses four domains: eye response, motor response, brainstem reflexes, and breathing patterns, with total scores ranging from 0 (completely unresponsive) to 16 (fully responsive) (Table 2).

Table 1. Glasgow Coma Scale

Eye response	No response	Eyes open to painful stimuli	Eyes open to verbal stimuli	Eyes open spontaneously		
Verbal response	No response	Sounds	Words	Confused	Oriented	
Motor response	No response	Extension (abnormal)	Flexion (abnormal)	Flexion (normal)	Localise pain	Obey commands
Score	1	2	3	4	5	6

Table 2. Full Outline of UnResponsiveness Score

Eye response	Eyelids remain closed with pain	Eyelids closed but open to pain	Eyelids closed but open to loud voice	Eyelids open but not tracking	Eyelids open, tracking, or blinking to command
Motor response	No response to pain or generalised myoclonus status	Extension response to pain	Flexion response to pain	Localising to pain	Thumbs-up, fist, or peace sign
Brainstem reflexes	Absent pupillary, corneal, and cough reflex	Pupillary and corneal reflexes absent	Pupillary or corneal reflexes absent	One pupil wide and fixed	Pupillary and corneal reflexes present
Respiration	Intubated, breathes at ventilator rate or apnea	Intubated, breathes above ventilator rate	Not intubated, irregular breathing	Not intubated, Cheyne–Stokes breathing pattern	Not intubated, regular breathing pattern
Score	0	1	2	3	4

Brainstem reflexes

Brainstem function is commonly assessed via the pupillary light reflex (PLR) and corneal reflex. Qualitative and quantitative PLR assessments show high specificity (94–100%) for predicting poor neurological outcome, though sensitivity remains low (20–30%).^{75, 76} Qualitative PLR achieves 100% specificity only after ~96 hours post-arrest, while quantitative methods can reach this earlier but are costly and lack standardised thresholds.^{77, 78} Similarly, bilateral absence of the corneal reflex ≥ 72 hours post-arrest predicts poor outcome with 100% specificity and 25–40% sensitivity.^{76, 79}

However, these reflexes can be affected by sedatives, neuromuscular blockers, and other pharmacologic agents.^{75, 80} Interrater reliability of qualitative assessments is also limited.^{81, 82} Current guidelines recommend using bilateral absence of PLR and corneal reflexes, in combination with at least one other concordant predictor, to assess poor neurological outcome post-cardiac arrest.^{76, 83}

Clinical seizures

Clinical seizures can often be observed after cardiac arrest.^{84–86} They can be classified as myoclonic, tonic-clonic, or a combination of both. In unconscious patients, myoclonic seizures within 96 hours and the so-called “status myoclonus”, with generalised myoclonus persisting >30 minutes, within 72 hours after cardiac arrest, may predict poor neurological outcome in combination with at least one more concordant predictor.⁴³ Clinical seizures should be confirmed with electroencephalogram (EEG).^{76, 80, 87}

Neurophysiology

Electroencephalogram

Electroencephalogram (EEG) measures cortical electrical fields generated by the summation of excitatory and inhibitory postsynaptic currents. Fluctuations in these electrical fields are recorded at the scalp, enabling real-time assessment of cortical function and neurological recovery. EEG is widely available and one of the most utilised methods for prognostication following cardiac arrest.^{88, 89}

Current guidelines recommend the use of specific “Highly Malignant EEG Patterns” (HMEP), together with at least one other concordant prognosticator, to predict poor neurological prognosis in unconscious patients ≥ 24 hours after cardiac arrest.⁴³ The HMEP include burst-suppression and suppressed background with or without superimposed periodic discharges.⁹⁰ In addition, unequivocal seizures on EEG, detected within the first 72 hours after ROSC, are also associated with poor prognosis following cardiac arrest.⁴³

In a multicentre prognostic study, the HMEP demonstrated a specificity of 93% and a sensitivity of 50% for predicting poor functional outcome in unconscious cardiac

arrest patients. The specificity further improved when HMEP were combined with an unreactive EEG background.⁹¹ In addition to its utility in predicting poor outcome, a non-highly malignant and reactive EEG pattern can predict good outcome post cardiac arrest, with approximately 80% specificity and 50% sensitivity.⁹²

Short-latency somatosensory evoked potentials

Short-latency somatosensory evoked potentials (SSEPs) assess the electrical response generated by peripheral nerve stimulation, typically the median nerve, recorded over the contralateral primary sensory cortex. With normal function, a cortical N20 wave, reflecting the depolarisation of pyramidal neurons in the postcentral gyrus, is registered approximately 20 milliseconds after the peripheral nerve stimulation.⁹³ Bilaterally absent SSEP N20 waves, when recorded with high quality and performed after at least 24 hours after cardiac arrest, together with at least one other concordant predictor, can be used to predict poor outcome in unconscious patients following cardiac arrest.⁴³ SSEPs show high specificity for predicting poor outcomes, with variable sensitivity (10–75%) and moderate to good interrater reliability.⁹⁴⁻⁹⁷

Blood based biomarkers

Biomarkers of brain injury represent breakdown products from damaged brain cells, with blood concentrations generally correlating to the extent of cellular injury.⁹⁸ Several biomarkers have been studied, but the only guideline recommended after cardiac arrest is currently neuron specific enolase (NSE).⁴³ NSE has been shown to accurately predict poor outcome post-cardiac arrest, with sensitivity and specificity varying depending on threshold.^{98,99} Since NSE is not entirely specific to the central nervous system and may be elevated for other reasons, especially haemolysis, serial measurements are advised. An increasing trend in NSE levels between 24 and 48 or 72 hours, combined with elevated values ($>60 \mu\text{g/L}$) at 48 and/or 72 hours can, together with at least one other concordant predictor, likely predict poor outcome in unconscious patients ≥ 72 hours after cardiac arrest.^{43,99}

Among novel brain injury biomarkers, neurofilament light chain (NfL) shows promise by enabling earlier and more accurate prediction of poor prognosis compared to NSE.¹⁰⁰⁻¹⁰² However, optimal diagnostic thresholds for NfL are not yet established.

Neuroimaging

The ERC/ESICM 2021 guidelines recommend performing head computed tomography (CT) early after hospital admission to exclude or confirm a neurological

cause of cardiac arrest and/or unconsciousness, as well as to identify any head trauma that might influence early management.⁴³ A recent review on prognostication following cardiac arrest reported that approximately 5% of cases are attributable to primary structural brain lesions, such as aneurysmal subarachnoid haemorrhage. This distinction has important implications for both clinical management and prognosis.¹⁰³

Neuroimaging is also an attractive prognostic tool due to its widespread 24/7 availability, rapid examination time, lack of interference from sedative medications, and ability to demonstrate morphological changes associated with HIE.⁷⁶ The most common CT findings indicative of HIE include reduced differentiation between grey and white matter and displacement of cerebral fluid (sulcal effacement).^{25, 76, 95} These imaging signs have demonstrated strong correlations with elevated levels of neuronal injury biomarkers¹⁰⁴ and histopathological findings of severe HIE.²²

The ERC/ESICM recommend that diffuse anoxic brain injury on CT or MRI, combined with at least one concordant prognostic marker, may predict poor outcome after cardiac arrest.⁴³ The Neurocritical Care Society (NCS) guidelines similarly state that a diffuse loss of grey-white differentiation with sulcal effacement on CT \geq 48 hours from ROSC and/or a diffuse pattern of restricted diffusion on MRI 2-7 days could be used as indicators of poor outcome. However, only with a very low level of quality of evidence.⁹⁵ ILCOR additionally recommends that absence of diffusion restriction on MRI between 3–7 days may indicate a favourable neurological outcome.¹⁰⁵

MRI

Magnetic resonance imaging (MRI) uses strong magnetic fields and radio waves to align and relax protons within body tissues to generate detailed anatomical images.¹⁰⁶ Compared to CT, MRI provides superior soft tissue contrast and greater sensitivity for detecting hypoxic-ischemic encephalopathy (HIE), with improved correlation to the spatial distribution of brain injury following cardiac arrest.¹⁰⁷ Additionally, serial MRI examinations enable better temporal characterisation of the evolution of brain injury compared to CT.³⁰

MRI utilises pulse field gradients and specialised sequences to generate contrast based on various tissue properties, allowing visualisation of physiological and pathological changes.¹⁰⁷ In cytotoxic oedema, cellular energy failure impairs ionic pumps, leading to intracellular water accumulation and consequent extracellular space reduction, which restricts the diffusion of extracellular water molecules.³⁰ The restricted free motion of extracellular water molecules is detectable within hours of injury as hyperintensity on diffusion-weighted images (DWI) sequences (Figure 5A) and can be quantitatively assessed using apparent diffusion coefficient (ADC) maps (Figure 5B).¹⁰⁸⁻¹¹² Although quantitative metrics such as “lowest mean ADC”¹¹³ and lesion “ADC burden”¹¹⁴ have been investigated for their prognostic

value in post-cardiac arrest patients, standardised threshold values for ADC metrics and lesion volumes remain to be established.¹¹⁵

T2-weighted fluid-attenuated inversion recovery (T2 FLAIR) can also detect brain injuries in HIE (Fig. 5C).¹¹⁶ Hyperintense signals on T2 FLAIR images, in conjunction with DWI and ADC findings, facilitate differentiation between cytotoxic and vasogenic oedema, thereby enabling comprehensive assessment of the extent and pathophysiology of brain injury in HIE.^{111, 112}

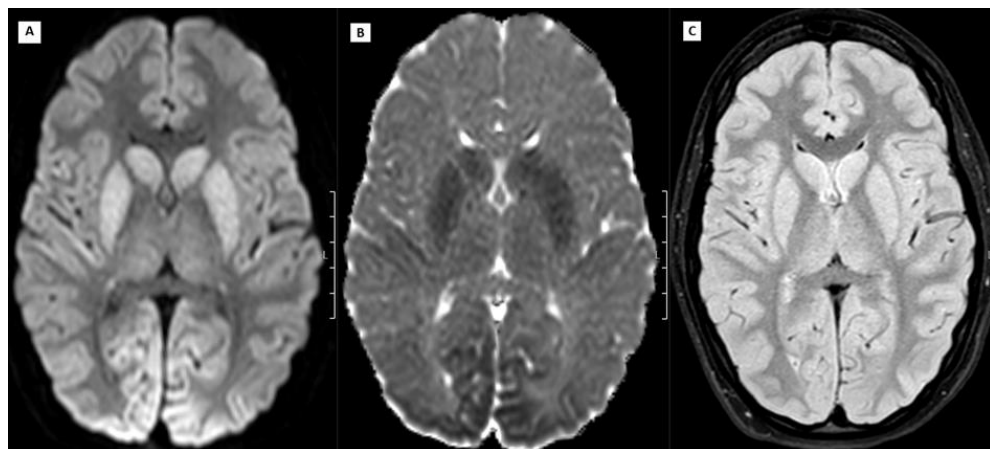


Figure 5A-C.

MRI images of diffuse and extensive anoxic injury here shown at the basal ganglia level in the putamina and the caudate nuclei as well as in the primary visual cortex on DWI (A) and ADC (B). On T2 FLAIR (C) the vasogenic oedema is only detectable in the putamina and the caudate nuclei.

Figure created by author.

In addition to unstandardised visual evaluation for the presence and extent of abnormalities on DWI- and T2 FLAIR- sequences, qualitative scoring systems have been developed to predict poor outcome with high accuracy and strong interrater agreement.¹¹⁷⁻¹²⁰

Compared to CT, diffusion-weighted imaging (DWI) on MRI has demonstrated higher sensitivity for predicting poor outcomes after cardiac arrest, albeit often at the expense of lower specificity. Furthermore, MRIs in these studies are typically performed at later time points than CT scans, which may confound direct comparisons between modalities.^{32, 76}

Emerging MRI techniques under investigation include functional MRI (fMRI), which detects regional cerebral blood flow changes reflecting neural activity, diffusion tensor imaging (DTI), and fractional anisotropy (FA), both of which provide quantitative insights into tissue microstructure and the integrity of white matter tracts. However, these advanced modalities are not yet incorporated into

routine clinical practice. Notably, portable MRI systems are now available, offering potential applicability in critically ill, unconscious cardiac arrest patients. Further research is needed to assess their prognostic performance.¹¹⁵

Outcome

Among patients with return to spontaneous circulation, cardiac causes constitute the leading cause of death within the first 72 hours following cardiac arrest. Beyond this early period, mortality is predominantly due to HIE sustained during and shortly after the arrest. As these patients often remain hemodynamically stable under full organ support, including mechanical ventilation, death frequently follows decisions regarding WLST, often based on a presumed poor neurologic prognosis.^{43, 46, 47, 121, 122}

Variability in WLST practices influences survival rates. Countries with prolonged organ support and low rates of WLST tend to report higher survival rates, but with an increased proportion of survivors in a persistent vegetative state.^{123, 124} Moreover, survival as a standalone outcome measure offers limited insight into the patient's post-resuscitation functional status or quality of life. As a result, functional outcome is increasingly recognised as a more clinically relevant and meaningful indicator of post-cardiac arrest recovery than survival alone.

Functional outcomes after cardiac arrest range from full recovery to severe neurological impairment. In healthcare systems where WLST is routinely practiced, the majority of OHCA-survivors have good neurological outcomes.^{24, 125, 126} The core outcome set for cardiac arrest (COSCA) initiative, led by the ILCOR, recommends using the clinician-reported modified Rankin scale (mRS) to classify global neurological function after cardiac arrest.¹²⁷⁻¹²⁹ The mRS evaluates the degree of disability or dependence in daily activities, with scores ranging from 0 (no symptoms) to 6 (dead) (Table 3).

Another frequently reported scale for global outcome measure is the cerebral performance category (CPC). CPC ranges from 1 (good cerebral performance) to 5 (brain death). While CPC has the advantage of including a vegetative state, the mRS allows for more detailed differentiation between mild and moderate disability and has demonstrated superior interrater reliability.^{130, 131}

Table 3. Modified Rankin Scale

Dichotomisation in Paper I-IV	Modified Rankin Scale	
Good outcome	mRS 0	No symptoms
	mRS 1	No significant disability: able to carry out all usual duties and activities despite some symptoms.
	mRS 2	Slight disability: able to look after own affairs without assistance, but unable to carry out all previous activities.
	mRS 3	Moderate disability: requires some help, but able to walk unassisted.
Poor outcome	mRS 4	Moderate severe disability: unable to walk alone without assistance and unable to attend to own bodily needs without assistance.
	mRS 5	Severe disability: bedridden, incontinent and requiring constant nursing care and attention.
	mRS 6	Dead.

The mRS is often dichotomised into “good” (mRS 0-3) and “poor” (mRS 4-6) outcomes. The dichotomisation facilitates statistical analyses and aligns with the binary decision of WLST. However, there is currently no universally accepted definition of what constitutes a poor functional outcome following cardiac arrest.

To provide a more comprehensive evaluation of recovery, the COSCA initiative recommends supplementing the mRS assessment with HRQoL (health-related quality of life) and assessment of cognitive function.¹²⁹

Neurological recovery following CA is often prolonged, with substantial improvements potentially occurring beyond the early post-resuscitation period. As a result, the minimum recommended time point for functional outcome assessment is 30 days post-arrest.¹²⁹ Given the dynamic nature of neurological recovery, reassessment at three to six months is advised to more accurately capture long-term outcomes.⁴⁵

Computed tomography

Allan M. Cormack, a South African physicist, published the theoretical foundations of computed tomography (CT) in the late 1950s.^{133, 134} Building on this work, Godfrey N. Hounsfield, an English electrical engineer, developed the first CT scanner between the mid-1960s and early 1970s.¹³⁵ The first clinical CT examination was performed in England in 1971, representing a major breakthrough in diagnostic imaging.¹³⁶ In 1979, Cormack and Hounsfield were jointly awarded the Nobel Prize in Physiology or Medicine for their contributions to the development of CT technology. Since its introduction, CT has undergone continuous advancements including increased scanning speed, expanded volume coverage, and improved temporal resolution, maintaining it as a cornerstone of modern medical imaging.¹³⁷

Methodology

Computed tomography (CT) produces cross-sectional images of the body by scanning thin slices (Greek:tomos) using a rotating X-ray tube and a detector array. During image acquisition, photons emitted from the X-ray tube interact with body tissues and are either scattered, absorbed (attenuated), or transmitted to the detectors, where they generate signals proportional to their remaining energy.

Each tissue type attenuates photons to a different extent, depending on its linear attenuation coefficient. This coefficient generally increases with the atomic number and/or density of the tissue and decreases with increasing photon energy.

Unlike, conventional x-ray film, which permits only subjective comparison of attenuation, CT enables quantitative analysis. CT numbers, expressed in Hounsfield units (HU), quantify the degree to which a given structure attenuates photons on an arbitrary scale where water is assigned 0 HU and air -1000 HU, irrespective of the CT scanner and/or the acquisition parameters. Each pixel in the CT image matrix is derived from a corresponding scanned volume element (voxel) and assigned a CT number that reflects the voxel's average linear attenuation coefficient. Thus, the CT image provides a direct representation of the spatial distribution of linear attenuation coefficients within the scanned tissue. The mean attenuation within a specific area of the CT image can be quantitatively assessed using Regions of Interest (ROIs).

CT numbers are converted into greyscale image for visual interpretation. Higher HU values are displayed as lighter shades of grey, and lower values as darker shades. Although each HU theoretically corresponds to a unique grey level, the human eye can only perceive contrast differences of approximately 10% and distinguishes far fewer shades of grey. To enhance visual interpretation, the grey scale can be adjusted to optimise image contrast and brightness, thereby allowing detection of subtle differences in attenuation. The range of HU values displayed is determined

by the window width (WW), while the window level (WL) defines the centre HU-value within that range. HU value below the lower limit of the WW will appear black, and those above the upper limit appear white. Figure 6 provides a simplified illustration of the CT image acquisition process.^{138, 139}

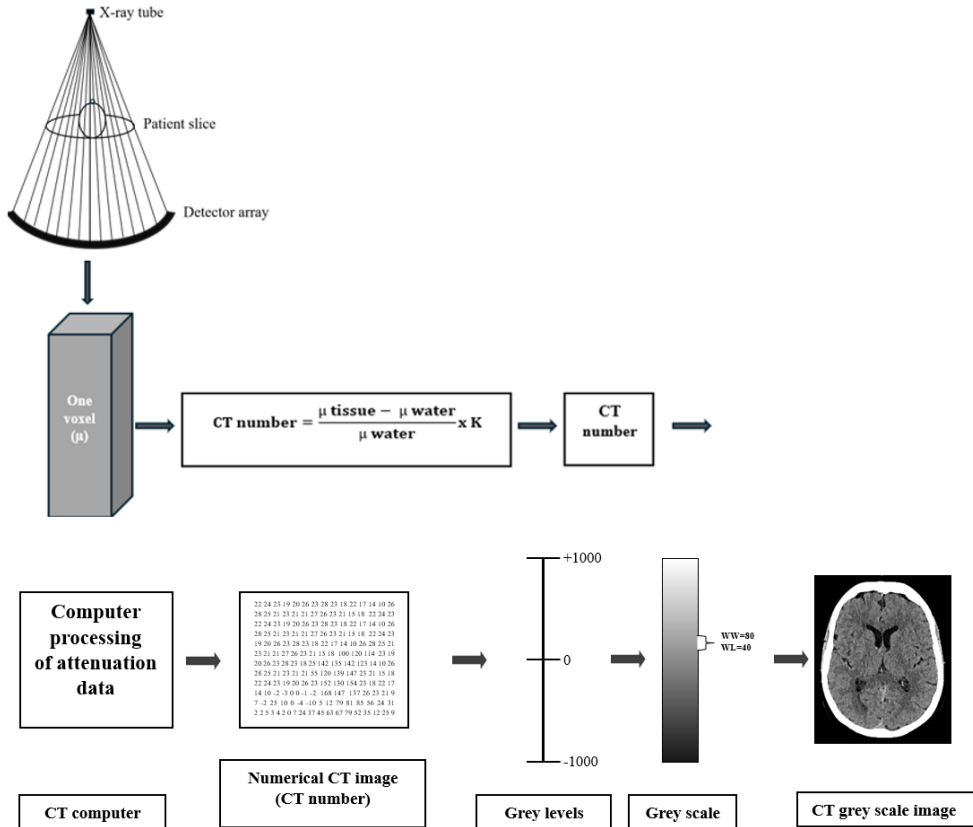


Figure 6. Schematic illustration of the CT image acquisition process.
CT; computed tomography, WL; window length, WW; window width.
Illustration inspired by Seeram et al. 2010.¹³⁹ Created by author.

Non-contrast head CT

The difference in attenuation between normal grey and white brain matter reflects the higher water- and blood content and lower lipid content in the densely cellular grey matter, resulting in slightly higher attenuation compared to white matter.¹⁴⁰ To detect these small differences, a narrow WW is used, enabling a finer range of grey to correspond to HU values in proximity. The optimal WL for brain CT images is

approximately the mean attenuation of grey matter, with a commonly used “brain window” setting of WW 80, WL 40 (Figure 7A).¹⁴¹ During image interpretation, radiologists may adjust the WW and WL, often utilising an even narrower WW of 40 to further enhance contrast. (Figure 7B).

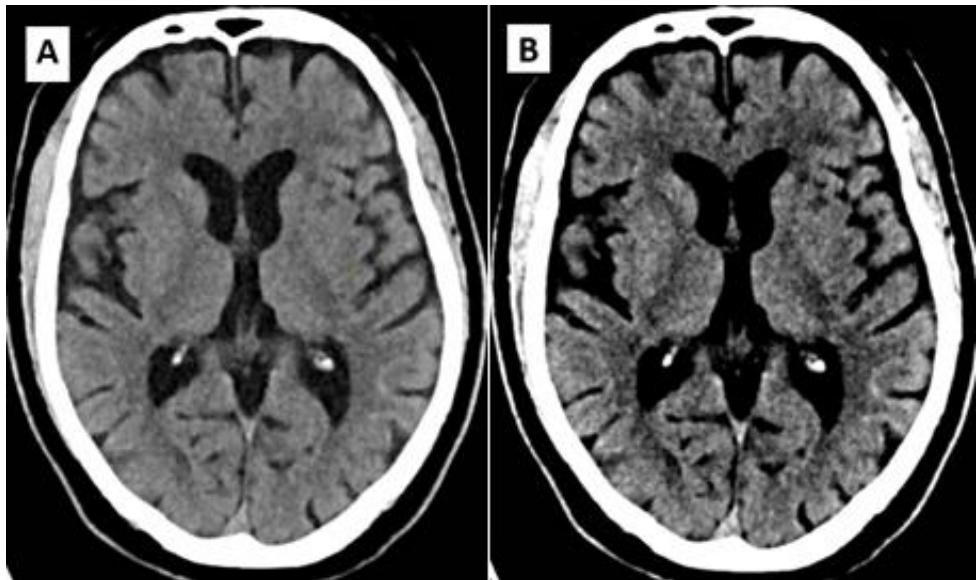


Figure 7A-B.

CT images at basal ganglia level with different manipulation of the grey scale. A) Often used standard brain window (WW 80, WL 40). B) A more narrow window (WW 40, WL 40) for better detection of subtle changes in the grey- white matter differentiation.

CT; computed tomography, WL; window length, WW; window width.

Figure created by author.

Different CT scanners and several acquisition parameters affect attenuation values,¹⁴² but generally accepted attenuation values on non-contrast CT from healthy subjects are 35-45 HU for grey matter and 20-30 HU for white matter.¹⁴³ In addition to variations in attenuation values from technical differences between CTs, poor scanner calibration, image artefacts and volume averaging may influence attenuation measurements.

Artefacts

One artefact that may alter the HU values is the beam hardening artefact, caused by a preferential attenuation of lower energy photons, resulting in “hardening” of the beam as higher energy photons reach the detector. Beam hardening commonly

occurs when the x-ray beam first passes through dense structures such as the skull and can manifest in two ways: *Streaking artefacts*, appearing as streaks or vague areas of decreased attenuation between two dense objects, for example, in the posterior fossa (Figure 8A), and *Cupping artifact*, characterised by an artificial increase in HU value in tissues adjacent to the skull bone (Figure 8B).^{144, 145}

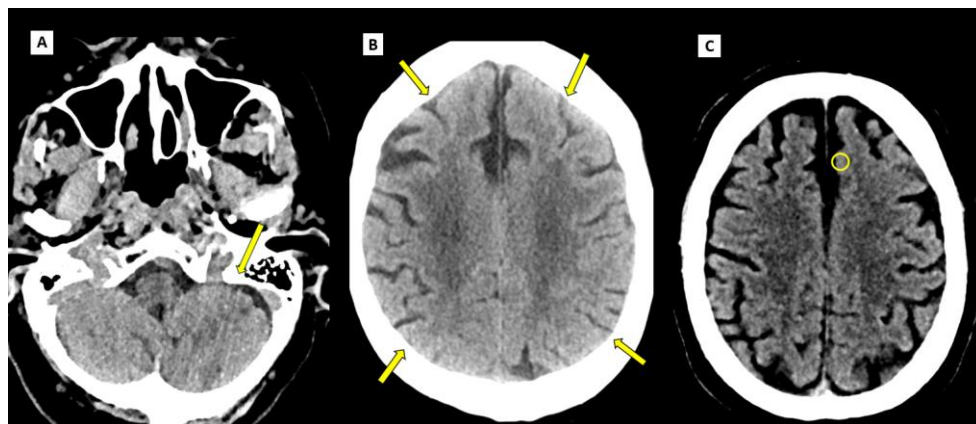


Figure 8A-C.

Factors that can influence attenuation measurements. Beam hardening artefacts shown as A) Streaking artefacts and B) Cupping artefacts. C) Partial volume effect. Intended measured attenuation in cortex will, due to a ROI size exceeding the border of cortex, be inaccurate and influenced by attenuation in CSF and subcortical white matter.

Figure created by author.

Another source of error when measuring attenuation on CT brain is volume averaging, which occurs when different tissue attenuations within a voxel are averaged, resulting in inaccurate pixel values. This partial volume effect can arise from thick CT slices and/or when the ROI exceeds the size of the structure being measured (Figure 8C).¹⁴⁵

Signs indicating hypoxic ischaemic encephalopathy on CT

The most common CT signs associated with hypoxic ischaemic encephalopathy include reduced differentiation between grey and white matter and a diffuse oedema with displacement of cerebral fluid (Figure 9C).^{25, 31, 32, 115} The primary cause of reduced grey-white matter differentiation is the brain net water uptake due to ionic oedema, which primarily affects grey matter and decreases its attenuation.^{30, 33} Additionally, a slight increase in white matter attenuation may occur as a result of distension of medullary veins.¹⁴⁶

Sulcal effacement reflects brain swelling caused by disruption of the blood-brain barrier and extracellular vasogenic oedema. In contrast to cytotoxic and ionic oedema, which develop within hours, vasogenic oedema typically emerges within days following cardiac arrest. Vasogenic oedema can cause significant mass effect, thereby exacerbating brain injury.^{31-33, 35}

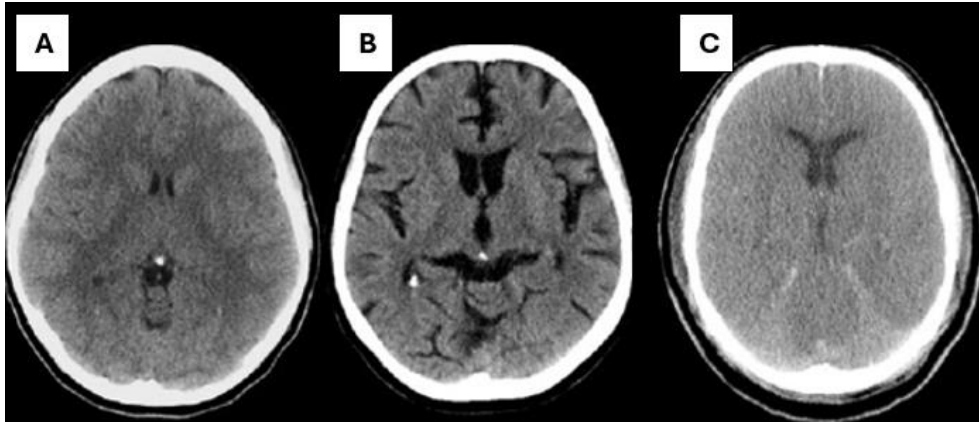


Figure 9A-C.

A) Normal findings in a young patient, characterised by preserved grey-white matter differentiation and narrow cerebrospinal fluid spaces. B) Normal findings in an older patient, with preserved grey-white matter differentiation and widened cerebrospinal fluid spaces. C) Findings indicative of severe hypoxic-ischaemic encephalopathy (HIE) with loss of grey-white matter differentiation and sulcal effacement. Figure created by Christoph Leithner. Reprinted with permission.

Since HIE after CA evolves over several days, imaging performed at least 24 hours post-arrest has demonstrated superior prognostic performance compared to earlier examinations.^{132, 147-149} The American Neurocritical Care Society recommends that CTs, intended for prognostic evaluation, should not be performed earlier than 48 hours after ROSC.⁹⁵

Additional radiological signs associated with HIE on CT include the *Pseudo Subarachnoid Haemorrhage Sign (p-SAH sign)* (Figure 10A), the *White Cerebellum Sign* (Figure 10B), and the *Reversal sign* (Figure 10C).

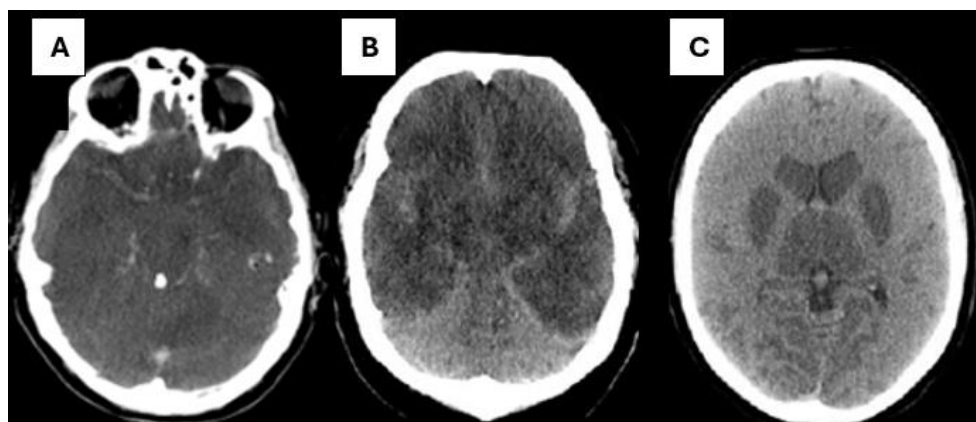


Figure 10A-C.

Radiological signs associated with HIE on CT. A) the Pseudo Subarachnoid Haemorrhage Sign, B) the White Cerebellum Sign, and C) the Reversal sign.

CT; computed tomography, HIE; hypoxic ischaemic encephalopathy.

Figure created by Christoph Leithner. Reprinted with permission.

p-SAH sign

The term *p*-SAH sign was first coined by Spiegel et al. in 1986, based on observations in 10 patients with extensive brain oedema but no evidence of subarachnoid haemorrhage (SAH) at autopsy.¹⁵⁰ In 1998, Avrahami et al. reviewed 100 comatose patients exhibiting brain oedema and radiological signs suggestive of SAH, but with no blood in cerebrospinal fluid analysis.¹⁵¹

The pathophysiology behind the *p*-SAH, characterised by increased attenuation along the sulci and basal cisterns mimicking true SAH, is not fully understood. It is thought to result from decreased attenuation of brain parenchyma combined with distension of superficial veins from increased intracranial pressure in severe oedema.

In unconscious patients following cardiac arrest, the *p*-SAH sign can appear within three days. It is reported to be highly specific for poor prognosis but with low sensitivity, ranging from 11.5 to 31%. *p*-SAH sign has been reported in up to 20% of post-cardiac arrest cases.^{152, 153}

The White Cerebellum Sign and the Reversal sign

The White Cerebellum sign refers to the relatively higher attenuation of the cerebellum, which is spared compared to the cerebrum, where diffuse decreased attenuation is seen in case of extensive brain oedema. It may appear concurrently with *the Reversal sign*, and some authors use the two terms interchangeably. However, *the Reversal sign* is better described as a distinct phenomenon, characterised by an inverse attenuation pattern with higher attenuation in white

matter compared to grey matter.^{154, 155} Both signs were originally, and continue to be, primarily reported in HIE with extensive brain oedema in the paediatric population.^{156, 157} Nonetheless, these signs have also been described in adults post-cardiac arrest and are associated with poor prognosis.³⁶

Qualitative CT assessment methods

Eye-balling

Due to the lack of consensus on standardised diagnostic criteria for HIE, unstandardised visual assessment, or *eyeballing*, of CT signs indicative of HIE remains common clinical practice. Several studies have demonstrated that such assessments yield high specificity for predicting poor neurological outcomes.^{158, 159} However, as with all subjective methods dependent on individual interpretation, there is an inherent risk of interrater variability.^{158, 160}

SEBES

The Subarachnoid haemorrhage Early Brain Edema Score (SEBES) visually assesses loss of grey-white matter differentiation and sulcal effacement (SE) at two predetermined anatomical levels bilaterally: the insular cortex and the centrum semiovale (Figure 11A-B).

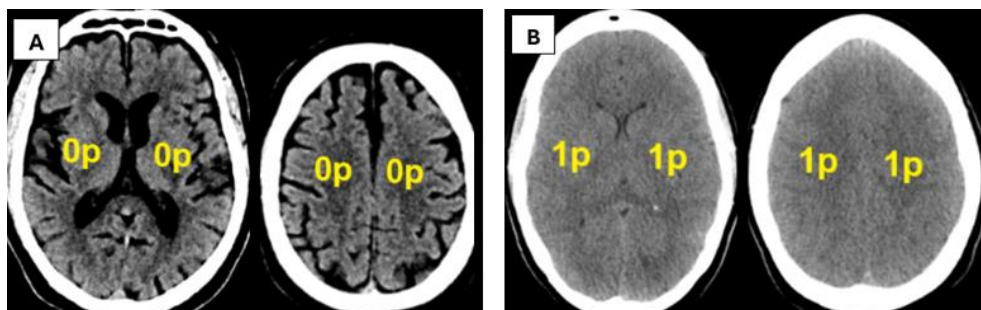


Figure 11A-B.

With SEBES sulcal effacement +/- disruption of the grey- white matter differentiation is assessed bilaterally at two anatomical levels; the level of the insular cortex (CT images to the left in A and B) and the level of centrum semiovale (CT images to the right in A and B). In the presence of sulcal effacement +/- disruption of the grey- white matter differentiation 1 pont is given, resulting in a total score ranging from 0 (no oedema) to 4 (general oedema).

A) CT images with no signs of oedema, SEBES 0 points.

B) CT images with signs of general oedema, SEBES 4 points.

CT; computed tomography, SEBES; Subarachnoid haemorrhage Early Brain Edema Score.

Figure created by author.

The absence of visible sulci, with or without loss of grey-white matter differentiation, scores one point per area, resulting in a total score ranging from 0 to 4 points. SEBES was originally developed for, and has shown promising results in, outcome prediction following subarachnoid haemorrhage.^{161, 162} In unconscious patients after cardiac arrest, standardised qualitative CT assessment using SEBES may improve sensitivity for poor outcome prediction and enhance interrater agreement.

ASPECT-b

The Alberta Stroke Program Early CT (ASPECT) score was originally developed to quantify the extent of ischaemic changes in middle cerebral artery (MCA) ischaemic stroke. The MCA vascular territory is segmented, and the score of 10 is reduced by one point for each region demonstrating involvement.¹⁶³ Subsequently, modified versions for the posterior circulation have been introduced (pc-ASPECTS).¹⁶⁴ The ASPECT score is widely used in stroke assessment and has demonstrated to be a reliable predictor of poor functional outcome.^{165, 166}

To address the frequently bilateral and symmetrical brain injury observed in HIE after cardiac arrest, the modified (m-ASPECT)¹⁶⁷ and the bilateral ASPECT (ASPECT-b)¹⁶⁸ scoring systems have been proposed. The m-ASPECT score involves a qualitative assessment of twelve bilateral regions on CT imaging, while the ASPECT-b score quantitatively evaluates ten bilateral areas in comparison to reference images. Preliminary findings from both scoring methods demonstrate promising interrater agreement as well as outcome prediction post-cardiac arrest.¹⁶⁷⁻¹⁶⁹

LOB-sign

The Loss of Boundary sign (LOB-sign) refers to the blurring of the distinct boundary between the grey and white matter. When assessed at the basal ganglia level on CTs, the LOB-sign demonstrated strong interrater agreement between two trained radiologists in one study. However, the sign lacked a clear definition and did not achieve perfect specificity.¹⁷⁰

Quantitative CT assessment methods

Grey- white matter ratio

The reduced differentiation between grey and white matter observed in HIE can be objectively quantified by measuring CT attenuation values. The greater susceptibility of grey matter to HIE-related injury is hypothesised to be attributed to its higher metabolic demand and higher vulnerability to excitotoxic mechanisms relative to white matter.^{36, 37, 171} Nevertheless, an isolated reduction in absolute grey

matter attenuation has not been consistently demonstrated as a reliable prognostic indicator for poor outcome after cardiac arrest.¹⁷²

The predictive value improves when the grey matter attenuation is expressed relative to white matter attenuation through the grey-white matter ratio (GWR). GWR is the most widely reported quantitative CT method for detecting cerebral oedema associated with HIE post-cardiac arrest and is currently the only quantitative CT method recommended by clinical guidelines.^{43, 173}

Torbey et al. conducted the first study investigating GWR in cardiac arrest patients and demonstrated that GWR differed significantly between unconscious cardiac arrest patients and control subjects.¹⁴⁶ They calculated GWR using attenuation measurements from ROIs at three anatomical levels: the basal ganglia level, the level of centrum semiovale, and the high convexity level. Among these, GWR at the basal ganglia level was found to be the most sensitive predictor of poor neurological outcome.

Following Torbey's initial study, numerous reports have examined the GWR using various combinations of attenuation measurements (Figure 12). Many of these studies have preferentially measured attenuation in deep brain structures, and most reports have used ROIs of approximately 0.1 cm² for attenuation measurements.^{109, 172, 174-183} The subcortical grey matter nuclei are particularly vulnerable to ischaemia and hypoxia, are distinctly visible on imaging, and, in comparison to cortical grey matter, at lower risk for partial volume effects, making them well suited for measurements.^{36, 146} Nonetheless, some studies suggest that including attenuation values from superficial grey and white matter in GWR, may enhance the predictive performance for poor neurological outcomes.^{174, 182, 184}

Regardless of brain regions included, GWRs have shown high specificity but variable sensitivity in predicting poor outcomes following cardiac arrest.^{107, 115} Reported GWR cut-off values that achieve 100% specificity for poor outcome prediction have ranged approximately from 1.08 to 1.23.³² This wide range likely reflects the considerable variation in factors such as the ROIs selected for GWR calculation, the interval between ROSC and CT examination, differences in CT scanners and acquisition protocol, the experience of investigators, as well as timing and methods of outcome assessment. To date, although current guidelines in neuroprognostication following cardiac arrest advocate for the use of quantitative CT assessment methods involving GWR, no standardised method has been recommended for calculating GWR from manual attenuation measurements, nor has a validated cut-off value been established to reliably predict poor neurological outcomes.^{115, 183}

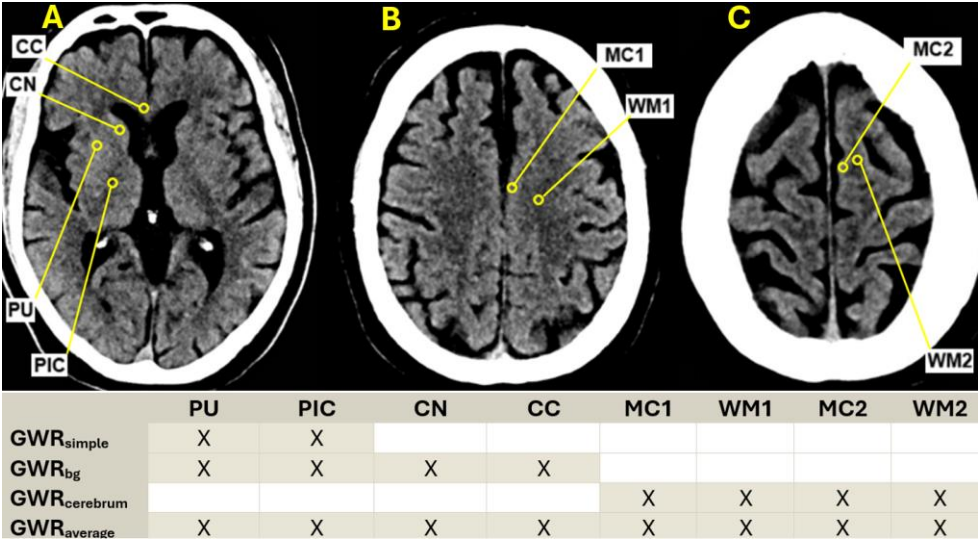


Figure 12. Attenuation measurements in specific grey- and white matter structures with approximately 0.1 cm² ROIs for GWR at three anatomical levels; A) the basal ganglia level, B) the centrum semiovale level, and C) the high convexity level. Various GWR models use different attenuation measurements marked with “X”. CT; head computed tomography, CC; genu corpus callosum, CN: head of the caudate nucleus, GWR grey- white matter ratio, MC1; medial cortex at the level of centrum semiovale, MC2; medial cortex at the high convexity level, PIC; posterior limb of the internal capsule, PU putamen, WM1; white matter at the level of the centrum semiovale, WM2; white matter at the high convexity level.

Figure created by author, including GWR models used in several previous studies.^{146, 172, 174-184}

Automated GWR

Manual GWR is time consuming and subject to both inter- and intra-rater variability. In addition, the often used approximately 0.1 cm² ROIs for attenuation measurements may not adequately represent larger anatomical structures, as minor alteration from vessels or calcifications can skew the ROI’s mean attenuation and thus the calculated GWR.

Automated, rater-independent approaches to GWR estimation on CTs offer the potential for more accurate, consistent, and anatomically representative measurements. These methods have demonstrated non-inferiority compared to manual GWR in predicting both poor- and good neurological outcomes post-cardiac arrest. A variety of automated techniques have been proposed, including probabilistic grey-white matter segmentation algorithms and image registration followed by atlas-based segmentation.¹⁸⁵⁻¹⁸⁸

Other CT methods

Regional Brain Net Water Uptake

In addition to automated GWR, preliminary data on a novel automated CT marker, the Regional brain net water uptake (NWU), have shown promising potential for outcome prediction following cardiac arrest.¹⁸⁹ Serially acquired CTs demonstrated regional variation in NWU, with the highest values observed in the basal ganglia. A NWU greater than 8% in putamina and caudate nuclei achieved the highest predictive value for poor neurological outcome (100% specificity and 43% sensitivity). In addition, CTs from patients with good outcomes exhibited minimal changes in NWU, which remained largely stable over time.

Proportion- and change in cerebrospinal fluid volume

Other objective, automatically generated CT markers for HIE include the Proportion cerebrospinal fluid volume (pCSFV) and the Change in cerebrospinal fluid. In a retrospective multicentre study involving unconscious cardiac arrest patients, pCSFV was independently associated with neurological outcome at six months follow-up. However, the overall prognostic power was poor.¹⁹⁰

Automated assessment of reductions in cerebrospinal fluid volume on serial CTs has demonstrated potential as a biomarker for development of cerebral oedema after ischaemic stroke. Theoretically, this methodology may also offer valuable prognostic information in unconscious patients following cardiac arrest.¹⁹¹

Machine learning methods

In recent years, several machine learning approaches applied to CT imaging analysis have also demonstrated promising potential in predicting outcomes after cardiac arrest.¹⁹²⁻¹⁹⁴

ONSD

The generalised oedema associated with HIE leads to an increase in the intracranial volume. The Monro-Kellie hypothesis describes a pressure-volume relationship that maintains a dynamic equilibrium among the non-compressible components within the rigid skull. Given the skull's limited compensatory capacity, any increase in intracranial volume soon results in a rise in ICP.¹⁹⁵

Direct measurement of ICP requires invasive procedures, which carry inherent risks. The optic nerve sheath, which directly connects to the subarachnoid space, expands in response to increased intracranial pressure (ICP).¹⁹⁶ An increased optic nerve sheath diameter (ONSD) serves as an indirect marker of elevated ICP. Measurement of ONSD via ultrasound, MRI, or CT has been shown to correlate with elevated ICP and is associated with poorer neurological outcomes.¹⁹⁷⁻¹⁹⁹

The most reported ONSD measurement is taken approximately 3 mm posterior to the globe. Although no universally established cut-off exists for predicting outcomes, an ONSD diameter below 5 mm is a generally accepted as indicative of good neurological outcome following cardiac arrest. Compared to ONSD measurements obtained via ocular ultrasound, those acquired from CT demonstrate similar specificity but lower sensitivity in predicting poor neurological outcomes after cardiac arrest.¹⁹⁷

CT perfusion

In recent years, CT perfusion (CTP) has seen increasing utilisation in ICU patients. CTP involves the acquisition of a temporal series of CT scans during the administration and clearance of an intravenous iodinated contrast agent. This imaging modality is well-established in the context of stroke, as it facilitates the differentiation between potentially salvageable ischaemic brain tissue (the penumbra) and irreversibly damaged infarcted tissue (the infarct core). In a prospective cohort study of unconscious patients following cardiac arrest, CTP findings indicative of non-survivable brain injury demonstrated high specificity and excellent interobserver agreement between two neuroradiologists in predicting poor neurological outcomes. However, sensitivity within this cohort was notably low, ranging from 2 to 19%.²⁰⁰

Photon counting detector CT

A recent study compared attenuation values in grey and white matter, as well as image quality, between conventional CT scanners and photon-counting detector CT (PCD-CT). The findings indicated a significant reduction in image noise and average offset with PCD-CT, suggesting that it may provide more reliable measurements. However, GWR remained consistent across both methods.²⁰¹

Knowledge gap

Although CT is a feasible, guideline-recommended, and widely used diagnostic tool after cardiac arrest,⁸⁹ several recent meta-analyses have concluded that the Grading of Recommendations Assessment, Development, and Evaluation (GRADE) level of evidence supporting its use for outcome prediction post-cardiac arrest remains very low.^{32, 76, 95} This low level of evidence is primarily attributed to the absence of multicentre validation studies and the lack of standardised approaches for both qualitative and quantitative assessments.^{43, 76, 95, 183, 202}

Aims of the thesis

The overall aim of this thesis was to strengthen the evidence of CT as a method for poor outcome prediction post-cardiac arrest.

The specific aims of the included Papers were:

- I. To explore prognostic performance and interrater agreement for various qualitative and quantitative CT methods for predicting poor outcomes, thereby informing the protocol for the subsequent validation study.
- II. To establish pre-specified radiological criteria for identifying signs indicative of HIE on CT, aimed at predicting poor functional outcomes after cardiac arrest.
- III. To validate both standardised manual qualitative and quantitative CT methods, as well as an automated quantitative CT technique, for prognostication of poor functional outcome post-cardiac arrest.
- IV. To assess the prognostic performance and interrater agreement of individual items within a qualitative CT assessment checklist, aiming to standardise radiological evaluation of HIE and ultimately improve interrater agreement.
- V. To investigate the grey- white matter ratio at the basal ganglia level in an age- and sex-matched reference population without previous cardiac arrest.

Materials and methods

This thesis includes five studies, summarised methodologically in Table 4. The data sources for Paper I (the TTM trial) and Papers II-IV (the TTM2 trial) are described in separate sections, whereas Paper V is based on a retrospective cohort from Helsingborg hospital. All five Papers are appended at the end of the thesis.

Table 4. Overview of studies included in the thesis

Paper	I	II	III	IV	V
Design	Post-hoc analysis of international multicentre study	Study protocol	Prospective international multicentre observational study	Subanalysis of prospective multicentre study	Retrospective single-center cross-sectional study
Study context, ClinicalTrials.gov identifier	The TTM trial, NCT01020916	The TTM2 trial, NCT02908308 The TTM2 CT-sub-study, NCT03913065			Convenience sample from one hospital
Study population	Patients from Swedish sites examined with CT ≤ 7 days post CA	Unconscious patients by routine examined with CT $>48\text{h} \leq 7$ days post CA			CTs without significant current pathology
	N = 106	N/A	N = 140 (341*)	N = 140	N = 155
Main CT parameters	All types of scanners and software	All types of scanners and software			Siemens Somatom Definition Flash
	Non-contrast	Non-contrast			Non-contrast
	120 kV	120 kV			120 kV
	Coronal, sagittal and axial slices of 3-5 mm	Axial slices of 4-5 mm			Axial slices of 5 mm
Platform	PACS	HON			HON
Method	Visual interpretation, SEBES, Manual GWR at three anatomical levels, $\approx 0.1 \text{ cm}^2$ ROIs	Checklist for qualitative assessment. Manual GWR at the basal ganglia level, 0.1 cm^2 ROIs. Automated GWR at the basal ganglia level		Single items within the checklist for qualitative assessment	Manual GWR at the basal ganglia level. $0.1 \text{ cm}^2 + 0.2 \text{ cm}^2$ ROIs

CA; Cardiac Arrest, CT; Head Computed Tomography, GWR; Grey-White matter Ratio, HON; Human Observer Net, PACS; Picture and Archiving System, SEBES; Subarachnoid Early Brain Edema Score, SOP; standardised operating procedures. TTM; Targeted Temperature Management.

* Post-hoc cohort including all patients with CT ≤ 7 days post CA within the TTM2 CT-sub-study.

TTM trial

Between November 2010 and January 2013, the Target Temperature Management After Out-of-hospital Cardiac Arrest (TTM) trial enrolled 950 adult patients (≥ 18 years) from 36 hospitals across Europe and Australia. Participants were randomised to receive targeted core temperature management at either 33 °C or 36 °C. The primary outcome was all-cause mortality assessed approximately 180 days post-enrolment. The secondary outcome comprised poor neurological outcome or death, defined as a score of 4 to 6 on the mRS or a CPC score of 3 to 5. Ethical committees in participating countries approved the study protocol. For Sweden, the Swedish Ethical Review Authority at Lund University approved the protocol in 2009 (Dnr 2009/324).

Eligible patients had a presumed cardiac origin of arrest (shockable or non-shockable rhythms) and were unconscious (GCS < 8) after at least twenty consecutive minutes of sustained ROSC. Key exclusion criteria included unwitnessed cardiac arrest with asystole as the initial rhythm, an interval exceeding four hours from ROSC to screening, a body temperature below 30 °C, and/or suspected or confirmed intracranial haemorrhage.

A schematic timeline from enrolment to outcome assessment is presented in Figure 13. Targeted temperature in both treatment arms was monitored via a urinary catheter and achieved and maintained with intravascular cooling catheters or surface cooling systems, initiated at the time of randomisation. Active rewarming to 37 °C commenced in both groups 28 hours post-randomisation at a controlled rate not exceeding 0.5 °C per hour. Throughout the 36-hour intervention period, patients in both groups were sedated and mechanically ventilated. After 36 hours, sedation was discontinued or decreased.

For patients remaining unconscious 72 hours after the completion of the intervention (i.e., 108 hours post-cardiac arrest), a neurological evaluation was performed by an independent physician blinded to the TTM allocation. The formal prognostication included a detailed clinical neurological examination, assessing the GCS, pupillary and corneal reflexes, alongside EEG and, when available, median nerve SSEP. Based on these findings, a recommendation was made regarding continuation or WLST. Decision of WLST was at the discretion of the treating physicians.

The following pre-specified criteria permitted WLST prior to formal prognostication:

- Severe myoclonus status within the first 24 hours post-admission combined with bilateral absence of the N20-peak on median nerve SSEP.
- Brain death due to cerebral herniation.

- Ethical considerations, including treatment-refractory shock or end-stage multi-organ failure.

Neurological outcomes were assessed by trained assessors at a minimum of six months post-randomisation (mean follow-up of slightly over eight months) via face-to-face or telephone interviews, utilising both the CPC- and the mRS.²⁰³

Following the initiation of the TTM2 trial, the original TTM trial has been referred to as the TTM1 trial, a designation that will also be used throughout this thesis.

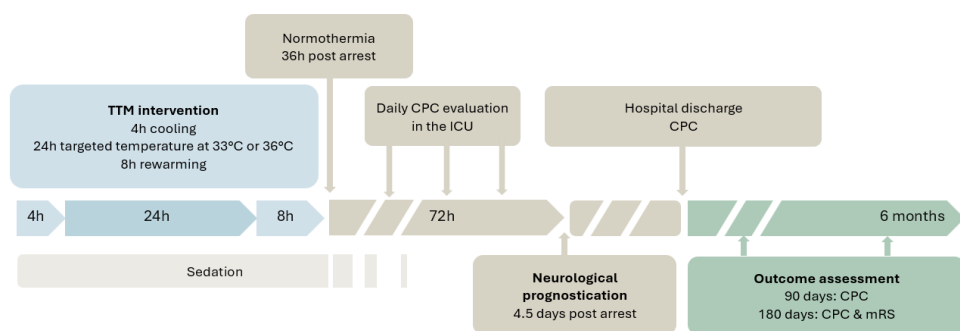


Figure 13.

TTM trial study overview

CPC; Cerebral performing scale, ICU; Intensive care unit, mRS; Modified Rankin scale

Illustration with some minor modification by Sofia Backman. Reprinted with permission.

Paper I

Study objective

In this pilot study, we sought to evaluate the prognostic performance and interrater agreement of multiple previously published as well as novel CT assessment methods for predicting poor outcomes post-cardiac arrest. The findings from this study informed the protocol design of the then ongoing TTM2 CT-sub-study.

Study design

This was a retrospective post-hoc analysis including unconscious patients (GCS score <8) who underwent a CT examination within seven days post cardiac arrest at Swedish sites participating in the TTM1 trial. CT examinations were performed on a clinical indication basis and were optional. In addition to the ethical approval obtained for the TTM1 trial (Dnr 2009/324, approved 2009-06-11), an amendment for Paper I was approved in January 2020 (Dnr 2019/324).

Irrespective of the CT scanner, all non-contrast CTs acquired at a tube voltage of 120 kV and reconstructed in coronal, sagittal, and axial planes with slice thicknesses of 3-5 mm were collected and anonymised. CTs demonstrating significant acute intracranial pathology (such as haemorrhage or infarction) or those affected by artefacts were excluded.

Included CTs were independently evaluated by two blinded radiologists (one neuroradiologist and one resident) at standard radiological workstations. Each rater was required to complete the assessment of one evaluation method for all patients before proceeding to the next method. The sequence of the various CT assessment methods is illustrated in Figure 14.

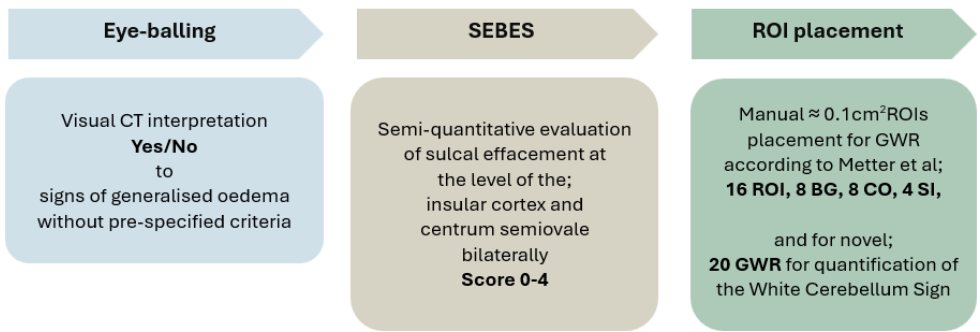


Figure 14.
Order and short description of the different CT assessment methods in Paper I.

Circular ROIs of approximately 0.1 cm² (corresponding to 60 pixels), were manually placed in predefined anatomical structures by the two raters. GWR was calculated as the sum of the mean attenuation values in HU from ROIs placed within grey matter, divided by the sum of the mean attenuation values from ROIs placed within white matter. The specific ROIs included in the different GWR models are shown in Table 5A.^{174, 177} Additionally, to quantify *the White Cerebellum sign*, a model incorporating the ratio between the 16 ROI AV GWR and the GWR in the cerebellum, referred to as the *20 ROI model*, was included. The equations for the various GWR models are provided in Table 5B.

Functional outcome, assessed by trained outcome assessors six months post-randomisation in the TTM1 trial, was dichotomised into “good” (mRS scores 0-3) and “poor” (mRS scores 4-6).

Table 5A-B.

A	GWR	ROIs in grey matter						ROIs in white matter				
		PU	CN	MC1	MC2	CBC	TH	PIC	CC	WM1	WM2	CBW
16 ROI AV	X	X	X	X	X			X	X	X	X	
8 ROI BG	X	X						X	X			
8 ROI CE			X	X						X	X	
4 ROI SI	X							X				
20 ROI	X	X	X	X	X	X		X	X	X	X	X
8 ROI RB*		X					X	X		X		

B	$16 \text{ ROI AV} = \frac{\text{PU} + \text{CN} + \text{MC1} + \text{MC2}}{\text{PIC} + \text{CC} + \text{WM1} + \text{WM2}}$						$8 \text{ ROI CE} = \frac{\text{MC1} + \text{MC2}}{\text{WM1} + \text{WM2}}$					
	$8 \text{ ROI BG} = \frac{\text{PU} + \text{CN}}{\text{PIC} + \text{CC}}$			$20 \text{ ROI} = \frac{16 \text{ ROI AV}}{(\text{CBC}/\text{CBW})}$				$8 \text{ ROI RB} = \frac{\text{CN} + \text{TH}}{\text{PIC} + \text{WM1}}$				

A) Attenuation measurements obtained in different structures with manual bilateral placement of ROIs according to the various GWR models. The included attenuation measurement is marked with "X".
 B) Equations for the various GWR models.

AV; average, BG; basal ganglia; CBC; cerebellar cortex, CBW; cerebellar white matter, CC; genu corpus callosum, CE; cerebrum CN; head of the caudate nucleus, GWR; grey- white matter ratio, MC1; medial cortex at the level of centrum semiovale, MC2; medial cortex at the high convexity level, PIC; posterior limb of the internal capsule, PU; putamen, RB; robust, SI; simple, TH; thalamus, WM1; white matter at the level of the centrum semiovale, WM2; white matter at the high convexity level.

*The 8 ROI RB GWR model was an exploratory post-hoc model including the four ROIs with the narrowest limits of agreement from the Bland-Altman analysis.

TTM2 trial

Between November 2017 and January 2020, the Targeted Hypothermia versus Targeted Normothermia After Out-of-hospital Cardiac Arrest (TTM-2) trial randomised 1861 adult patients (≥ 18 years) from 61 hospitals across Europe, Australia, and New Zealand to either targeted temperature management at 33 °C or normothermia with early fever treatment (37.8 °C or higher). The primary outcome was all-cause mortality assessed at or around six months post-randomisation. A key secondary outcome was poor functional outcome or death, defined as a mRS score of 4 to 6, evaluated approximately six months after enrolment.²⁰⁴ The study protocol received ethical approval from committees in all participating countries. For

Sweden, the Swedish Ethical Review Authority at Lund University approved the original protocol in 2015 (Dnr 2015/228) and a subsequent amendment in 2017 (Dnr 2017/36).

Eligible patients had a presumed cardiac or unknown aetiology of cardiac arrest (including both shockable and non-shockable rhythms), were unconscious (FOUR score below 4) after at least twenty consecutive minutes of ROSC and had no restrictions on intensive care interventions. Major exclusion criteria included unwitnessed cardiac arrest with asystole as the initial rhythm, more than three hours from ROSC to screening, admission temperature below 30 °C, extracorporeal membrane oxygenation (ECMO) prior to ROSC, intracranial haemorrhage, and any limitations in care.

A schematic timeline from enrolment to outcome assessment is shown in Figure 15. In the hypothermia group, target temperatures at 33 °C were rapidly achieved using intravascular cooling catheters or various surface cooling systems. This target temperature was maintained until 28 hours post-randomisation, followed by active rewarming to 37 °C at a controlled rate of approximately 0.3 °C per hour. In the normothermia group, intravascular cooling catheters or surface cooling systems were employed as needed when conservative and pharmacological interventions failed to maintain temperatures at or below 37.5 °C, particularly when temperatures reached 37.8 °C. Throughout the 40-hour intervention period, patients in both groups remained sedated or comatose and mechanically ventilated.

Patients remaining in the ICU ≥ 96 hours post-enrolment underwent neurological evaluation by a physician blinded to treatment allocation. The assessment protocol mandated clinical examination, including FOUR score, pupillary- and corneal reflex testing, as well as EEG. Neuroradiology (CT and/or MRI), SSEP, and NSE measurements were optional.

A poor neurological outcome was deemed likely if, at ≥ 96 hours after randomisation, the patient exhibited an absent or extensor motor response to painful stimuli in combination with at least two of the following criteria:

- Bilateral absent pupillary and corneal reflexes.
- Absence of SSEP N20-responses.
- Diffuse anoxic brain injury on CT or MRI.
- Presence of status myoclonus within 48 hours of randomisation.
- Elevated NSE levels.
- EEG demonstrating a highly malignant pattern without observed reactivity to auditory or painful stimuli.

If the previously stated criteria for likely poor neurological prognosis were met, and confounding effects of sedation on consciousness were ruled out, WLST due to presumed poor prognosis was permitted. Only two exceptions allowed for WLST prior to neurological evaluation ≥ 96 hours post-randomisation: confirmed brain death or ethical considerations, such as irreversible organ failure or significant medical comorbidities. The decision of WLST was at the discretion of the treating physicians.

Outcome assessments were conducted approximately six months post-randomisation through face-to-face or telephone interviews performed by trained assessors, who evaluated neurological outcome according to the mRS.²⁰⁴

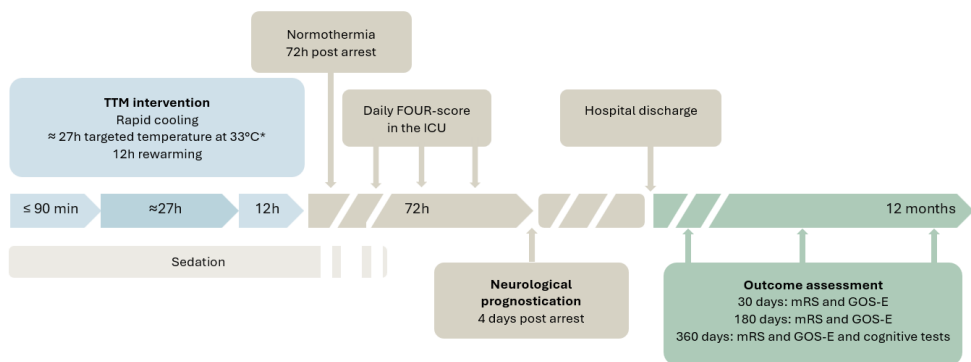


Figure 15.

TTM2 trial study overview

GOS-E; Glasgow Outcome Scale Extended, ICU; Intensive care unit, mRS; Modified Rankin scale.

Illustration inspired by Sofia Backman. Reprinted with permission.

Paper II-III

Study objective

Through these studies, we aimed to validate standardised manual qualitative and quantitative CT assessment methods, as well as an automated quantitative CT assessment, for prediction of poor functional outcomes post-cardiac arrest.

Study design

Paper II served as the protocol for Paper III, which was a prospective, international, multicentre, observational sub-study conducted within the framework of the TTM2 trial, known as the TTM2 CT-sub-study. Participating sites in the TTM2 CT-sub-study performed routine CT examinations on unconscious (FOUR score below 4)

cardiac arrest patients at >48 hours post-cardiac arrest. Ethical approval for the sub-study was obtained from the Swedish Ethical Review Authority at Lund University in 2018 (Dnr 2018/127).

Pseudonymised original CT examinations were collected from thirteen sites across four countries and securely uploaded to a two-way encrypted digital platform managed by Lund University (LUSEC). Randomisation, clinical management, neurological prognostication, WLST, and follow-up were conducted according to the main TTM2 trial protocol.²⁰⁴

Eligible patients underwent CTs from any type of scanner and software, with axial reconstructions of 4-5 mm thickness acquired at a tube voltage of 120 kV. CTs demonstrating acute ischaemic lesions, haemorrhage, other acute significant intracranial pathology, and/or artefacts were excluded.

Five radiologists (four neuroradiologists and one general radiologist) and two neurologists, all with between 3 and 15 years of experience in interpreting CTs after cardiac arrest, from four countries independently assessed the included CTs using a virtual private network-secured platform (Human Observer Net).²⁰⁵ The standardised qualitative assessments were completed for all patients by all raters prior to the initiation of the manual quantitative assessments. When all raters had finished both the qualitative and the quantitative assessments for all patients, 20% of CTs (the identical CTs for all raters) were re-evaluated in the same manner, first qualitative, followed by quantitative assessment, by all raters to assess intra-rater agreement (Figure 16).

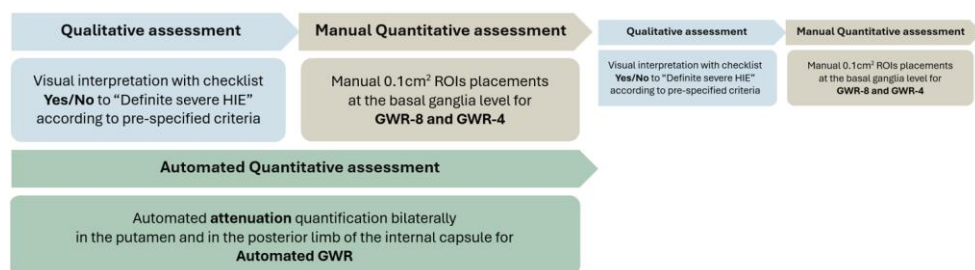


Figure 16.
Order and short description of the different CT assessment methods in Paper III.

For the qualitative assessment, CT images were evaluated at four predefined axial anatomical levels according to a checklist (Figure 17). Subsequently, raters confirmed or declined: “Are there *definite signs of severe HIE* defined as complete or near complete loss of grey-white matter differentiation at the basal ganglia level

and in the frontoparietal cortex with additional evidence of brain swelling/sulcal effacement?”.

For the quantitative assessment, circular ROIs measuring 0.1 cm² were manually placed bilaterally at the basal ganglia level in the caudate nucleus, the putamen, the genu corpus callosum, and the posterior limb of the internal capsule. GWR was calculated by dividing the sum of the mean attenuation values measured in grey matter ROIs by the sum of the mean attenuation values in white matter ROIs.

All CTs performed within seven days post-cardiac arrest, without significant pathology and/or artefacts, were co-registered to a publicly available MRI based digital brain atlas.¹⁸⁵ Tissue probability maps from the atlas identified anatomical regions on CTs, and mean attenuation values in the putamen and the posterior limb of the internal capsule were measured to assess automated GWR. The attenuation measurements and the three evaluated GWR methods are presented in Figure 18A-C.

Functional outcome, assessed by trained outcome assessors six months post-randomisation in the main study (TTM2 trial), was dichotomised into “good” (mRS scores 0-3) and “poor” (mRS scores 4-6).

Checklist - SOP for qualitative analysis in the TTM2 CT-Substudy

Patient: _____

Rater: _____

Prerequisites

Artifacts precluding analysis	<input type="checkbox"/> yes	<input type="checkbox"/> no
Brain diseases precluding analysis	<input type="checkbox"/> yes	<input type="checkbox"/> no
Residual contrast agent visible	<input type="checkbox"/> yes	<input type="checkbox"/> no

CT Levels

Qualitative Analysis

Start using standard brain window and then adapt to optimize visibility of grey-white matter differentiation. Evaluate axial images at these 4 different levels. Consider the best grey-white-differentiation, best visibility of sulci

1 - Brain stem + Cerebellum

Effacement of CSF spaces	<input type="checkbox"/> yes	<input type="checkbox"/> no
Pseudo-SAH	<input type="checkbox"/> yes	<input type="checkbox"/> no
White Cerebellum Sign	<input type="checkbox"/> yes	<input type="checkbox"/> no

2 - Basal ganglia

Bilateral loss of grey-white distinction	<input type="checkbox"/> yes	<input type="checkbox"/> no
Bilateral sulcal effacement	<input type="checkbox"/> yes	<input type="checkbox"/> no
Reversal sign	<input type="checkbox"/> yes	<input type="checkbox"/> no

3 - Frontoparietal cortex corona radiata level

Bilateral loss of grey-white distinction	<input type="checkbox"/> yes	<input type="checkbox"/> no
Bilateral sulcal effacement	<input type="checkbox"/> yes	<input type="checkbox"/> no

4 - High convexity cortex

Bilateral loss of grey-white distinction	<input type="checkbox"/> yes	<input type="checkbox"/> no
Bilateral sulcal effacement	<input type="checkbox"/> yes	<input type="checkbox"/> no

Result of qualitative analysis

Definite severe HIE: complete or near complete loss of grey-white distinction in the basal ganglia and in the frontoparietal cortex with additional evidence of brain swelling/sulcal effacement. Consider patient age while evaluating.

- ☐ Definite signs of severe HIE
☐ No definite signs of severe HIE

In the clinical setting, would you have diagnosed severe HIE despite the fact that the current SOP's stated criteria for definitive severe HIE are not being met?

- ☐ yes
☐ no

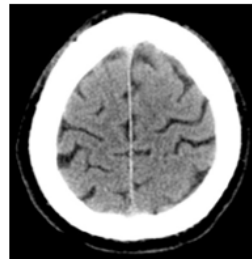
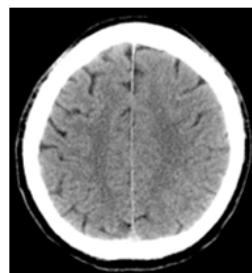
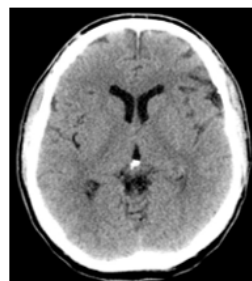


Figure 17.

Checklist for the qualitative assessment and the definition of "Definite severe HIE".
 Figure adopted from Paper II.

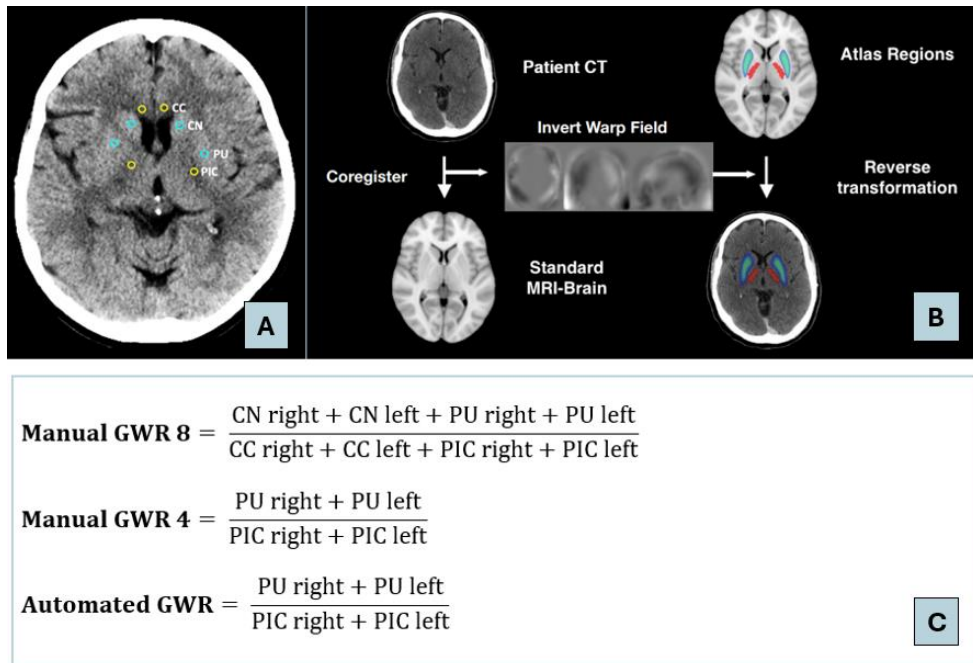


Figure 18A-C.

Attenuation measurements in different structures at the basal ganglia level with A) manual bilateral placement of ROIs and B) automated attenuation measurements. C) Included measurements for the various GWR models.

CC; genu corpus callosum, CN; head of the caudate nucleus, CT; computed tomography, GWR; grey-white matter ratio, MRI; magnetic resonance imaging, PIC; posterior limb of the internal capsule, PU; putamen.

Figure adapted from Paper III.

Paper IV

Study objective

In this study, we aimed to evaluate the prognostic performance and interrater agreement of individual items within our previously presented qualitative CT assessment checklist (Figure 17). The overall goal was to advance the standardisation of radiological assessment of HIE manifestations on CT and ultimately improve interrater agreement.

Study design

This was an in-depth analysis within the prospective TTM2 CT-sub-study, which included unconscious cardiac arrest patients who underwent CT between > 48 hours

≤7 days post-arrest. The raters, patient selection criteria, and CTs were consistent with those employed in the prospective cohort described in Paper III.

The prognostic performance of poor functional outcome (defined as a mRS score 4 - 6 at six months post-cardiac arrest) and interrater agreement were assessed for the individual items within the qualitative CT assessment checklist. These items included *the Pseudo Subarachnoid Haemorrhage Sign*, *the White Cerebellum Sign*, *the Reversal sign*, *loss of grey-white distinction* at three anatomical levels, and *sulcal effacement* at four anatomical levels (Figure 9A-C, Figure 17).

Paper V

A GWR <1.10 at the basal ganglia level on CT previously predicted poor functional outcome after cardiac arrest with high specificity and moderate sensitivity. However, since most unconscious cardiac arrest patients die following withdrawal of life-sustaining therapy (WLST) based on a presumed poor prognosis, there is a risk of a self-fulfilling prophecy. To improve the accuracy of outcome prognostication based on GWR on CT, we aimed to establish these parameters in a reference population.

Study objective

The objective was to describe attenuation values and GWR at the basal ganglia level in an age- and sex-matched reference population without previous cardiac arrest. We hypothesised that no study participant would have GWR <1.10. Additionally, we explored differences in attenuation values, GWR, and interrater variability for measurements obtained from 0.2 cm² ROIs compared to those from 0.1 cm² ROIs.

Study design

This was a retrospective, single-centre, cross-sectional study conducted at Helsingborg hospital. The design and statistical analysis plan were pre-published (DOI:10.5281/zenodo.13880313). Adult (≥18 years) patients who underwent non-contrast CT on a single scanner due to symptoms of stroke or transient ischaemic attack (TIA) between the 1st of January and the 17th of August 2021, were consecutively collected. The cohort was then filtered to achieve a group with a mean age of 70 years and 65% male patients.

CTs and/or radiology reports indicating significant current findings or artefacts were excluded. Included CTs were anonymised, except for the patient age and gender. The study protocol was approved by the Swedish Ethical Review Authority on the 15th of June 2022, with a waiver of consent (Dnr 2022-02755-01).

All CTs were performed on a single Siemens Somatom Definition Flash with acquisition parameters consistent with the standard clinical protocol: 40 x 0.6 mm collimation, 320 effective mAs, 120 kVp, pitch of 0.55, 1 second rotation time, 512 x 512 Matrix, and 22 cm Display Field of View.

Axial reconstructions of 5 mm thickness were assessed at the basal ganglia level by three raters from two countries, a general radiologist, a neuroradiologist, and a neurologist experienced in interpreting CTs after cardiac arrest, using a secured platform. Circular ROIs of 0.1 cm² were manually placed bilaterally in the head of the caudate nucleus, the putamen, the genu of the corpus callosum, and the posterior limb of the internal capsule, as described in Papers II and III. Additionally, circular 0.1 cm² ROIs were manually placed bilaterally in the lateral ventricles and the thalamus. After completing the assessments using the 0.1 cm² ROIs, 0.2 cm² ROIs were manually placed in the same structures bilaterally in all included CTs (see Figure 19 and 20). GWR was calculated according to the *Manual GWR* 8 (Figure 18C).

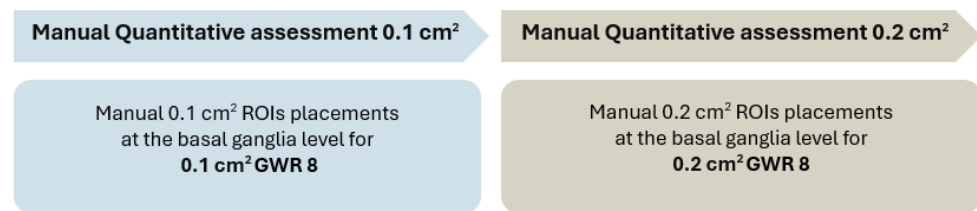


Figure 19.
Order of the different CT assessment methods in Paper V.

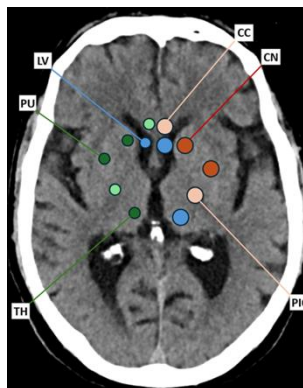


Figure 20.
Placement of circular ROIs at the basal ganglia level. ROI sizes of 0.1 cm² are presented in the right hemisphere and ROI sizes of 0.2 cm² in the left hemisphere.
CC; genu corpus callosum, CN; head of the caudate nucleus, LV; lateral ventricle, PIC; posterior limb of the internal capsule, PU; putamen, TH; thalamus.
Figure created by author.

Statistical analyses

The statistical methods used across all Papers in this study were developed in consultation with professional statisticians during the study design phase and subsequently reviewed during data analysis and manuscript preparation. For Paper I, analyses were performed using IBM SPSS (IBM Corp, Armonk, New York, USA) version 26, and R, version 3.5.1 (The R Foundation for Statistical Computing). For Papers III through V, IBM SPSS version 29, and R version 4.0.4 were utilised.

Continuous variables were reported as means (standard deviations) or medians (interquartile ranges), and categorical variables were reported in numbers (percentages). A paired t-test was used to compare GWR values, and Wilcoxon signed-rank test was used to compare attenuation measurements (Paper V). A two-sided p-value of less than 0.05 was considered statistically significant.

Prognostic performance

To clarify the terminology, *negative* (N) describes a CT without signs of HIE, indicating a good outcome, and *positive* (P) describes a CT with signs of HIE, indicating a poor outcome. When the CT assessment matched the reported outcome (mRS score at six months), the prediction was classified as *true* (T), conversely, discordant predictions were classified as *false* (F) (Figure 21).²⁰⁶

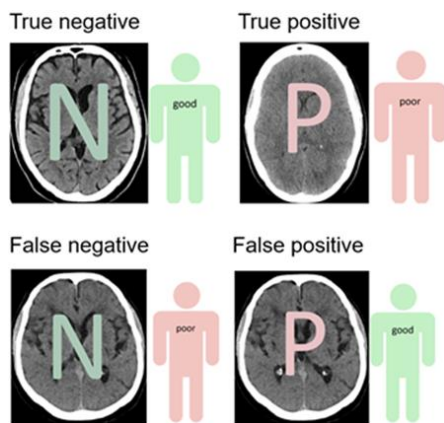


Figure 21.

CT images reported without signs of HIE *N* indicating good outcome (green) and with signs of HIE indicating poor outcome *P* (pink). Besides the CT images, the illustration of that patient's outcome at 6 months follow-up: green (good) mRS 0-3, pink (poor) mRS 4-6. **True negative (TN)**; good outcome patient correctly assessed as such by having no signs of HIE on CT, **True positive (TP)**; poor outcome patient correctly identified as such by having signs of HIE on CT, **False negative (FN)**; poor outcome patient not identified as having signs of HIE on CT, **False positive (FP)**; good outcome patient incorrectly assessed as having signs of HIE on CT.

Illustration inspired by Marion Moseby-Knappe. Reprinted with permission.

The *sensitivity* (true positive fraction (TPF)) of a test is its ability to identify patients with poor outcome:

$$\text{Sensitivity} = \text{TPF} = \frac{\text{TP}}{\text{TP} + \text{FN}}$$

The *specificity* (true negative fraction (TNF)) of a test is its ability to classify good outcome patients as normal:

$$\text{Specificity} = \text{TNF} = \frac{\text{TN}}{\text{TN} + \text{FP}}$$

The receiver operating characteristic (ROC) curves graphically illustrates the proportion true positives (sensitivity) against the false positive fraction (Figure 22).²⁰⁷ For the overall performance of a diagnostic test, the Area Under the ROC curve (AUROC) can be calculated. The maximum area 1.0 (100%) means that the test only delivers correct diagnoses. If the area is 0.5 (50%) the test is no better than a random classification of the patients.²⁰⁶

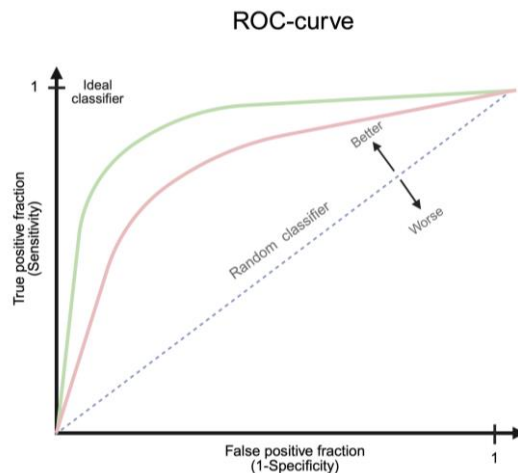


Figure 22. ROC curves. The ideal classifier has an AUROC of 1 while a random classifier has an AUROC of 0.5. The green ROC curve represents a method with better diagnostic performance (larger AUROC) than the pink ROC curve. ROC; Receiver Operating Characteristics, AUROC; area under the ROC curve. *Illustration inspired by Veronica Fransson. Reprinted with permission. Created in BioRender.com*

In Papers I and III, the overall diagnostic performance of various GWR models for predicting poor outcome (mRS score 4-6) was evaluated by calculating the area under the receiver operating characteristic curve (AUROC) with 95% confidence intervals, using a bootstrap procedure with 2000 iterations. Comparisons between ROC-curves were performed using DeLong's test.

Tests that only deliver correct diagnoses (100% sensitive and 100% specific) are exceedingly rare, therefore, a trade-off between sensitivity and specificity is often necessary. In neurological prognostication after cardiac arrest, high specificity is prioritised to minimise false-positive predictions, as an incorrect poor prognosis could potentially lead to premature WLST and patient death.⁴³

In Papers I, III, and IV, specificities and sensitivities for poor outcome prediction, with 95% confidence intervals, were calculated using Wilson's method. To encompass the range of previously published GWR cut-offs associated with poor outcome prediction without false positives, three different GWR cutoffs: 1.10, 1.15, and 1.20, were evaluated in our pilot study (Paper I). Additionally, GWR cut-off values and sensitivities at 100% specificity were determined. The validation study (Paper III) analysed the pre-specified GWR cut-offs of 1.10 and 1.15.

To evaluate the impact of timing on prognostic performance, CT examinations were categorised as *early* (<24 hours post-cardiac arrest) or *late* (\geq 24 hours post-cardiac arrest) in the pilot study (Paper I). This temporal aspect of prognostic accuracy was further explored in our post-hoc cohort within Paper III. Automated GWR, with the pre-specified cut-off of 1.10 for poor outcome prediction, were analysed across specific time windows: <2 hours, 2-6 hours, >6-48 hours, >48-96 hours, and >96-168 hours after cardiac arrest.

Inter- and intra- rater agreement

In Paper I, inter-observer agreement for binary variables between the two examiners was assessed using percentage agreement. Since percentage agreement does not account for agreement occurring by chance, 80 percent agreement has generally been cited as the minimum threshold for acceptable interrater agreement.²⁰⁸

To account for random agreement, Cohen's kappa (for comparisons involving two raters) and Fleiss' kappa (for more than two raters) were calculated in Papers III and IV to evaluate interrater agreement for binary variables.^{206, 208, 209} While kappa is widely accepted for assessing interrater agreement, it is known to be frequency-dependent, which can sometimes lead to an underestimation of the true strength of agreement.

In Paper III, the strength of agreement based on kappa values was categorised as follows:

<0.20 = poor
0.21 – 0.40 = fair
0.41 – 0.60 = moderate
0.61 – 0.80 = good
0.81 – 1.00 = very good

However, the interpretation of kappa values is not universally agreed upon in the literature. Some authors emphasise that kappa values below 1.00 reflect not only levels of agreement but also the reverse, presence of disagreement. For instance, if 41% of CT images were incorrectly assessed in a clinical setting, this would constitute a significant quality concern. Consequently, categorising kappa values between 0.41 and 0.60 as indicating “moderate” agreement may be misleading.²⁰⁸ For this reason, we adopted an alternative categorisation of agreement strength in our in-depth analyses of various radiological signs of HIE in Paper IV:

<0.20 = none
0.21 – 0.39 = minimal
0.40 – 0.59 = weak
0.60 – 0.79 = moderate
0.80 – 0.90 = strong
>0.90 = almost perfect

An alternative approach to interpreting kappa values is to avoid categorical labels altogether and instead consider any value below 0.60 as indicative of inadequate agreement.

For quantitative variables in Papers I and V, inter- and intra- observer agreement was assessed using Bland-Altman plots (Figure 23).

Bland-Altman plots display the differences between two sets of measurements against their means, producing a scatter plot with the mean difference and upper and lower limits of agreement.^{210, 211} The paired t-test or the Wilcoxon signed-rank test can be used to detect systematic errors, while the limits of agreement reflect the extent of random errors.

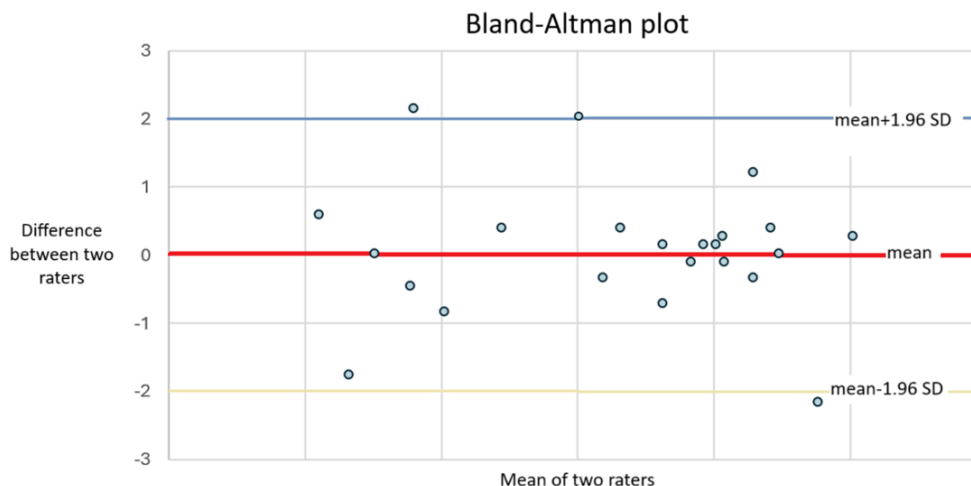


Figure 23.
Figure created by author.

Percentage concordance

In Paper III, the percentage concordance was assessed between the qualitative classification of *definite severe HIE* and a GWR-8 cut-off < 1.10 by four or more of the study investigators and pathological findings from other routine prognostic methods.

In Paper IV, concordance was calculated between each rater's confirmation of an individual radiological sign and their final evaluation of *definite signs of severe HIE*.

Self-fulfilling prophecy bias

Assessment of the diagnostic performances described above requires ground truth data. HIE is linked to poor functional outcomes. However, since local radiologists' reports were disclosed to the physicians responsible for WLST decisions, and WLST in these patients almost invariably resulted in death, our findings may be affected by self-fulfilling prophecy bias and thus overestimated.

A systemic review on neuroprognostication after cardiac arrest revealed that 88% of the included studies were susceptible to self-fulfilling prophecy bias.^{212, 213} In a retrospective study of unconscious cardiac arrest patients, neuroimaging findings alone prompted changes in clinical management in approximately 50% of cases, frequently resulting in the initiation of withdrawal of life-sustaining therapy (WLST).¹⁵⁸ This underscores the influence of neuroprognostic test results on real-

time clinical decision-making, which may contribute to premature WLST and death.^{59, 214, 215} Furthermore, in healthcare settings where WLST is not routinely practiced, the specificity of neuroimaging for predicting poor neurological outcomes following cardiac arrest has been shown to be lower compared to settings where WLST is employed.²¹⁶

To minimise self-fulfilling prophecy bias, conservative and standardised WLST protocols were employed in the TTM1- and the TTM2 trials. Prognostication was conducted no earlier than 108 hours (TTM1) or 96 hours (TTM2) post-randomisation, with only a limited set of prespecified criteria permitting WLST prior to this formal prognostication.^{203, 204} Validation studies of comparable prognostication strategies have demonstrated 100% specificity for predicting poor neurological outcomes, including in settings where WLST is not practiced, supporting the safety and reliability of this approach.^{99, 217} In regions where WLST is restricted due to cultural, legal, or religious factors, such as South Korea and Italy, recovery among patients with poor neurological prognosis remains exceedingly rare.^{123, 218, 219}

A further potential source of overestimation in the predictive performance of prognostic tests following cardiac arrest is the inclusion of non-neurological causes of death. Therefore, it is essential to document the mode of death and account for it in analyses of outcome prediction accuracy.

Ethics

Radiation exposure

CT imaging exposes tissue to ionising radiation, which carries a potential risk of deoxyribonucleic acid (DNA) damage, potentially resulting in cell death, mutations, or carcinogenesis. All exposure to ionising radiation should be considered potentially harmful, with the magnitude of harm generally increasing with cumulative dose. Radiation dose in CT is commonly quantified using the Computed Tomography Dose Index volume (CTDI_{vol}), measured in milliGray (mGy). Other dosimetric parameters include the dose length product (DLP), which reflects the total radiation output over the scan length, and the size specific dose estimate (SSDE), which adjusts for patient body habitus to provide a more individualised dose estimate.^{220, 221} Compared to other imaging modalities, CT delivers a relatively high dose of ionising radiation, and, as with all imaging that involves ionising radiation, the radiation protection principle of "As Low As Reasonably Achievable" (ALARA) should be applied.

In the studies included in this thesis, participants underwent CTs either based on clinical indication (Papers I and V) or according to established clinical protocols (Papers III and IV). All images were anonymised, and no additional CT examinations or clinical follow-ups were performed. Thus, our studies did not result in additional radiation exposure.

A standard non-contrast head CT typically involves a CTDI of approximately 45 mGy and a DLP of around 900 mGy cm. Our cohorts included only adult participants (≥ 18 years), who generally have lower radiosensitivity than paediatric populations. In the context of excluding alternative intracranial pathologies and predicting outcomes in unconscious cardiac arrest patients, the radiation dose associated with CT in the adult population is generally considered acceptable. While MRI provides a radiation-free alternative, its use is often limited by availability, longer acquisition times, and logistical challenges, particularly in critically ill, mechanically ventilated, and unconscious patients in the ICU.

Research on unconscious patients

All studies included in this thesis were conducted in accordance with the ethical principles outlined in the Declaration of Helsinki and its subsequent amendments.²²² The four fundamental ethical principles guiding research involving human subjects are shown in Figure 24.²²³

AUTONOMY Respect patient's right of self-governance
NONMALEFICENCE Avoid causing harm and minimise harm to the patient
BENEFICENCE Maximise benefits and enhance patient's well-being
JUSTICE Treat patients fairly and equitably

Figure 24.

These ethical principles are universal and apply worldwide, transcending national, cultural, legal, or economic boundaries.

Approval of study protocols for studies included in this thesis was obtained from the appropriate ethics committees in each participating country. The treatment algorithms tested in the TTM1 and TTM2 trials were guideline-recommended to be initiated as soon as possible after hospital admission, necessitating justification of randomisation prior to obtaining informed consent. For patients who regained consciousness, written and oral informed consent was obtained, and for all included patients, declaration was obtained from legal representatives and/or patients according to local legislation (Papers I-IV).

When ongoing treatment is no longer considered beneficial, withdrawal of life-sustaining therapy (WLST) is legally permitted for unconscious post-cardiac arrest patients in Sweden and most other countries. However, in some countries, cultural and religious factors make WLST uncommon. Although rare, cases of neurological improvement have been reported in such settings.¹²³

By strengthening the evidence and improving the accuracy of CT for prognostication in unconscious cardiac arrest patients, this thesis can reduce inappropriate WLST decisions and prevent unnecessary prolonged intensive care in patients with a futile prognosis, promoting both nonmaleficence and beneficence. Additionally, by limiting non-beneficial intensive care, critical resources can be reallocated to patients with a chance of recovery, promoting fairness and optimal use of healthcare resources (justice).

Results

Paper I

Participants

Of the 117 patients from Swedish TTM1-trial sites who underwent CT examination within seven days post-cardiac arrest, 106 were eligible for inclusion. The patient selection- and exclusion-process is illustrated in Figure 25.

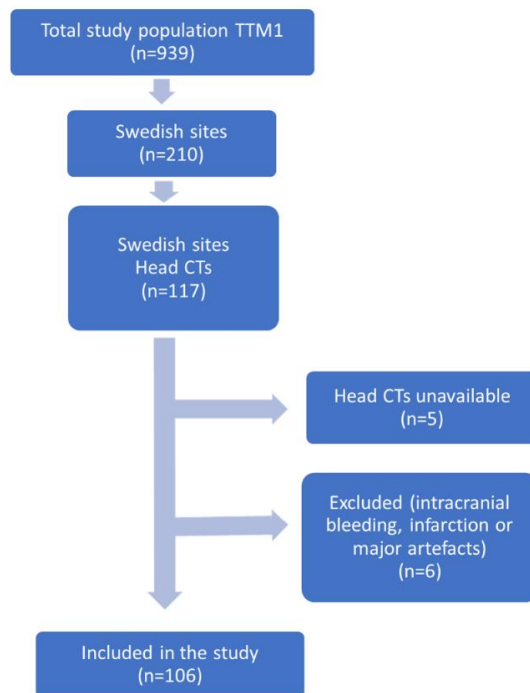


Figure 25.
Flowchart of patient selection and exclusion.

CT; computed tomography, n; number of patients, TTM; Targeted Temperature Management. Examiner 2 excluded n=7 patients for certain ROIs and thus only included n=105 images for some of the GWR models.

Figure adopted from Paper I.

Among the included patients, 84/106 (79%) were male, median age was 68 years (IQR 60-75). The median time from ROSC to CT was 4 hours (IQR 2-72 hours), with 68/106 64% of the CT examinations performed within 24 hours post-ROSC. At six months, 70/106 (66%) had poor functional outcomes (mRS 4-6).

Prognostic performance

The overall predictive performance for functional outcome, measured by AUROC, varied across different GWR models. For CTs performed <24 hours post-cardiac arrest, AUROCs ranged from 0.50 to 0.64 for rater (examiner) 1 and from 0.40 to 0.63 for rater 2. For CTs conducted \geq 24 hours post-cardiac arrest, AUROCs ranged from 0.58 to 0.87 for rater 1 and from 0.60 to 0.94 for rater 2 (Figure 26).

All GWR models tested at cut-off < 1.10 achieved 100% specificity for both raters. The highest sensitivity at this cut-off, for both raters, was observed with the GWR 8 ROIs BG model on CTs performed \geq 24 post-cardiac arrest, 50% (95% CI: 33-67) for rater 1 and 63% (95% CI: 46-78) for rater 2. The prognostic performance of the various CT assessment methods for predicting poor functional outcome, together with the inter-rater agreement percentages, are presented in Table 6.

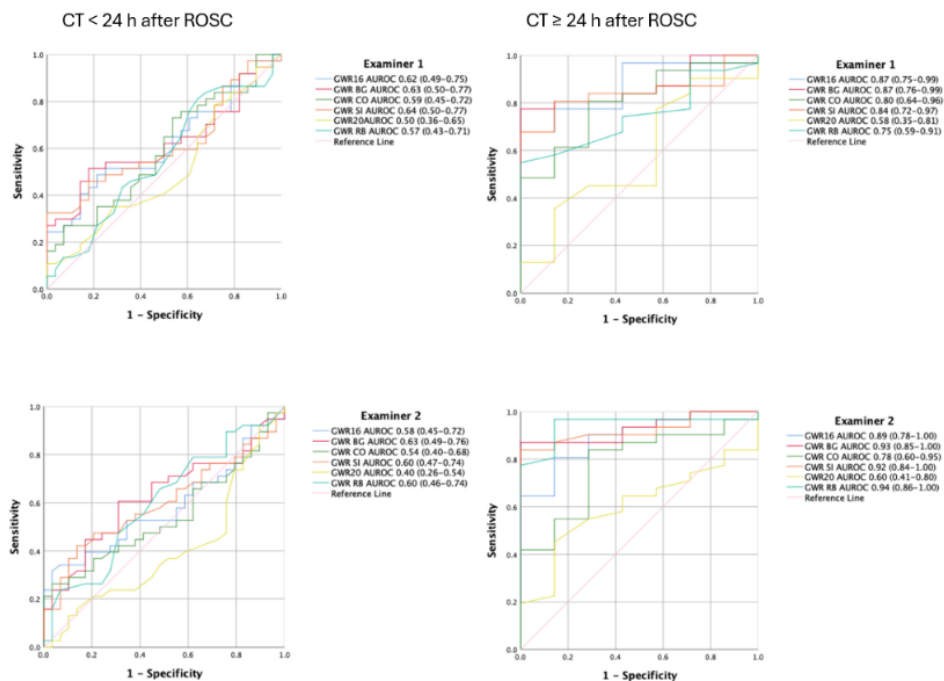


Figure 26. ROC curves and AUROC with 95% confidence intervals of the various GWR models predicting functional outcome in CTs performed <24 hours or \geq 24 hours after ROSC for the two raters. Figure adapted from Paper I.

Table 6. Prognostic performance and percentage agreement for the various GWR models

CT method	Cut-off	<24 h post arrest (N = 68)			≥24 h post arrest (N = 38)		
		Percent agreement	Spec.	Sens.	Percent agreement	Spec.	Sens.
Eye-balling	HIE	84	89-100	15-20	74	100	43-78
SEBES	4 points	84	93-100	10-10	74	100	30-53
GWR:							
16 ROIs AV	1.20	91*	96-100	20-33	92	88-100	63-70
	1.15	91*	100	10-15	87	100	50-53
	1.10	96*	100	5-8	90	100	40
8 ROIs CE	1.20	77	79-89	23-35	76	62-88	50-60
	1.15	93	100	8-15	84	88-100	43-47
	1.10	97	100	5	74	100	13-40
8 ROIs BG	1.10	82*	82-100	23-36	97	100	70-73
	1.15	93*	100	15-18	90	100	63
	1.10	93*	100	8-10	79	100	50-63
4 ROI SI	1.20	78*	89-100	28-33	92	100	63-67
	1.15	91*	96-100	15-18	82	100	57-60
	1.10	93*	100	8-10	74	100	37
8 ROIs RB	1.20	87	93-100	18-30	84	88-100	57-60
	1.15	97	100	8-13	97	100	40
	1.10	100	100	3	79	100	37-50

Excerpt from the summary table (Paper I) presenting the prognostic performance of various CT assessment methods for predicting poor outcome (mRS 4-6) at six months, alongside the percentage agreement between the two raters.

* One additional CT examination was excluded from some analyses by one of the raters due to noted artefacts.

AV; average, BG; basal ganglia; CBC; cerebellar cortex, CBW; cerebellar white matter, CC; genu corpus callosum, CE; cerebrum CN; head of the caudate nucleus, GWR; grey- white matter ratio, MC1; medial cortex at the level of centrum semiovale, MC2; medial cortex at the high convexity level, PIC; posterior limb of the internal capsule, PU; putamen, RB; robust, SI; simple, TH; thalamus, WM1; white matter at the level of the centrum semiovale, WM2; white matter at the high convexity level.

*The 8 ROI RB GWR model was an exploratory post-hoc model including the four ROIs with the narrowest limits of agreement from the Bland-Altman analysis.

Interrater agreement

The percentage agreement for the unstandardised visual interpretation and the SEBES ranged from 74% to 84%. All GWR models demonstrated interrater agreement ≥74%.

Bland-Altman plots for some of the GWR models are presented in Figure 27. These GWR models showed varying ranges between upper and lower limits of agreement and several of the GWR models exhibited small but statistically significant bias.

The 8 ROIs CE model displayed the widest limits of agreement between the two examiners, whereas the 8 ROIs BG and 16 ROIs AV models demonstrated the narrowest ranges.

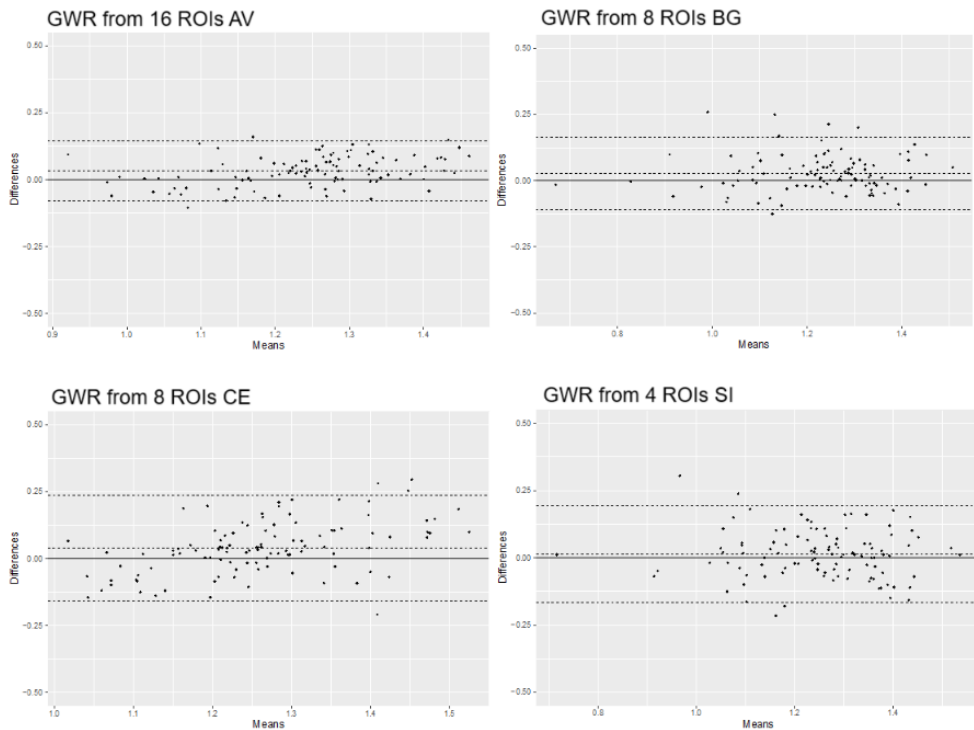


Figure 27. Bland-Altman plots comparing the GWR of each patient calculated from manually placed approximately 0.1 cm² ROIs by rater 1 with those placed by rater 2 for some of the tested GWR models in Paper I. *Figure adapted from Paper I.*

Paper III-IV

Participants

Thirteen sites across four countries participated in the TTM2 CT-sub-study. Among their patients, 387 (61%) provided informed consent and underwent CT ≤ 7 days post cardiac arrest. Forty-six CTs were excluded due to unfulfilled technical requirements, significant artefacts, or evidence of current intracranial ischaemia or haemorrhage. Of the 341 approved CTs, 140 were eligible for the prospective cohort (defined as unconscious patients with a CT > 48 hours ≤ 7 days post-cardiac arrest). All 341 approved CTs were included in the post-hoc analysis (CTs ≤ 7 days after

cardiac arrest). The flowchart of patient selection and exclusion is presented in Figure 28.

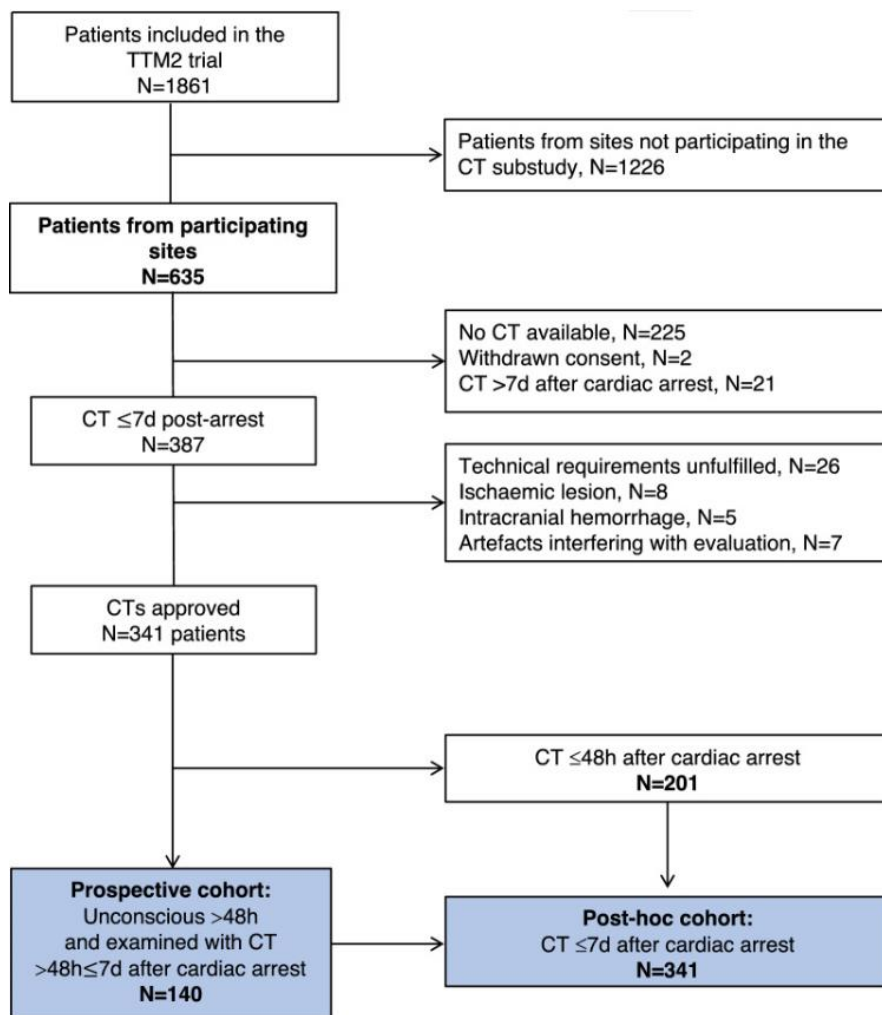


Figure 28.

Flowchart of patient selection and exclusion.

CT; computed tomography, N; number of patients, TTM; Targeted Temperature Management.

Figure adopted from Paper III.

The median age of the prospective cohort was 68 years (IQR 59-76), and 106 (76%) were male. The median time from cardiac arrest to CT was 84 hours (IQR 66-109). Compared to patients who underwent CT ≤ 48 hours after cardiac arrest, and those who were excluded for other reasons, the prospective cohort had a higher proportion

of poor outcome, with 105 (75%) exhibiting poor functional outcome (mRS 4-6 at six months follow-up).

Paper III

Prognostic performance

The standardised qualitative assessment of “definite signs of severe HIE” predicted poor outcome with 100% specificity across all raters, while sensitivity ranged from 11% to 57% (Table 7).

Median GWR at both at cut-offs (<1.10 and <1.15) were significantly lower in patients with poor outcomes compared to those with good outcomes ($p < 0.0001$). The overall predictive performance for poor functional outcome, as measured by the AUROC, ranged from 0.78 to 0.86 for manual GWR4 and from 0.83 to 0.89 for manual GWR8 across the seven raters (Figure 29).

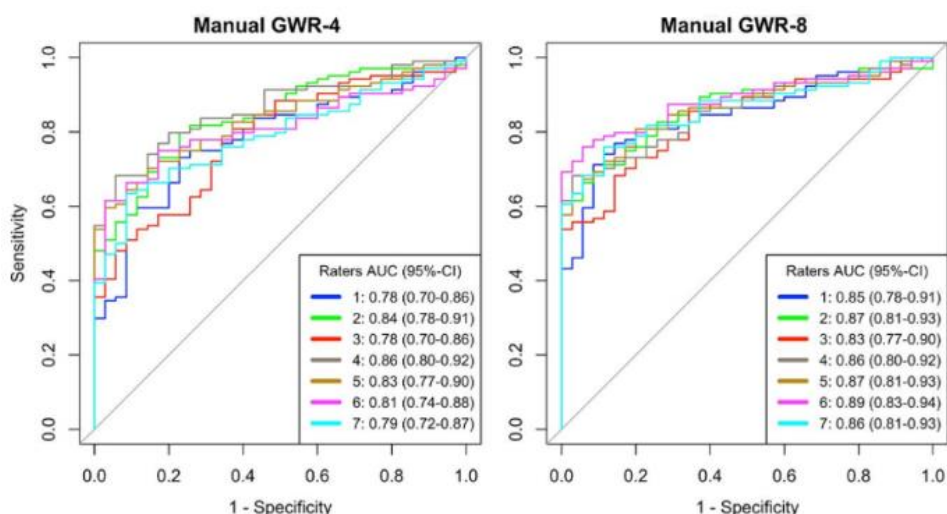


Figure 29.

ROC curves and AUROC with 95% confidence intervals for GWR-4 and GWR-8 for predicting poor functional outcome in CTs performed >48 hours <7 days after ROSC for the seven raters.

Figure adopted from Paper III.

Table 7. Prognostic performance for the various GWR models

Method Rater	Specificity (95% CI)	Sensitivity (95% CI)	TP	TN	FP	FN
Qualitative						
1	100 (90-100)	11 (7-19)	12	35	0	93
2	100 (90-100)	37 (29-47)	39	35	0	66
3	100 (90-100)	36 (28-46)	38	35	0	67
4	100 (90-100)	61 (51-70)	64	35	0	41
5	100 (90-100)	35 (27-45)	37	35	0	68
6	100 (90-100)	57 (48-66)	60	35	0	45
7	100 (90-100)	40 (31-50)	42	35	0	63
GWR-8 cut-off <1.10						
1	100 (90-100)	31 (23-41)	33	35	0	72
2	100 (90-100)	34 (26-44)	36	35	0	69
3	100 (90-100)	38 (29-48)	40	35	0	65
4	100 (90-100)	46 (37-55)	48	35	0	57
5	100 (90-100)	47 (37-56)	49	35	0	56
6	100 (90-100)	39 (30-49)	41	35	0	64
7	100 (90-100)	46 (37-55)	48	35	0	46
GWR-4 cut-off <1.10						
1	100 (90-100)	30 (22-39)	31	35	0	74
2	100 (90-100)	18 (12-27)	19	35	0	86
3	100 (90-100)	22 (15-31)	23	35	0	82
4	100 (90-100)	27 (19-36)	28	35	0	77
5	100 (90-100)	31 (23-41)	33	35	0	72
6	100 (90-100)	28 (20-37)	29	35	0	76
7	100 (90-100)	37 (29-47)	39	35	0	66
GWR-8 cut-off <1.15						
1	94 (81-98)	48 (38-57)	50	33	2	55
2	100 (90-100)	44 (35-53)	46	35	0	59
3	100 (90-100)	47 (37-56)	49	35	0	56
4	100 (90-100)	53 (44-63)	56	35	0	49
5	100 (90-100)	52 (43-62)	55	35	0	50
6	100 (90-100)	46 (37-55)	48	35	0	57
7	100 (90-100)	56 (47-65)	59	35	0	46
GWR-4 cut-off <1.15						
1	91 (78-97)	36 (28-46)	38	32	3	67
2	100 (90-100)	30 (22-39)	31	35	0	74
3	100 (90-100)	29 (21-38)	30	35	0	75
4	100 (90-100)	45 (36-54)	47	35	0	58
5	100 (90-100)	43 (34-52)	45	35	0	60
6	100 (90-100)	38 (29-48)	40	35	0	65
7	94 (81-98)	47 (37-56)	49	33	2	56
Automated GWR cut-off <1.10						
	100 (90-100)	41 (32-51)	43	35	0	62

At cut-off <1.10, both manual GWR methods across all raters and the automated method achieved 100% specificity. Sensitivity ranged from 31% to 47% for the GWR-8 method and from 18% to 37% for the GWR-4 method among the seven raters.

At cut-off <1.15, the GWR-8 method resulted in two false-positive predictions by one rater, yielding specificity ranging from 94% to 100% and sensitivity from 44% to 56% across raters. For the GWR-4 method, at cut-off <1.15, specificity ranged from 91% to 100%, and sensitivity from 29% to 47% across the seven raters. One rater had three- and another rater had two false-positive predictions.

Concordance with other routine prognostic methods

The concordance between “definite signs of severe HIE” assessed by at least four raters and other prognostic markers ranged from 37% for bilaterally absent pupillary reflexes to 96% for NSE ≥ 60 $\mu\text{g/L}$. Similarly, the concordance between at least four raters assessing GWR-8 <1.10 and other prognostic markers ranged from 32% for bilaterally absent pupillary reflexes to 97% for NSE ≥ 60 $\mu\text{g/L}$.

Grey-white matter ratio from automated measurements and comparisons

The median automated GWR was significantly lower in patients with poor outcome compared to those with good outcome ($p < 0.0001$). The overall predictive performance for poor functional outcome, measured by the AUROC was 0.84. The AUROC for the automated GWR did not differ significantly from the mean manual GWR-8 (0.87) or GWR-4 (0.84) (Figure 30).

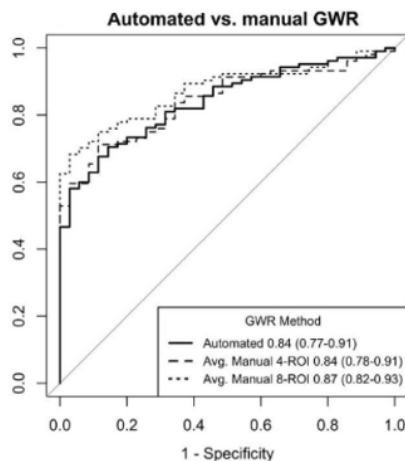


Figure 30.

ROC curves and AUROC with 95% confidence intervals for the automated GWR method and for mean of the seven raters' manual GWR-4 and GWR-8 methods for prediction of poor functional outcome in CTs performed ≥ 48 hours <7 days.

Figure adopted from Paper III.

Inter- and intra- rater agreement

The interrater agreement ranged from κ 0.57 for GWR-4 at both cut-offs to κ 0.83 for GWR-8 at the cut-off <1.15 (Table 8).

Table 8. Interrater agreement for the various CT assessment methods

Method	Fleiss' kappa (95% CI)	Strength of agreement*
Qualitative	0.6 (0.56-0.64)	Moderate
GWR-8		
cut-off <1.10	0.72 (0.69-0.76)	Good
cut-off <1.15	0.83 (0.79-0.86)	Very good
GWR-4		
cut-off <1.10	0.57 (0.53-0.6)	Moderate
cut-off <1.15	0.57 (0.53-0.61)	Moderate

* The interpretation of κ -values lacks universal consensus, this categorisation was applied in Paper III.

The intrarater agreement for the qualitative assessment ranged from κ 0.33 to 0.93 (Table 9). For the GWR-8 method, intrarater agreement ranged from κ 0.58 to 0.84 at cut-off <1.10, and from κ 0.62 to 1.00 at cut-off <1.15, across the seven raters. For GWR-4, the intrarater agreement ranged from approximately 0.30 to 0.75 at both cut-offs.

Table 9. Intrarater agreement for the various CT assessment methods

Rater	Qualitative assessment Cohen's kappa Strength of agreement*		GWR-8, cut-off Cohen's kappa Strength of agreement*			GWR-4, cut-off Cohen's kappa Strength of agreement*		
1	0.78	Good	<1.10	0.66	Good	<1.10	0.63	Good
			<1.15	0.67	Good	<1.15	0.36	Fair
2	0.76	Good	<1.10	0.58	Moderate	<1.10	0.26	Fair
			<1.15	0.76	Good	<1.15	0.35	Fair
3	0.91	Very good	<1.10	0.84	Very good	<1.10	0.27	Fair
			<1.15	1	Very good	<1.15	0.33	Fair
4	0.93	Very good	<1.10	0.76	Good	<1.10	0.36	Fair
			<1.15	1	Very good	<1.15	0.50	Moderate
5	0.75	Good	<1.10	0.84	Very good	<1.10	0.75	Good
			<1.15	0.77	Good	<1.15	0.74	Good
6	0.85	Very good	<1.10	0.74	Good	<1.10	0.70	Good
			<1.15	1	Very good	<1.15	0.40	Fair
7	0.33	Fair	<1.10	0.77	Good	<1.10	0.41	Good
			<1.15	0.62	Good	<1.15	0.32	Fair

* The interpretation of κ -values lacks universal consensus, this categorisation was applied in Paper III. Table adapted from Paper III where full tables including confidence intervals can be found in the supplementary data.

Post-hoc analyses of automated GWR

Except for CTs performed within 2 hours post-cardiac arrest, the median automated GWR was significantly lower in poor functional outcome patients compared to good functional outcome patients across all other time intervals (Figure 31).

A single false-positive prediction occurred in the >2 to 6-hour interval, resulting in a specificity of 98% for poor outcome prediction. All other time categories demonstrated 100% specificity. The highest sensitivity was observed in CTs performed between >48 and 96 hours after cardiac arrest.

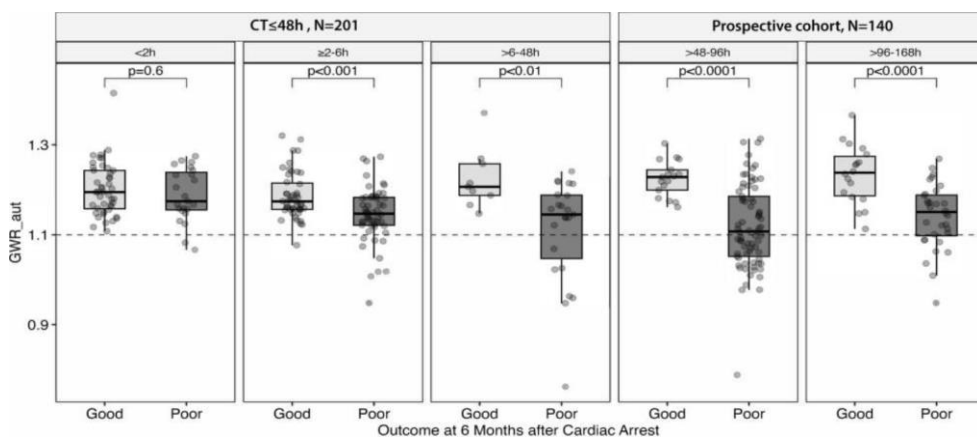


Figure 31.

Box-scatter plots for automated GWR for prediction of poor functional outcome (mRS 4-6 at 6 months) grouped by timing of CT in hours after cardiac arrest. Except for CTs performed within 2 hours post-cardiac arrest, the median automated GWR was significantly lower in poor functional outcome patients compared to good functional outcome patients across all other time intervals.

Figure adopted from Paper III.

Paper IV

Prognostic performance

The mean prognostic performances for predicting poor functional outcome for the different signs indicating HIE on CT are presented in Table 10.

- Loss of grey-white distinction

Bilateral loss of grey-white matter distinction demonstrated 100% specificity for predicting poor functional outcome across all raters at each of the three assessed anatomical levels. The mean sensitivity among the

seven raters ranged from 45% at the basal ganglia level to 50% at the high convexity level.

- **Sulcal effacement**

The mean specificity for predicting poor outcome for bilateral sulcal effacement ranged from 93% at the corona radiata level to 99% at both the basal ganglia- and at the high convexity level. Mean sensitivity ranged from 29% at the basal cisterns to 49% at the corona radiata level. Among the 35 patients with good functional outcomes at six months, 11 (18 individual ratings) were assessed as exhibiting signs of bilateral sulcal effacement at one- or several anatomical levels on CTs. The median age among these misclassified patients was 54 years (IQR 41-57), compared to a median age of 68 years (IQR 59-76) in the overall cohort.

- **Other signs indicating HIE**

The p-SAH Sign and *the Reversal Sign* both demonstrated 100% specificity for poor outcome prediction across all raters. *The White Cerebellum Sign* yielded two false-positive predictions, resulting in a mean specificity of 99%. The mean sensitivity for these three signs ranged from 8% to 11%.

Table 10. Prognostic performance for the various radiological signs

Sign	Specificity mean (min-max)	Sensitivity mean (min-max)
Loss of grey-white distinction at the level of:		
Basal ganglia	100 (100-100)	45 (14-69)
Corona radiata	100 (100-100)	46 (33-59)
High convexity	100 (100-100)	50 (38-60)
Sulcal effacement at the level of:		
Basal cisterns	98 (89-100)	29 (8-53)
Basal ganglia	99 (94-100)	38 (21-58)
Corona radiata*	93 (80-100)	49 (23-64)
High convexity*	99 (97-100)	41 (25-54)
Signs of:		
p-SAH	100 (100-100)	8 (3-13)
White cerebellum	99 (94-100)	11 (1-31)
Reversal	100 (100-100)	9 (3-13)

Prognostic performance for prediction of poor functional outcome (mRS 4–6) at six months post-arrest. Specificity and sensitivity for all items in the qualitative CT-assessment checklist reported as means of the raters with full range (**minimum and maximum**) not (95% CI).

* The sulcal effacement at corona radiata- and high convexity level was rated retrospectively by four of the seven raters.

p-SAH; the Pseudo Subarachnoid Haemorrhage Sign.

Interrater agreement

The interrater agreement for loss of grey-white distinction ranged from κ 0.57 at the basal ganglia level to κ 0.74 at the high convexity level (Table 11). For sulcal effacement, the level of interrater agreement ranged from κ 0.41 at the basal cisterns to κ 0.65 at the high convexity level. The interrater agreement for the *White Cerebellum Sign* was κ 0.36, for the *p-SAH Sign* κ 0.49, and for the *Reversal Sign* κ 0.52.

Table 11. Interrater agreement for the various radiological signs

Sign	Fleiss' kappa (95% CI)	Strength of agreement [#]
Loss of grey-white distinction at the level of:		
Basal ganglia	0.57 (0.53-0.6)	Weak
Corona radiata	0.67 (0.64-0.71)	Moderate
High convexity	0.74 (0.7-0.78)	Moderate
Sulcal effacement at the level of:		
Basal cisterns	0.41 (0.38-0.45)	Weak
Basal ganglia	0.61 (0.57-0.64)	Moderate
Corona radiata*	0.57 (0.5-0.63)	Weak
High convexity*	0.65 (0.59-0.72)	Moderate
Signs of:		
p-SAH	0.49 (0.45-0.53)	Weak
White cerebellum	0.36 (0.33-0.4)	Minimal
Reversal	0.52 (0.49-0.56)	Weak

Fleiss' kappa (95% CI) for the seven raters for the qualitative CT assessment signs.

* The sulcal effacement at corona radiata- and high convexity level was rated retrospectively by four of the seven raters.

[#] The interpretation of κ -values lacks universal consensus, this categorisation was applied in Paper IV.

Concordance between an individual radiological sign and “definite signs of HIE”

The concordance between each rater's confirmation of an individual radiological sign and their final evaluation of *definite signs of severe HIE* ranged from 92% to 100% for *loss of grey-white distinction* across the seven raters and the various anatomical levels. For *sulcal effacement*, concordance ranged from 39% to 100%. The concordance for the *p-SAH Sign* ranged between 5% to 50%, for the *White Cerebellum Sign* from 2% to 45%, and for the *Reversal Sign* from 8% to 31%.

Paper V

Participants

A total of 228 consecutive (but filtered to match a cardiac arrest population) non-contrast CTs were screened to reach the predetermined inclusion target of 155 CTs. The flowchart outlining patient selection and exclusion is presented in Figure 32. The mean and median age of participants was 75 years (IQR 74-75), and 91 (59%) were male.

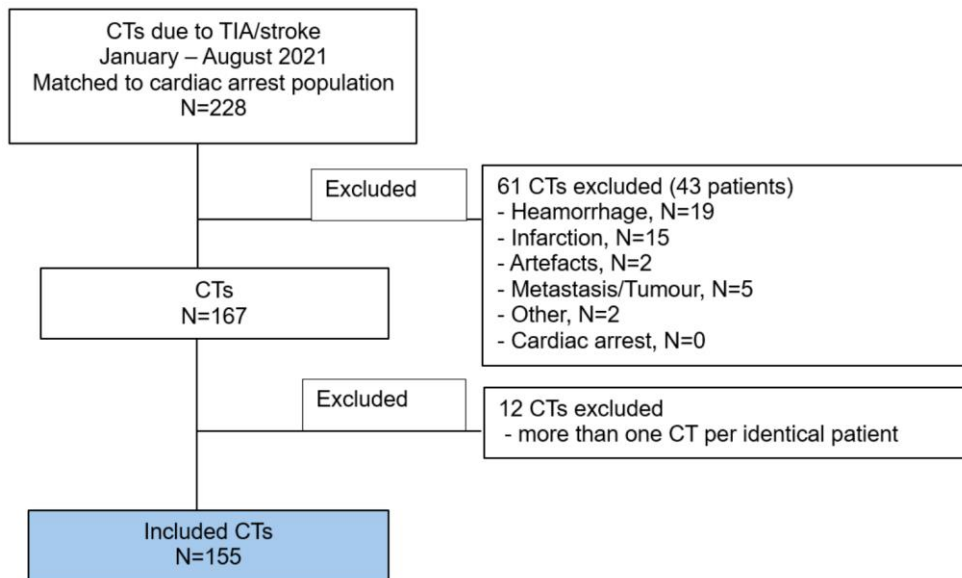


Figure 32.

Flowchart of patient selection and exclusion.

CT; computed tomography, N; number of patients, TIA; Transient Ischaemic Attack.

Figure adopted from Paper V.

GWR

The distribution of the GWR from 0.1 cm² and 0.2 cm² ROIs for each patient, as assessed by all three raters, is presented in Figure 33A. For the 0.1 cm² ROIs, the median GWR (min-max) for the three raters were: 1.30 HU (1.14-1.56), 1.31 HU (1.16-1.54), and 1.32 HU (1.18-1.49), respectively. For the 0.2 cm² ROIs, the corresponding median GWR (min-max) for the three raters were: 1.29 (1.15-1.48), 1.32 (1.20-1.52), and 1.27 (1.14-1.48). None of the participants were assigned a GWR below 1.10.

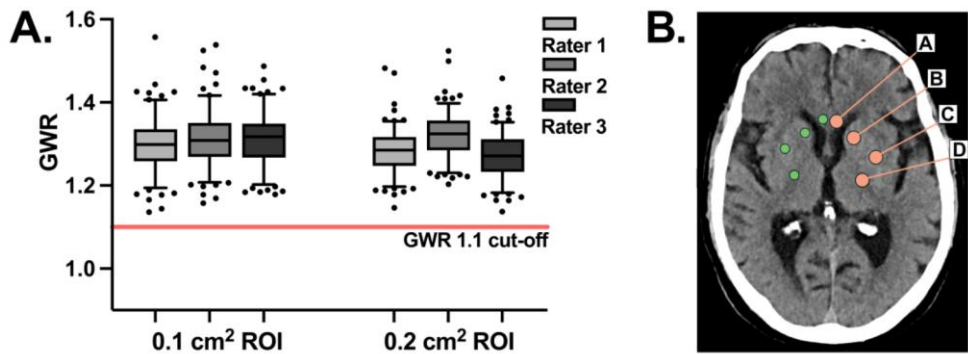


Figure 33A-B.

A) Box- and whiskers plots of GWR from manually placed 0.1 cm² and 0.2 cm² ROIs at the basal ganglia level for the included N=155 patients presented separately for the three raters. Whiskers between 5-95% CI. B) Circular ROIs of 0.1 cm² (size presented by green ROIs in right hemisphere) and 0.2 cm² (size presented by red ROIs in left hemisphere) manually placed in the genu corpus callosum [A], in the head of the caudate nucleus [B], in the putamen [C], and in the posterior limb of the internal capsule [D]. The GWR was calculated by the mean attenuation in the head of the caudate nucleus [B] and the putamen [C] bilaterally divided by the mean attenuation in the genu corpus callosum [A] and the posterior limb of the internal capsule [D] bilaterally.

Figure adopted from Paper V.

Interrater agreement

Several pairwise comparisons between raters revealed a statistically significant but small bias, with mean GWR differences ranging from 0 to 0.05 for both the 0.1 cm² and the 0.2 cm² ROIs GWR (Figure 34A-F). The limits of agreement between raters were approximately ± 0.1 around the mean difference. GWR measurements using the 0.2 cm² ROIs demonstrated narrower limits of agreement compared to those using 0.1 cm² ROIs.

Variability between GWR calculated from 0.1 cm² compared with 0.2 cm²

All raters demonstrated statistically significant but small bias, with mean GWR differences ranging from 0 to 0.04, when comparing their measurements from 0.1 cm² ROIs GWR to those from 0.2 cm² ROIs GWR (Figure 35A-C). The limits of agreement were approximately ± 0.1 around the mean difference.

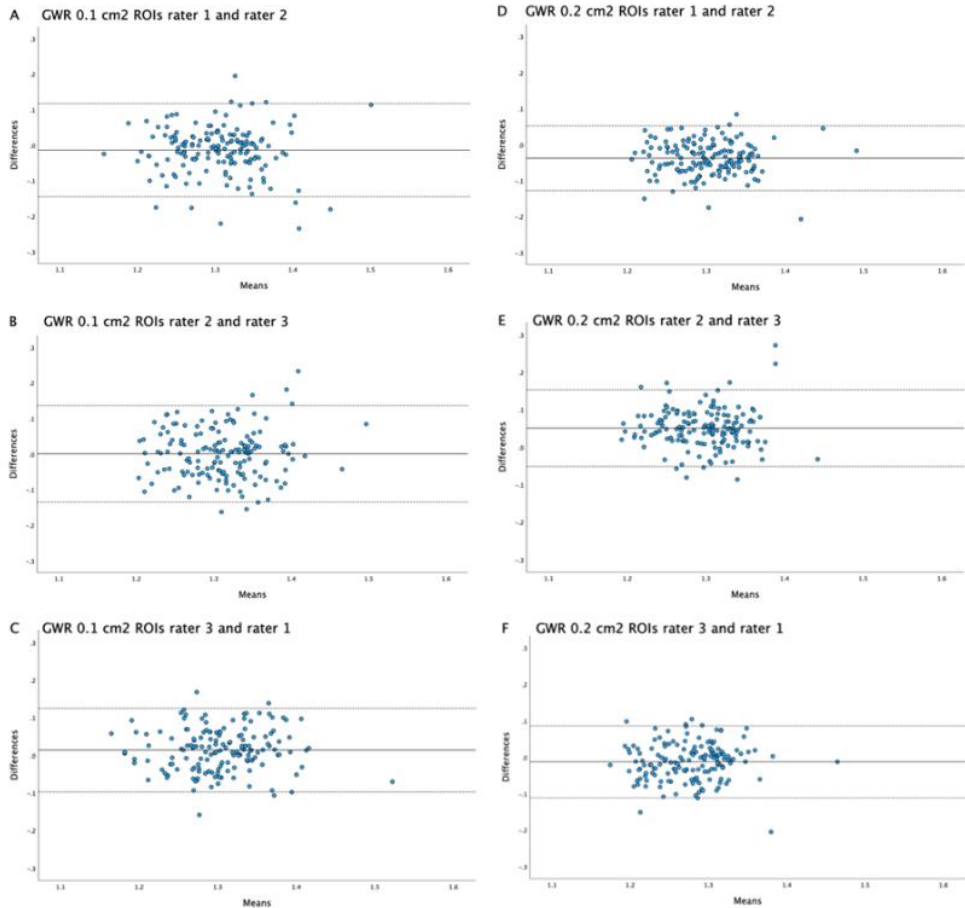


Figure 34A-F.

Bland-Altman plots comparing GWR of each patient (N=155) calculated from manually placed 0.1 cm² ROIs; **A**) by rater 1 with those placed by rater 2, **B**) by rater 2 with rater 3, **C**) by rater 3 with rater 1, and comparing GWR of each patient (N=155) calculated from 0.2 cm² manually placed ROIs; **D**) by rater 1 with those placed by rater 2, **E**) by rater 2 with rater 3, and **F**) by rater 3 with rater 1. Each plot indicates the mean of each GWR (x-axis) with mean differences (y-axis).

Figure adopted from Paper V.

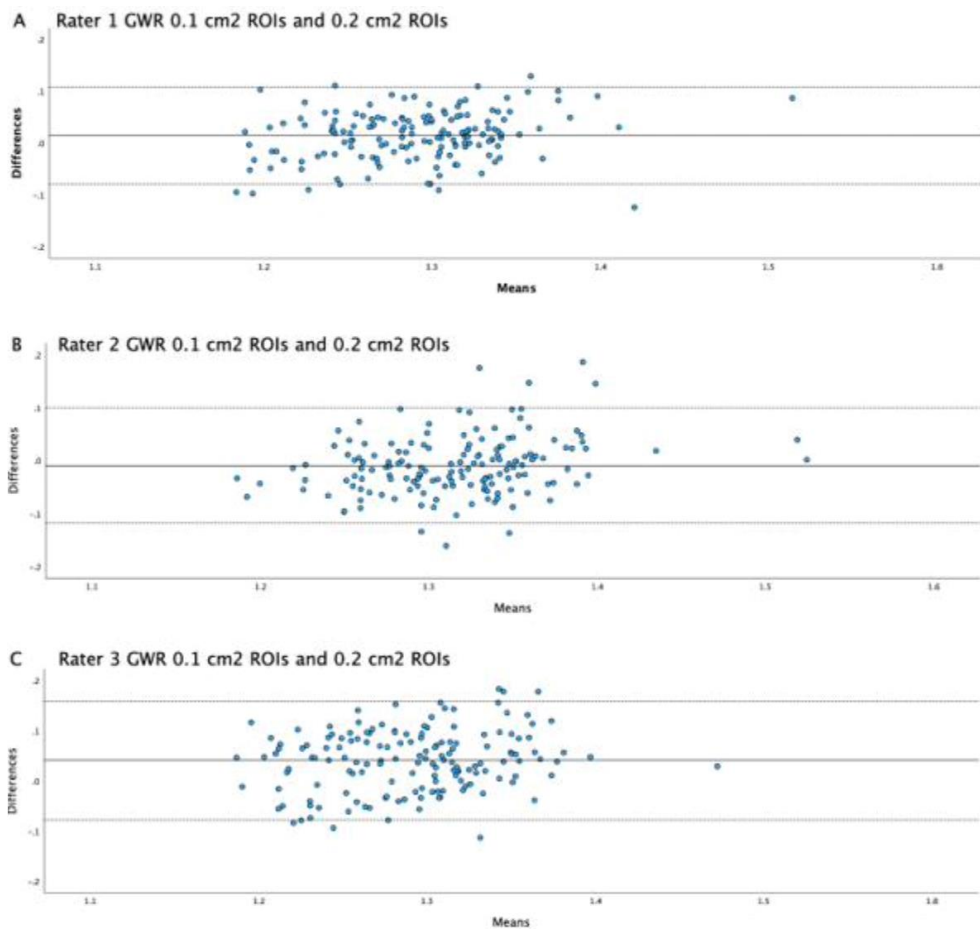


Figure 35A-C.

Bland-Altman plots comparing the GWR of each patient (N=155) calculated from manually placed 0.1 cm² ROIs with manually placed 0.2 cm² ROIs by; A) rater 1, B) rater 2, and C) rater 3. Each plot indicates the mean of each GWR (x-axis) with mean differences (y-axis).

Figure adopted from Paper V.

Discussion

Based on data from two prospective multicentre studies, among other sources, the findings presented in this thesis demonstrate that CT serves as a highly specific prognostic tool for predicting poor functional outcomes following cardiac arrest, irrespective of the assessment method employed. However, sensitivity varies depending on the timing of imaging, the assessment method, and the rater, with a moderate median sensitivity.

Timing of CT

To maximise the prognostic performance of CT, it is crucial to determine the optimal timing for image acquisition following ROSC. Current ERC/ESCIM prognostication guidelines do not specify a fixed interval for performing CT, but recommend that formal multimodal prognostication should not be conducted earlier than 72 hours after ROSC.⁴³ The American Neurocritical Care Society advises performing CT for prognostic assessment no earlier than 48 hours after ROSC.⁹⁵

In the pilot study (Paper I), patients were categorised based on CT timing: *early* (<24 hours) or *late* (\geq 24 hours) after cardiac arrest. Most established and novel qualitative and quantitative methods for diagnosing poor outcomes demonstrated high specificity both on *early* and *late* CTs. Sensitivity, however, increased from low on *early* CTs to moderate or high on *late* CTs.

In the post-hoc analysis in Paper III, the prognostic performance of GWR with a cut-off <1.10, assessed automatically, was evaluated across different time intervals following cardiac arrest. Except for one false-positive prediction in the >2 to 6-hour interval post-cardiac arrest, all other time intervals demonstrated 100% specificity. The highest sensitivity, 48%, was observed between 48 and 96 hours post-cardiac arrest.

Although CTs performed shortly after hospital admission are justified and valuable for excluding or confirming a neurological cause of CA and/or unconsciousness,¹⁰³ evidence from this thesis as well as from other studies,^{175, 224} indicate that CTs conducted within a few hours post-cardiac arrest have limited prognostic value. Our findings of increased sensitivity for predicting poor outcome within the initial days

are consistent with previous studies^{132, 147-149, 175} and align with the temporal pathophysiological progression of HIE.^{25, 30-33}

Assessment methods

Qualitative CT assessment methods

Signs indicating hypoxic-ischaemic encephalopathy (HIE) and poor prognosis on CT are most often assessed visually without standardisation and reported qualitatively in clinical practice.²²⁵ This unstandardised visual interpretation, *eye-balling*, was evaluated in the pilot study, (Paper I). *Eye-balling* resulted in three false-positive predictions on *early* CTs, with specificities of 89% and 100% for the two raters. Sensitivity for *eye-balling* on *early* CTs was low for both raters. For *late* CTs, specificity was 100% for both raters, and sensitivity ranged from 43% to 78%. Inter-rater agreement was 84% for *early* and 74% for *late* CTs. The standardised qualitative assessment, *SEBES*, did not improve the percentage agreement and showed lower sensitivity than *eye-balling* across both time groups and raters. However, *SEBES* resulted in one fewer false positive, two in total, both on *early* CTs and from the same rater, indicating a potentially safer assessment when standardised.

In Paper III, the application of a standardised qualitative assessment checklist, incorporating a more precise definition of *definite severe HIE* than those proposed in current guidelines, yielded a specificity of 100% for predicting poor outcomes across all seven raters (980 ratings) on CTs performed between $> 48 \text{ hours} \leq 7 \text{ days}$ post-cardiac arrest. However, sensitivity exhibited considerable variability, ranging from 11% to 61%.

The predictive performance of our qualitative assessments, with high median specificity but only moderate median sensitivity, is consistent with previous studies.^{76, 115} Albeit infrequently, false-positive predictions were observed in *early* CTs (Paper I), aligning with prior findings.^{170, 226} This highlights the importance of a multimodal approach to prognostication in unconscious cardiac arrest patients and the inherent risks of relying solely on qualitative CT assessment for evaluating HIE, the most common current practice.

The reliability of qualitative CT assessment is limited by the absence of standardised radiological criteria, resulting in inadequate interrater agreement.^{115, 158, 160} Even with the implementation of standardised criteria in Paper III, inter-rater reliability was limited (κ 0.6), indicating a need for further improvements to standardise the qualitative CT evaluation after cardiac arrest.

To investigate this, we analysed the prognostic performance and interrater agreement of individual items within the qualitative CT checklist in Paper IV, including *the p-SAH Sign*, *the White Cerebellum Sign*, *the Reversal Sign*, *loss of grey-white distinction*, and *sulcal effacement*. Among these, bilateral loss of grey-white matter distinction demonstrated the highest prognostic value, achieving 100% specificity across all raters and anatomical levels, with mean sensitivity ranging from 45% at the basal ganglia level to 50% at the high convexity level. This sign also showed the strongest concordance with raters' conclusions of *definite severe HIE* and the highest interrater agreement (κ 0.74) (at the high convexity level). These findings highlight that reduced grey-white matter distinction should constitute an essential part of the radiological evaluation for signs indicating HIE on CTs following cardiac arrest, as supported by previous studies.^{132, 149} In contrast to several quantitative CT studies, which preferably assess radiodensities at the basal ganglia level,^{36, 146, 149, 176-178, 182} our results suggest that including the high convexity level in qualitative assessments may provide additional prognostic value.

When evaluated in isolation, the radiological sign of sulcal effacement resulted in several false-positive predictions, predominantly at the corona radiata level, with mean specificity ranging from 93% to 99%. This implies that sulcal effacement may be more challenging to assess than loss of grey-white matter distinction, particularly in younger patients with physiologically higher brain volume. Consistent findings have been reported in previous studies.²²⁷ Furthermore, the prognostic mean sensitivity of sulcal effacement exhibited considerable variability, ranging from 29% to 49% across anatomical levels.

While cytotoxic and ionic oedema typically develop within hours after cardiac arrest, vasogenic oedema evolves over the first few days.²²⁸ Paper IV included CTs obtained between >48 hours and ≤7 days post-cardiac arrest, a timeframe theoretically sufficient for the development of both cytotoxic and vasogenic oedema. Nevertheless, the slightly lower sensitivity of sulcal effacement compared to loss of grey-white matter distinction may partly reflect temporal differences in the pathophysiological evolution of these signs. Interrater agreement for sulcal effacement was also lower than for loss of grey-white matter distinction.

Consistent with previous studies, *the White Cerebellum Sign*, *the p-SAH sign*, and *the Reversal sign* demonstrated high specificity but limited sensitivity.^{36, 152, 153} Relative to the other assessed radiological signs of HIE, these signs provided comparatively limited additional prognostic value.

Quantitative CT assessment methods

In the pilot study (Paper I), several GWR models at varying cut-offs were evaluated for the assessment of HIE on CTs following cardiac arrest. At a cut-off <1.10, all GWR models demonstrated 100% specificity across both raters and on both *early*

and *late* CTs. As noted previously, sensitivity for predicting poor outcome increased substantially when GWR was obtained on *late* CTs (≥ 24 hours to 7 days post-cardiac arrest). On these *late* CTs, the highest sensitivity at the <1.10 cut-off was observed with the GWR model based on eight ROIs placed at the basal ganglia level (8 GWR BG), yielding sensitivity ranging from 50% to 63%. In addition to its superior prognostic performance, the 8 GWR BG model also demonstrated one of the highest levels of interrater percentage agreement (79%). This aligns with findings from previous studies and is likely attributed, at least in part, to the particular susceptibility of subcortical nuclei to HIE, as well as the relatively low risk of partial volume effects in these often well-defined structures.^{36, 146, 149, 176-178, 182}

Even at higher cut-offs (1.15 and 1.20), several GWR models maintained 100% specificity, with some achieving sensitivities up to approximately 70% (GWR 8 BG). In the literature, GWR cut-off values proposed to predict poor functional outcome with 100% specificity post-cardiac arrest have ranged from approximately 1.08 to 1.23.³² In Paper I we observed that the false-positive rate with GWR at cut-off <1.15 could be reduced when the quantitative assessment was supplemented with *eye-balling*. Nevertheless, in planned Paper III, we chose to validate a conservative cut-off to minimise the risk of false-positive predictions.

In Paper III, seven raters from four countries independently placed ROIs at the basal ganglia level on 140 CTs obtained >48 hours ≤ 7 days post-cardiac arrest from thirteen sites across four countries. Both the GWR-8 and GWR-4 models demonstrated 100% specificity for poor outcome prediction at cut-off <1.10 across all raters. The GWR-8 demonstrated higher median sensitivity (39%) and stronger interrater (κ 0.72) and intrarater agreement (κ 0.58 – 0.84) than the GWR-4 among the seven raters. Both the caudate nuclei and the putamina are particularly vulnerable to hypoxic-ischemic encephalopathy (HIE),^{38, 39} and our results suggest that including both structures in manual grey matter attenuation measurements improves the prognostic performance of the GWR compared to assessing the putamina alone. However, our objective alternative, the automated GWR based solely on putamina grey matter attenuation measurements, achieved 100% specificity and 41% sensitivity at cut-off <1.10 .

In Paper III, using a cut-off <1.15 , sensitivity increased and showed more consistent results across the seven raters (44% to 56%), contrasting the qualitative assessment. However, one rater produced two false-positive predictions at this cut-off. Notably, none of these patients were identified with HIE signs by any rater using qualitative criteria, underlining the potential value of combining quantitative and qualitative approaches.

There is a potential risk that quantitative measurements based on small ROIs may not accurately represent the entire structure, as localised factors such as calcifications or blood vessels can bias mean attenuation and GWR values.

Automated, atlas-based measurements encompassing the entire structure may mitigate this risk and provide more reliable assessments, however, these methods still require stringent quality control to exclude artefacts and acute pathological changes.

Another hindrance to relying solely on quantitative assessment and establishing a universally reliable GWR cut-off for poor outcome prediction is the variability in attenuation values (HU-values) across different scanners and acquisition protocols, which GWR has not been shown to fully compensate for.^{142, 229} The “marked reduction” in GWR for poor outcome prediction referenced in current guidelines lacks specification regarding ROIs, cut-off values, scanner types, acquisition protocols, or timing of examination post-cardiac arrest.⁴³ In Paper III, to reflect real-world clinical conditions, we accepted all scanners and acquisition protocols, with the only prerequisites being tube voltage of 120 kV and axial slice thickness of 4-5 mm. Under these conditions, in CT scans performed between 48 hours and 7 days post-cardiac arrest, a GWR below 1.10 serves as a strong prognostic marker for HIE. However, as shown in Paper V, although no participant had a GWR below 1.10, the limits of agreement of ± 0.1 GWR, observed both between different raters and within a single rater using varying ROI sizes, underscore the challenges and risks of relying on fixed GWR cut-offs for prognostication.

Raters

Across all prognostic studies in this thesis, specificity for predicting poor outcomes was consistently high among all raters. However, sensitivity varied considerably, especially in the qualitative assessment of HIE signs. Experienced neuroradiologists achieved moderate to high sensitivity, while less experienced raters exhibited substantially lower sensitivity during unstandardised visual evaluations.

Current guidelines recommend that signs of HIE identified through conventional visual analysis should be confirmed by an experienced neuroradiologist.⁴³ Had only experienced neuroradiologists assessed the CTs included in Papers I-IV, our findings would imply that qualitative assessment of CTs obtained ≥ 24 hours (Paper I) and >48 hours ≤ 7 days (Paper III) post-cardiac arrest demonstrates high prognostic performance in predicting poor outcome in unconscious patients. Notably, two of the neuroradiologists in Paper III exhibited substantially lower sensitivity in the quantitative assessment compared to their qualitative evaluations (approximately 40% versus 60%).

The highest concordance between these two neuroradiologists' conclusions of *definite severe HIE* and isolated radiological signs was observed for loss of grey-white matter distinction, indicating that this sign was the most critical indicator in

their assessments. This pattern of concordance was also evident among the less experienced raters.

An alternative explanation for the lower sensitivity in some less experienced raters compared to the most experienced neuroradiologists is that the former strictly adhered to the defined criteria, whereas the experienced neuroradiologists relied more on their clinical judgement. This would indicate that the proposed criteria for *definite severe HIE* may have been too rigid.

The findings in this thesis support current guideline recommendations that assessment should be performed by neuroradiologists to ensure optimal accuracy. However, despite the widespread use of external radiological review, only a limited number of CTs are assessed by neuroradiologists in clinical practice. Given the involvement of less experienced and general radiologists, the results in this thesis suggest that combining quantitative and qualitative assessments can enhance the prognostic performance of CT. Ultimately, it may be that providing raters with automated or machine-learned GWR measurements could be most beneficial, as this approach would also assist in training less experienced raters to recognise subtle visual changes indicative of HIE.

Strengths

Strengths of Papers I-IV include their multicentre designs, nested within large international cardiac arrest trials employing standardised criteria for neuroprognostication, WLST, and structured six-month functional outcome assessments. Paper III was additionally a pre-planned study.

In both Papers III and IV, CTs were obtained at a clinically relevant time point for neuroprognostication. Across all Papers included in this thesis, radiological assessments were performed by at least two independent and blinded raters. In Papers III-V, the raters represented different countries, contributing to the external validity.

Papers III and V were conducted according to pre-specified protocols that included sample size calculations. For Paper III, the protocol also incorporated standard operating procedures for both qualitative and quantitative CT assessments.

Papers I and III-IV included CTs from all scanners and acquisition protocols, except for requiring a tube voltage of 120 kV and axial reconstructions of 4-5 mm, thereby supporting the external validity.

Limitations

Several limitations apply to the studies included in this thesis. Papers I and V were conducted retrospectively. In addition, Paper V was a single-centre study, and all measurements were performed using images from one single CT scanner with identical acquisition parameters, which limits the generalisability and external reliability of the findings. This study also lacked detailed demographic data, further restricting interpretability.

In Paper I, CT examination was not mandatory but instead performed upon clinical indication, introducing a considerable risk of selection bias. The small sample size limited statistical power and precluded further subgroup analyses, which would have been valuable given the dynamic changes in neuronal injury that can occur within the first 24 hours and the days that follow.

Papers III and IV were also constrained by moderate sample sizes, leading to wide 95% confidence intervals for specificity. Additionally, a notable proportion of patients underwent CT imaging prior to the pre-specified time-point, introducing a potential risk of selection bias in these studies as well.

To enable participation from raters in different countries, CT assessments in Papers III-V were conducted using a VPN-secured platform equipped with only basic windowing tools. Ratings were in most cases made on standard computer screens, which typically have lower luminance and resolution than clinical radiology workstations. This may have reduced diagnostic confidence and impacted both qualitative and quantitative assessments. Unlike clinical practice, raters were restricted to axial images only, and assessments of qualitative and quantitative features were conducted separately. Ratings were final, the rater had to complete the assessment of one patient before proceeding to the next and was not permitted to revisit previous CT examinations. Additionally, raters could neither consult with colleagues nor access prior examinations for comparison. These constraints may have adversely affected the prognostic performance for predicting poor outcomes post-cardiac arrest based on CT imaging.

Lastly, applicable to Papers I-IV, is the potential for self-fulfilling prophecy bias, as CT reports from local radiologists were available to treating clinicians involved in decisions regarding WLST. Strategies implemented to minimise this risk are discussed on page 69. In Paper III, we further addressed this concern by evaluating the concordance between either *definite severe HIE* or $\text{GWR-8} < 1.10$ in at least 4 raters, and the more objective predictor $\text{NSE} \geq 60 \mu\text{g/L}$. The resulting concordance rates were 96% and 97%, respectively. In Paper V, we demonstrated that in an elderly reference population, corresponding to the age group with the highest incidence of cardiac arrest, none had a $\text{GWR} < 1.10$ when assessed using the same quantitative method as in the cardiac arrest cohort. This finding provides additional support for the robustness and specificity of the applied GWR threshold.

Conclusions

CT is a highly specific tool for predicting poor functional outcomes after cardiac arrest and should be considered in patients who remain unconscious >48 hours post-arrest, as part of a multimodal neuroprognostication strategy.

Combining a structured qualitative assessment of definite severe HIE with a GWR <1.10, assessed manually or via an automated method at the basal ganglia level, enables prediction of poor functional outcome with high specificity and moderate sensitivity.

Improving interrater agreement will require further refinement of standardised qualitative assessment, with a focus on the robust predictive marker of loss of grey-white matter distinction.

Future perspectives

Several important questions remain to be addressed to further evaluate and optimise the predictive value of computed tomography in unconscious patients following cardiac arrest. Key areas for future research include:

The value of serial CTs

Many patients undergo CT shortly after hospital admission, and those who remain unconscious may receive additional scanning at clinically relevant time points for neuroprognostication. However, the prognostic value of serial CT assessments remains underexplored. The ability to compare imaging across time points may improve the prognostic performance and better reflect routine radiological practice. Future studies should also aim to more accurately replicate clinical conditions by considering aspects such as radiological workstations, workflow integration, and the handling of inconclusive ratings, to strengthen the external validity and clinical applicability of findings. Additionally, larger prospective trials of serial CT scans are needed to validate promising automated neuroprognostic markers, such as the regional brain net water uptake.

Timing of CT for neuroprognostication

This thesis demonstrated that CTs performed >48 hours after cardiac arrest can predict poor functional outcome with 100% specificity. The pilot study (Paper I), albeit underpowered, showed tendencies that prognostication with CT is safe from 24 hours after cardiac arrest. Many HIE pathophysiological processes occur before 48 hours, with the more reliable indicator, loss of grey-white matter distinction, typically emerging earlier than sulcal effacement. This suggests that a shorter time window, such as >24 hours post-arrest, may be sufficient to identify signs of HIE. Future studies should explore this possibility and define the earliest reliable time point for CT-based prognostication.

Refining the qualitative definition of HIE

Hypoxic ischaemic encephalopathy lacks standardised radiological criteria. A more precise qualitative definition of *HIE* on CT could be, “Extensive and bilateral loss or reduction of grey-white matter distinction in the basal ganglia and/or frontoparietal cortex.” Prospective validation of this definition is needed to improve interrater agreement.

Integration of qualitative and quantitative assessments

In this thesis, A GWR cut-off <1.10 was associated with no false positives, while a cut-off <1.15 introduced a small number of false positives. As quantitative GWR is intended to complement qualitative CT assessment, future research should evaluate their combined prognostic performance. This approach may allow for increased sensitivity with a slightly higher GWR cut-off, without compromising specificity.

Development of automated and machine-learned tools

Automated methods for calculating GWR should be further developed and validated. In the long term, these tools could provide a reliable and widely accessible adjunct for clinical evaluation of HIE on CT, especially in settings with limited neuroradiological expertise. They may also aid in training less experienced clinicians to recognise subtle imaging features associated with HIE. Additionally, machine-learned GWR estimation could efficiently generate normative reference data across different scanners, acquisitions protocols and age groups for future studies.

Integration of combinations of predictors for poor outcome

Given the recommendation for multimodal prognostication, patients often undergo multiple complementary assessments. Future studies should investigate the predictive value of CT combined with other markers to enhance the accuracy of poor outcome prediction. Specifically, combining NfL with CT may not only improve prognostic performance but also serve as a robust surrogate marker for HIE, thereby strengthening the reliability of CT findings.

Technical development of CT

The recent developments in CT technology, including dual-energy, spectral, and photon-counting CT, are likely to improve the sensitivity for detecting signs of HIE and predicting poor outcomes post-cardiac arrest. This should also be explored in future studies.

The predictive value of a normal CT

In addition to assessing the predictive performance of CT for poor outcomes after cardiac arrest, it would also be important to investigate the prognostic value of a normal CT, particularly when combined with other concordant predictors, for identifying patients likely to have a good outcome.

Acknowledgements

This thesis would not have been possible without the support, guidance, and collaboration of many individuals, to whom I am deeply grateful.

I would like to express my sincere gratitude to all patients and their families for their participation in the trials.

Niklas Nielsen, my main supervisor. Thank you for granting me this opportunity, for welcoming me into various research networks, and for your unwavering guidance and support. Your approach to scientific methodology is truly exemplary, and it has been an honour to pursue my PhD under your mentorship.

Marion Moseby-Knappe, my co-supervisor and dear friend. I am so thankful to have had you as my closest collaborator on most of the projects in this thesis. You possess a remarkable instinct for supporting, challenging, and guiding a student, and I have learned so much from you. A sincere thank you for all the enjoyable conversations and shared moments, including those that went beyond the topic of cardiac arrest.

Tobias Cronberg, my co-supervisor. Thank you for your invaluable input and wise advice on our manuscripts. I also appreciate your excellent literature suggestions on brain injury and prognostication post-cardiac arrest. Your extensive knowledge on these topics has been an incredible resource.

Johan Wassélius, my co-supervisor. A sincere thank you for your thorough and constructive evaluation during my half-time review, and for your dedicated supervision throughout the second half of my doctoral studies. Your expertise in CT and radiological research has been invaluable. I also greatly appreciate the advice you have shared on navigating a research career.

A heartfelt thank you to our collaborators at Charité, Berlin. **Martin Kenda**, thank you so much for generously sharing your vast expertise in automated GWR, for all your help in setting up a functional platform, and for the many enjoyable meetings during my doctoral years. **Christoph Leithner**, your comments, reflections, and input on our manuscripts and abstracts have often been the final touch that made everything come together. Your knowledge of CT-based prognostication after cardiac arrest is immense, and I've learned so much from you. **Michael Scheel**, thank you for all your support with the TTM2-CT sub-study. Writing the protocol paper together with all of you on-site, with lots of cinnamon buns and coffee, was

an incredibly inspiring experience. A big thank you to each of you for contributing to the ratings in our studies.

Kasim Abul-Kasim, former co-supervisor. Thank you for getting me started, for the engaging research discussions, the thought-provoking questions, and for a great collaboration in Paper I.

Mikael Johnsson, my radiology colleague in Helsingborg, neuroradiologist superstar and friend, thank you so much for your ratings in all our projects, and for your steady presence and little pep talks along the way.

Thanks to all other radiologists who participated in the time-consuming qualitative and quantitative CT assessment methods, **Juha Martola**, **Matthew Wheeler**, and **Stephanie Owen**. Juha, I am also very grateful for your valuable comments on neuroradiological signs associated with HIE.

All co-authors, I am deeply grateful and honoured to have written these manuscripts together with you. Your comments have improved the manuscripts and made publication in well-regarded journals possible. Thank you for your encouraging feedback and dedicated engagement.

Kristina Källén, thank you for your insightful and thoughtful evaluation during my half-time review. Your feedback highlighted important aspects to address in the research ahead.

Susann Ullén, **Sara Jespersen**, and **Axel Ström**, thank you for your valuable advice on statistical methods.

Anneli Stoll Troedsson, **Michael Borring**, **Pia Nilsson**, and **Anneli Andersson**, thank you for help with data collection and storage.

Simon Heissler and **Ulla-Britt Karlsson**, research coordinators and coordinators of PhD courses at Helsingborg Hospital, thank you for being there for all the big and little things throughout my PhD.

Many thanks to everyone at the outstanding hospital library of Helsingborg.

Krister Aronsson, Librarian/Information specialist at Lund University, thank you for your thorough and professional literature review.

A heartfelt thank you to everyone at the Centre for Cardiac Arrest at Lund University for sharing your outstanding research and for creating such a welcoming environment for me, somewhat of an outsider as the only radiologist and based in Helsingborg. I always leave our meetings feeling energised and inspired with exciting new research ideas.

Cornelia Lelinge, thank you for expert language editing of this thesis.

Sincere thanks to the heads of the radiology department at Helsingborg Hospital, **Karin Fristedt**, **Anders Navntoft**, and **Sven Truong**, for granting me the time and flexibility to pursue research.

A warm thank you to all my radiology colleagues for generously sharing your knowledge and for fostering such a pleasant and collegial atmosphere. Special thanks to **Axel Johansson** and **Jenny Eliasson** for keeping me sane and for your thoughtful answers to my questions about neuroradiology. Thanks to **Torbjörn Ahl**, **Irene Karlsson**, and everyone who assisted me with questions regarding CT acquisition protocols. I am also deeply grateful to everyone at the Radiology Department at Ängelholm Hospital for your warm welcome, encouragement, and support during my thesis writing period.

Thanks to everybody who provided valuable feedback on this thesis (**Niklas, Johan, Christoph, Martin, Marion, Torbjörn, Sebastian, Bea, and Susann**).

Thanks to my friends and family for your love, support and unwavering belief in me. **Rita**, ohne deine Hilfe wäre diese Dissertation nicht möglich gewesen. Vielen Dank für alles, was du für unsere Familie tust.

Sebastian (SMAT), **Benjamin**, **Jakob**, and **Filip** 

Financial support

This thesis has been made possible by generous grants from governmental funding of clinical research within the Swedish National Health Service (ALF), the Thelma Zoega Foundation, the Stig and Ragna Gorthon Foundation, and the Vera and Carl J. Michaelsen Foundation.

The TTM trials were supported by the Swedish Research Council (Vetenskapsrådet), the Swedish Heart-Lung Foundation, the Stig and Ragna Gorthon Foundation, the Knutsson Foundation, the Laerdal Foundation, the Hans-Gabriel and Alice Trolle-Wachtmeister Foundation for Medical Research, Regional Research Support in Region Skåne, and by governmental funding of clinical research within the Swedish National Health Service.

References

1. Myat A, Song KJ, Rea T. Out-of-hospital cardiac arrest: current concepts. *Lancet*. 2018; **391**(10124): 970-9.
2. Goto Y, Maeda T, Nakatsu-Goto Y. Prognostic implications of conversion from nonshockable to shockable rhythms in out-of-hospital cardiac arrest. *Crit Care*. 2014; **18**(5): 528.
3. Taglieri N, Saia F, Bacchi Reggiani ML, Ghetti G, Bruno AG, Rosetti C, et al. Prognostic significance of shockable and non-shockable cardiac arrest in ST-segment elevation myocardial infarction patients undergoing primary angioplasty. *Resuscitation*. 2018; **123**: 8-14.
4. Terman SW, Hume B, Meurer WJ, Silbergleit R. Impact of presenting rhythm on short- and long-term neurologic outcome in comatose survivors of cardiac arrest treated with therapeutic hypothermia. *Crit Care Med*. 2014; **42**(10): 2225-34.
5. Nolan JP, Berg RA, Andersen LW, Bhanji F, Chan PS, Donnino MW, et al. Cardiac Arrest and Cardiopulmonary Resuscitation Outcome Reports: Update of the Utstein Resuscitation Registry Template for In-Hospital Cardiac Arrest: A Consensus Report From a Task Force of the International Liaison Committee on Resuscitation (American Heart Association, European Resuscitation Council, Australian and New Zealand Council on Resuscitation, Heart and Stroke Foundation of Canada, InterAmerican Heart Foundation, Resuscitation Council of Southern Africa, Resuscitation Council of Asia). *Circulation*. 2019; **140**(18): e746-e57.
6. Adielsson A, Djärv T, Rawshani A, Lundin S, Herlitz J. Changes over time in 30-day survival and the incidence of shockable rhythms after in-hospital cardiac arrest - A population-based registry study of nearly 24,000 cases. *Resuscitation*. 2020; **157**: 135-40.
7. Yonis H, Ringgren KB, Andersen MP, Wissenberg M, Gislason G, Køber L, et al. Long-term outcomes after in-hospital cardiac arrest: 30-day survival and 1-year follow-up of mortality, anoxic brain damage, nursing home admission and in-home care. *Resuscitation*. 2020; **157**: 23-31.
8. Gräsner JT, Wnent J, Herlitz J, Perkins GD, Lefering R, Tjelmeland I, et al. Survival after out-of-hospital cardiac arrest in Europe - Results of the EuReCa TWO study. *Resuscitation*. 2020; **148**: 218-26.
9. Martin SS, Aday AW, Almarzooq ZI, Anderson CAM, Arora P, Avery CL, et al. 2024 Heart Disease and Stroke Statistics: A Report of US and Global Data From the American Heart Association. *Circulation*. 2024; **149**(8): e347-e913.

10. Claesson A, Djarv T, Nordberg P, Ringh M, Hollenberg J, Axelsson C, et al. Medical versus non medical etiology in out-of-hospital cardiac arrest-Changes in outcome in relation to the revised Utstein template. *Resuscitation*. 2017; **110**: 48-55.
11. Perkins GD, Callaway CW, Haywood K, Neumar RW, Lilja G, Rowland MJ, et al. Brain injury after cardiac arrest. *Lancet*. 2021; **398**(10307): 1269-78.
12. Berdowski J, Berg RA, Tijssen JG, Koster RW. Global incidences of out-of-hospital cardiac arrest and survival rates: Systematic review of 67 prospective studies. *Resuscitation*. 2010; **81**(11): 1479-87.
13. Gräsner JT, Lefering R, Koster RW, Masterson S, Böttiger BW, Herlitz J, et al. EuReCa ONE-27 Nations, ONE Europe, ONE Registry: A prospective one month analysis of out-of-hospital cardiac arrest outcomes in 27 countries in Europe. *Resuscitation*. 2016; **105**: 188-95.
14. Zeppenfeld K, Tfelt-Hansen J, de Riva M, Winkel BG, Behr ER, Blom NA, et al. 2022 ESC Guidelines for the management of patients with ventricular arrhythmias and the prevention of sudden cardiac death. *Eur Heart J*. 2022; **43**(40): 3997-4126.
15. Yan S, Gan Y, Jiang N, Wang R, Chen Y, Luo Z, et al. The global survival rate among adult out-of-hospital cardiac arrest patients who received cardiopulmonary resuscitation: a systematic review and meta-analysis. *Crit Care*. 2020; **24**(1): 61.
16. Kiguchi T, Okubo M, Nishiyama C, Maconochie I, Ong MEH, Kern KB, et al. Out-of-hospital cardiac arrest across the World: First report from the International Liaison Committee on Resuscitation (ILCOR). *Resuscitation*. 2020; **152**: 39-49.
17. Nishiyama C, Kiguchi T, Okubo M, Alihodžić H, Al-Araji R, Baldi E, et al. Three-year trends in out-of-hospital cardiac arrest across the world: Second report from the International Liaison Committee on Resuscitation (ILCOR). *Resuscitation*. 2023; **186**: 109757.
18. Magnusson C, et. al. Annual report of cardiac arrest from the Swedish Heart-Lung-Registry. (<https://www.hlr.nu/svenska-hlr-registret/>). 2024.
19. Hillgren J, et. Al. Annual report of Intensive care from the Swedish Intensive Care Register. (<http://www.icuregswe.org>). 2023.
20. Cummins RO OJ, Thies WH, Pepe PE. Improving survival from sudden cardiac arrest: the "chain of survival" concept. A statement for health professionals from the Advanced Cardiac Life Support Subcommittee and the Emergency Cardiac Care Committee, American Heart Association. *Circulation*. 1991; **83**(5).
21. Peberdy MA CC, Neumar RW, Geocadin RG, Zimmerman JL, Donnino M, Gabrielli A, Silvers SM, Zaritsky AL, Merchant R, Vanden Hoek TL, Kronick SL. Post-cardiac arrest care: 2010 American Heart Association guidelines for cardiopulmonary resuscitation and emergency cardiovascular care. *Circulation*. 2010; **122**.
22. Endisch C, Westhall E, Kenda M, Streitberger KJ, Kirkegaard H, Stenzel W, et al. Hypoxic-Ischemic Encephalopathy Evaluated by Brain Autopsy and Neuroprognostication After Cardiac Arrest. *JAMA Neurol*. 2020; **77**(11): 1430-9.
23. Thannhauser J, Nas J, Waalewijn RA, van Royen N, Bonnes JL, Brouwer MA, et al. Towards individualised treatment of out-of-hospital cardiac arrest patients: an update on technical innovations in the prehospital chain of survival. *Neth Heart J*. 2022; **30**(7-8): 345-9.

24. Dankiewicz J, Cronberg T, Lilja G, Jakobsen JC, Levin H, Ullén S, et al. Hypothermia versus Normothermia after Out-of-Hospital Cardiac Arrest. *N Engl J Med*. 2021; **384**(24): 2283-94.
25. Cronberg T, Greer DM, Lilja G, Moulaert V, Swindell P, Rossetti AO. Brain injury after cardiac arrest: from prognostication of comatose patients to rehabilitation. *Lancet Neurol*. 2020; **19**(7): 611-22.
26. Blennow Nordström E, Vestberg S, Evald L, Mion M, Segerström M, Ullén S, et al. Neuropsychological outcome after cardiac arrest: results from a sub-study of the targeted hypothermia versus targeted normothermia after out-of-hospital cardiac arrest (TTM2) trial. *Crit Care*. 2023; **27**(1): 328.
27. Andrew E, Nehme Z, Wolfe R, Bernard S, Smith K. Long-term survival following out-of-hospital cardiac arrest. *Heart*. 2017; **103**(14): 1104-10.
28. Rey JR, Caro-Codón J, Rodríguez Sotelo L, López-de-Sa E, Rosillo SO, González Fernández Ó, et al. Long term clinical outcomes in survivors after out-of-hospital cardiac arrest. *Eur J Intern Med*. 2020; **74**: 49-54.
29. Buunk G, van der Hoeven JG, Meinders AE. Cerebral blood flow after cardiac arrest. *Neth J Med*. 2000; **57**(3): 106-12.
30. Von Kummer R, Van der Lugt. Major Artery Ischemic Stroke: Imaging and Management. European Society of Neuroradiology. Springer Nature Switzerland; 2019. p. 1-30.
31. Sandroni C, Cronberg T, Sekhon M. Brain injury after cardiac arrest: pathophysiology, treatment, and prognosis. *Intensive Care Med*. 2021; **47**(12): 1393-414.
32. Keijzer HM, Hoedemaekers CWE, Meijer FJA, Tonino BAR, Klijn CJM, Hofmeijer J. Brain imaging in comatose survivors of cardiac arrest: Pathophysiological correlates and prognostic properties. *Resuscitation*. 2018; **133**: 124-36.
33. Stokum JA, Gerzanich V, Simard JM. Molecular pathophysiology of cerebral edema. *J Cereb Blood Flow Metab*. 2016; **36**(3): 513-38.
34. Busl KM, Greer DM. Hypoxic-ischemic brain injury: pathophysiology, neuropathology and mechanisms. *NeuroRehabilitation*. 2010; **26**(1): 5-13.
35. Kalogeris T, Baines CP, Krenz M, Korthuis RJ. Cell biology of ischemia/reperfusion injury. *Int Rev Cell Mol Biol*. 2012; **298**: 229-317.
36. Gutierrez LG, Rovira A, Portela LA, Leite Cda C, Lucato LT. CT and MR in non-neonatal hypoxic-ischemic encephalopathy: radiological findings with pathophysiological correlations. *Neuroradiology*. 2010; **52**(11): 949-76.
37. Arbelaez A, Castillo M, Mukherji SK. Diffusion-weighted MR imaging of global cerebral anoxia. *American Journal of Neuroradiology*. 1999; **20**(6): 999-1007.
38. Falini A, Barkovich AJ, Calabrese G, Origgi D, Triulzi F, Scotti G. Progressive brain failure after diffuse hypoxic ischemic brain injury: a serial MR and proton MR spectroscopic study. *AJNR Am J Neuroradiol*. 1998; **19**(4): 648-52.
39. Freeman WD BM, Barrett KM. Hypoxiv-ischaemic brain injury (HIBI) after cardiopulmonary arrest. *Current Anaesthesia and Critical Care*. 2007; **18**(5-6): 261-76.

40. Jou C, Shah R, Figueroa A, Patel JK. The Role of Inflammatory Cytokines in Cardiac Arrest. *J Intensive Care Med.* 2020; **35**(3): 219-24.
41. Penketh J, Nolan JP. Post-Cardiac Arrest Syndrome. *J Neurosurg Anesthesiol.* 2023; **35**(3): 260-4.
42. Nolan JP, Neumar RW, Adrie C, Aibiki M, Berg RA, Böttiger BW, et al. Post-cardiac arrest syndrome: epidemiology, pathophysiology, treatment, and prognostication. A Scientific Statement from the International Liaison Committee on Resuscitation; the American Heart Association Emergency Cardiovascular Care Committee; the Council on Cardiovascular Surgery and Anesthesia; the Council on Cardiopulmonary, Perioperative, and Critical Care; the Council on Clinical Cardiology; the Council on Stroke. *Resuscitation.* 2008; **79**(3): 350-79.
43. Nolan JP, Sandroni C, Böttiger BW, Cariou A, Cronberg T, Friberg H, et al. European Resuscitation Council and European Society of Intensive Care Medicine guidelines 2021: post-resuscitation care. *Intensive Care Med.* 2021; **47**(4): 369-421.
44. Waraich M ME. Hypoxic ischaemic brain injury. *Anaesthesia and Intensive Care Medicine.* 2024; **25**(1): 23-9.
45. Geocadin RG, Callaway CW, Fink EL, Golan E, Greer DM, Ko NU, et al. Standards for Studies of Neurological Prognostication in Comatose Survivors of Cardiac Arrest: A Scientific Statement From the American Heart Association. *Circulation.* 2019; **140**(9): e517-e42.
46. Dragancea I, Rundgren M, Englund E, Friberg H, Cronberg T. The influence of induced hypothermia and delayed prognostication on the mode of death after cardiac arrest. *Resuscitation.* 2013; **84**(3): 337-42.
47. Laver S, Farrow C, Turner D, Nolan J. Mode of death after admission to an intensive care unit following cardiac arrest. *Intensive Care Med.* 2004; **30**(11): 2126-8.
48. Coimbra C, Wieloch T. Moderate hypothermia mitigates neuronal damage in the rat brain when initiated several hours following transient cerebral ischemia. *Acta Neuropathol.* 1994; **87**(4): 325-31.
49. Sterz F, Safar P, Tisherman S, Radovsky A, Kuboyama K, Oku K. Mild hypothermic cardiopulmonary resuscitation improves outcome after prolonged cardiac arrest in dogs. *Crit Care Med.* 1991; **19**(3): 379-89.
50. Olai H, Thornéus G, Watson H, Macleod M, Rhodes J, Friberg H, et al. Meta-analysis of targeted temperature management in animal models of cardiac arrest. *Intensive Care Med Exp.* 2020; **8**(1): 3.
51. Arrich J, Herkner H, Müllner D, Behringer W. Targeted temperature management after cardiac arrest. A systematic review and meta-analysis of animal studies. *Resuscitation.* 2021; **162**: 47-55.
52. Zeiner A, Holzer M, Sterz F, Schörkhuber W, Eisenburger P, Havel C, et al. Hyperthermia after cardiac arrest is associated with an unfavorable neurologic outcome. *Arch Intern Med.* 2001; **161**(16): 2007-12.
53. Bro-Jeppesen J, Hassager C, Wanscher M, Søholm H, Thomsen JH, Lippert FK, et al. Post-hypothermia fever is associated with increased mortality after out-of-hospital cardiac arrest. *Resuscitation.* 2013; **84**(12): 1734-40.

54. Bernard SA, Gray TW, Buist MD, Jones BM, Silvester W, Gutteridge G, et al. Treatment of comatose survivors of out-of-hospital cardiac arrest with induced hypothermia. *N Engl J Med*. 2002; **346**(8): 557-63.
55. Mild therapeutic hypothermia to improve the neurologic outcome after cardiac arrest. *N Engl J Med*. 2002; **346**(8): 549-56.
56. Nolan JP, Morley PT, Vanden Hoek TL, Hickey RW, Kloeck WG, Billi J, et al. Therapeutic hypothermia after cardiac arrest: an advisory statement by the advanced life support task force of the International Liaison Committee on Resuscitation. *Circulation*. 2003; **108**(1): 118-21.
57. Arrich J, Holzer M, Herkner H, Müllner M. Hypothermia for neuroprotection in adults after cardiopulmonary resuscitation. *Cochrane Database Syst Rev*. 2009 Oct **7**; (4): Cd004128.
58. Arrich J, Holzer M, Havel C, Müllner M, Herkner H. Hypothermia for neuroprotection in adults after cardiopulmonary resuscitation. *Cochrane Database Syst Rev*. 2012 Sep **12**; (9): Cd004128.
59. May TL, Ruthazer R, Riker RR, Friberg H, Patel N, Soreide E, et al. Early withdrawal of life support after resuscitation from cardiac arrest is common and may result in additional deaths. *Resuscitation*. 2019; **139**: 308-13.
60. Elmer J, Torres C, Aufderheide TP, Austin MA, Callaway CW, Golan E, et al. Association of early withdrawal of life-sustaining therapy for perceived neurological prognosis with mortality after cardiac arrest. *Resuscitation*. 2016; **102**: 127-35.
61. Shrestha DB, Sedhai YR, Budhathoki P, Gaire S, Adhikari A, Poudel A, et al. Hypothermia versus normothermia after out-of-hospital cardiac arrest: A systematic review and meta-analysis of randomized controlled trials. *Ann Med Surg (Lond)*. 2022; **74**: 103327.
62. Nielsen N, Friberg H, Gluud C, Herlitz J, Wetterslev J. Hypothermia after cardiac arrest should be further evaluated - a systematic review of randomised trials with meta-analysis and trial sequential analysis. *Int J Cardiol*. 2011; **151**(3): 333-41.
63. Nielsen N, Wetterslev J, Cronberg T, Erlinge D, Gasche Y, Hassager C, et al. Targeted temperature management at 33 °C degrees versus 36 °C after cardiac arrest. *N Engl J Med*. 2013; **369**(23): 2197-206.
64. Donnino MW, Andersen LW, Berg KM, Reynolds JC, Nolan JP, Morley PT, et al. Temperature Management After Cardiac Arrest: An Advisory Statement by the Advanced Life Support Task Force of the International Liaison Committee on Resuscitation and the American Heart Association Emergency Cardiovascular Care Committee and the Council on Cardiopulmonary, Critical Care, Perioperative and Resuscitation. *Circulation*. 2015; **132**(25): 2448-56.
65. Lascarrou JB, Merdji H, Le Gouge A, Colin G, Grillet G, Girardie P, et al. Targeted Temperature Management for Cardiac Arrest with Nonshockable Rhythm. *N Engl J Med*. 2019; **381**(24): 2327-37.
66. Beekman R, Khosla A, Buckley R, Honiden S, Gilmore EJ. Temperature Control in the Era of Personalized Medicine: Knowledge Gaps, Research Priorities, and Future Directions. *J Intensive Care Med*. 2024; **39**(7): 611-22.

67. Dragancea I, Horn J, Kuiper M, Friberg H, Ullén S, Wetterslev J, et al. Neurological prognostication after cardiac arrest and targeted temperature management 33 °C versus 36 °C: Results from a randomised controlled clinical trial. *Resuscitation*. 2015; **93**: 164-70.
68. Nakstad ER, Stær-Jensen H, Wimmer H, Henriksen J, Alteheld LH, Reichenbach A, et al. Late awakening, prognostic factors and long-term outcome in out-of-hospital cardiac arrest - results of the prospective Norwegian Cardio-Respiratory Arrest Study (NORCAST). *Resuscitation*. 2020; **149**: 170-9.
69. Paul M, Bougouin W, Geri G, Dumas F, Champigneulle B, Legriel S, et al. Delayed awakening after cardiac arrest: prevalence and risk factors in the Parisian registry. *Intensive Care Med*. 2016; **42**(7): 1128-36.
70. Tsai MS, Chen WJ, Chen WT, Tien YT, Chang WT, Ong HN, et al. Should We Prolong the Observation Period for Neurological Recovery After Cardiac Arrest? *Crit Care Med*. 2022; **50**(3): 389-97.
71. Nolan JP, Cariou A. Post-resuscitation care: ERC–ESICM guidelines 2015. *Intensive Care Med*. 2015; **41**(12): 2204-6.
72. Teasdale G JB. Assessment of coma and impaired consciousness. A practical scale. *Lancet*. 1974; **2**(7872): 81-4.
73. Stead LG, Wijdicks EF, Bhagra A, Kashyap R, Bellolio MF, Nash DL, et al. Validation of a new coma scale, the FOUR score, in the emergency department. *Neurocrit Care*. 2009; **10**(1): 50-4.
74. Iyer VN, Mandrekar JN, Danielson RD, Zubkov AY, Elmer JL, Wijdicks EF. Validity of the FOUR score coma scale in the medical intensive care unit. *Mayo Clin Proc*. 2009; **84**(8): 694-701.
75. Oddo M, Sandroni C, Citerio G, Miroz JP, Horn J, Rundgren M, et al. Quantitative versus standard pupillary light reflex for early prognostication in comatose cardiac arrest patients: an international prospective multicenter double-blinded study. *Intensive Care Med*. 2018; **44**(12): 2102-11.
76. Sandroni C, D'Arrigo S, Cacciola S, Hoedemaekers CWE, Kamps MJA, Oddo M, et al. Prediction of poor neurological outcome in comatose survivors of cardiac arrest: a systematic review. *Intensive Care Med*. 2020; **46**(10): 1803-51.
77. Paramanathan S, Grejs AM, Søreide E, Duez CHV, Jeppesen AN, Reinertsen Å J, et al. Quantitative pupillometry in comatose out-of-hospital cardiac arrest patients: A post-hoc analysis of the TTH48 trial. *Acta Anaesthesiol Scand*. 2022; **66**(7): 880-6.
78. Nyholm B, Obling LER, Hassager C, Grand J, Møller JE, Othman MH, et al. Specific thresholds of quantitative pupillometry parameters predict unfavorable outcome in comatose survivors early after cardiac arrest. *Resusc Plus*. 2023; **14**: 100399.
79. Wijdicks EF, Hijdra A, Young GB, Bassetti CL, Wiebe S. Practice parameter: prediction of outcome in comatose survivors after cardiopulmonary resuscitation (an evidence-based review) [RETIRED]: report of the Quality Standards Subcommittee of the American Academy of Neurology. *Neurology*. 2006; **67**(2): 203-10.
80. Rossetti AO, Rabinstein AA, Oddo M. Neurological prognostication of outcome in patients in coma after cardiac arrest. *Lancet Neurol*. 2016; **15**(6): 597-609.

81. Maciel CB, Youn TS, Barden MM, Dhakar MB, Zhou SE, Pontes-Neto OM, et al. Corneal Reflex Testing in the Evaluation of a Comatose Patient: An Ode to Precise Semiology and Examination Skills. *Neurocrit Care*. 2020; **33**(2): 399-404.
82. Olson DM, Stutzman S, Saju C, Wilson M, Zhao W, Aiyagari V. Interrater Reliability of Pupillary Assessments. *Neurocrit Care*. 2016; **24**(2): 251-7.
83. Youn CS, Callaway CW, Rittenberger JC. Combination of initial neurologic examination, quantitative brain imaging and electroencephalography to predict outcome after cardiac arrest. *Resuscitation*. 2017; **110**: 120-5.
84. Dhakar MB, Sivaraju A, Maciel CB, Youn TS, Gaspard N, Greer DM, et al. Electro-clinical characteristics and prognostic significance of post anoxic myoclonus. *Resuscitation*. 2018; **131**: 114-20.
85. Seder DB, Sunde K, Rubertsson S, Mooney M, Stammet P, Riker RR, et al. Neurologic outcomes and postresuscitation care of patients with myoclonus following cardiac arrest. *Crit Care Med*. 2015; **43**(5): 965-72.
86. Lybeck A, Friberg H, Aneman A, Hassager C, Horn J, Kjærgaard J, et al. Prognostic significance of clinical seizures after cardiac arrest and target temperature management. *Resuscitation*. 2017; **114**: 146-51.
87. Chakraborty T, Braksick S, Rabinstein A, Wijdicks E. Status Myoclonus with Post-cardiac-arrest Syndrome: Implications for Prognostication. *Neurocrit Care*. 2022; **36**(2): 387-94.
88. Friberg H, Cronberg T, Dünser MW, Duranteau J, Horn J, Oddo M. Survey on current practices for neurological prognostication after cardiac arrest. *Resuscitation*. 2015; **90**: 158-62.
89. Elmer J, Steinberg A, Callaway CW. Paucity of neuroprognostic testing after cardiac arrest in the United States. *Resuscitation*. 2023; **188**: 109762.
90. Westhall E, Rossetti AO, van Rootselaar AF, Wesenberg Kjaer T, Horn J, Ullén S, et al. Standardized EEG interpretation accurately predicts prognosis after cardiac arrest. *Neurology*. 2016; **86**(16): 1482-90.
91. Turella S, Dankiewicz J, Friberg H, Jakobsen JC, Leithner C, Levin H, et al. The predictive value of highly malignant EEG patterns after cardiac arrest: evaluation of the ERC-ESICM recommendations. *Intensive Care Med*. 2024; **50**(1): 90-102.
92. Turella S, Dankiewicz J, Ben-Hamouda N, Nilsen KB, Düring J, Endisch C, et al. EEG for good outcome prediction after cardiac arrest: A multicentre cohort study. *Resuscitation*. 2024; **202**: 110319.
93. Bauer E, Funk GC, Gendo A, Kramer L, Zauner C, Sterz F, et al. Electrophysiological assessment of the afferent sensory pathway in cardiac arrest survivors. *Eur J Clin Invest*. 2003; **33**(4): 283-7.
94. Nobile L, Pognuz ER, Rossetti AO, Franchi F, Verginella F, Mavroudakakis N, et al. The characteristics of patients with bilateral absent evoked potentials after post-anoxic brain damage: A multicentric cohort study. *Resuscitation*. 2020; **149**: 134-40.
95. Rajajee V, Muehlschlegel S, Wartenberg KE, Alexander SA, Busl KM, Chou SHY, et al. Guidelines for Neuroprognostication in Comatose Adult Survivors of Cardiac Arrest. *Neurocrit Care*. 2023; **38**(3): 533-63.

96. Pfeifer R, Weitzel S, Günther A, Berrouschot J, Fischer M, Isenmann S, et al. Investigation of the inter-observer variability effect on the prognostic value of somatosensory evoked potentials of the median nerve (SSEP) in cardiac arrest survivors using an SSEP classification. *Resuscitation*. 2013; **84**(10): 1375-81.
97. Zandbergen EG, Hijdra A, de Haan RJ, van Dijk JG, Ongerboer de Visser BW, Spaans F, et al. Interobserver variation in the interpretation of SSEPs in anoxic-ischaemic coma. *Clin Neurophysiol*. 2006; **117**(7): 1529-35.
98. Stammet P, Collignon O, Hassager C, Wise MP, Hovdenes J, Åneman A, et al. Neuron-Specific Enolase as a Predictor of Death or Poor Neurological Outcome After Out-of-Hospital Cardiac Arrest and Targeted Temperature Management at 33°C and 36°C. *J Am Coll Cardiol*. 2015; **65**(19): 2104-14.
99. Youn CS, Park KN, Kim SH, Lee BK, Cronberg T, Oh SH, et al. External validation of the 2020 ERC/ESICM prognostication strategy algorithm after cardiac arrest. *Crit Care*. 2022; **26**(1): 95.
100. Wihersaari L, Reinikainen M, Furlan R, Mandelli A, Vaahersalo J, Kurola J, et al. Neurofilament light compared to neuron-specific enolase as a predictor of unfavourable outcome after out-of-hospital cardiac arrest. *Resuscitation*. 2022; **174**: 1-8.
101. Moseby-Knappe M, Mattsson N, Nielsen N, Zetterberg H, Blennow K, Dankiewicz J, et al. Serum Neurofilament Light Chain for Prognosis of Outcome After Cardiac Arrest. *JAMA Neurol*. 2019; **76**(1): 64-71.
102. Levin H, Lybeck A, Frigyesi A, Arctadius I, Thorgeirsdóttir B, Annborn M, et al. Plasma neurofilament light is a predictor of neurological outcome 12 h after cardiac arrest. *Crit Care*. 2023; **27**(1): 74.
103. Wijdsicks EFM. Brain Injury after Cardiac Arrest: Refining Prognosis. *Neurol Clin*. 2025; **43**(1): 79-90.
104. Lagebrant A, Lang M, Nielsen N, Blennow K, Dankiewicz J, Friberg H, et al. Brain injury markers in blood predict signs of hypoxic ischaemic encephalopathy on head computed tomography after cardiac arrest. *Resuscitation*. 2023; **184**: 109668.
105. Berg KM, Bray JE, Ng KC, Liley HG, Greif R, Carlson JN, et al. 2023 International Consensus on Cardiopulmonary Resuscitation and Emergency Cardiovascular Care Science With Treatment Recommendations: Summary From the Basic Life Support; Advanced Life Support; Pediatric Life Support; Neonatal Life Support; Education, Implementation, and Teams; and First Aid Task Forces. *Circulation*. 2023; **148**(24): e187-e280.
106. Bitar R, Leung G, Perng R, Tadros S, Moody AR, Sarrazin J, et al. MR pulse sequences: what every radiologist wants to know but is afraid to ask. *Radiographics*. 2006; **26**(2): 513-37.
107. Lopez Soto C, Dragoi L, Heyn CC, Kramer A, Pinto R, Adhikari NKJ, et al. Imaging for Neuroprognostication After Cardiac Arrest: Systematic Review and Meta-analysis. *Neurocrit Care*. 2020; **32**(1): 206-16.
108. Wijman CA, Mlynash M, Caulfield AF, Hsia AW, Eyngorn I, Bammer R, et al. Prognostic value of brain diffusion-weighted imaging after cardiac arrest. *Ann Neurol*. 2009; **65**(4): 394-402.

109. Jeon CH, Park JS, Lee JH, Kim H, Kim SC, Park KH, et al. Comparison of brain computed tomography and diffusion-weighted magnetic resonance imaging to predict early neurologic outcome before target temperature management comatose cardiac arrest survivors. *Resuscitation*. 2017; **118**: 21-6.
110. Wu O, Sorensen AG, Benner T, Singhal AB, Furie KL, Greer DM. Comatose patients with cardiac arrest: predicting clinical outcome with diffusion-weighted MR imaging. *Radiology*. 2009; **252**(1):173-81.
111. Mlynash M, Campbell DM, Leproust EM, Fischbein NJ, Bammer R, Eyngorn I, et al. Temporal and spatial profile of brain diffusion-weighted MRI after cardiac arrest. *Stroke*. 2010; **41**(8): 1665-72.
112. Wijdicks EF, Campeau NG, Miller GM. MR imaging in comatose survivors of cardiac resuscitation. *AJNR Am J Neuroradiol*. 2001; **22**(8): 1561-5.
113. Yoon JA, Kang C, Park JS, You Y, Min JH, In YN, et al. Quantitative analysis of apparent diffusion coefficients to predict neurological prognosis in cardiac arrest survivors: an observational derivation and internal-external validation study. *Crit Care*. 2024; **28**(1): 138.
114. Moon HK, Jang J, Park KN, Kim SH, Lee BK, Oh SH, et al. Quantitative analysis of relative volume of low apparent diffusion coefficient value can predict neurologic outcome after cardiac arrest. *Resuscitation*. 2018; **126**: 36-42.
115. Beekman R, Hirsch KG. Brain imaging after cardiac arrest. *Curr Opin Crit Care*. 2023; **29**(3): 192-8.
116. Keijzer HM, Verhulst M, Meijer FJA, Tonino BAR, Bosch FH, Klijn CJM, et al. Prognosis After Cardiac Arrest: The Additional Value of DWI and FLAIR to EEG. *Neurocrit Care*. 2022; **37**(1): 302-13.
117. Hirsch KG, Mlynash M, Jansen S, Persoon S, Eyngorn I, Krasnokutsky MV, et al. Prognostic value of a qualitative brain MRI scoring system after cardiac arrest. *J Neuroimaging*. 2015; **25**(3): 430-7.
118. Vanden Berghe S, Cappelle S, De Keyzer F, Peeters R, Coursier K, Depotter A, et al. Qualitative and quantitative analysis of diffusion-weighted brain MR imaging in comatose survivors after cardiac arrest. *Neuroradiology*. 2020; **62**(11): 1361-9.
119. Chan WP, Nguyen C, Kim N, Tripodis Y, Gilmore EJ, Greer DM, et al. A practical magnetic-resonance imaging score for outcome prediction in comatose cardiac arrest survivors. *Resuscitation*. 2024; **202**: 110370.
120. Park JY, Kim YH, Ahn SJ, Lee JH, Lee DW, Hwang SY, et al. Association between the extent of diffusion restriction on brain diffusion-weighted imaging and neurological outcomes after an out-of-hospital cardiac arrest. *Resuscitation*. 2023; **187**: 109761.
121. Witten L, Gardner R, Holmberg MJ, Wiberg S, Moskowitz A, Mehta S, et al. Reasons for death in patients successfully resuscitated from out-of-hospital and in-hospital cardiac arrest. *Resuscitation*. 2019; **136**: 93-9.
122. Lemiale V, Dumas F, Mongardon N, Giovanetti O, Charpentier J, Chiche JD, et al. Intensive care unit mortality after cardiac arrest: the relative contribution of shock and brain injury in a large cohort. *Intensive Care Med*. 2013; **39**(11): 1972-80.

123. Kim YJ, Ahn S, Sohn CH, Seo DW, Lee YS, Lee JH, et al. Long-term neurological outcomes in patients after out-of-hospital cardiac arrest. *Resuscitation*. 2016; **101**: 1-5.
124. Scarpino M, Carrai R, Lolli F, Lanzo G, Spalletti M, Valzania F, et al. Neurophysiology for predicting good and poor neurological outcome at 12 and 72 h after cardiac arrest: The ProNeCA multicentre prospective study. *Resuscitation*. 2020; **147**: 95-103.
125. Elliott VJ, Rodgers DL, Brett SJ. Systematic review of quality of life and other patient-centred outcomes after cardiac arrest survival. *Resuscitation*. 2011; **82**(3): 247-56.
126. Harve H, Tiainen M, Poutiainen E, Maunu M, Kajaste S, Roine RO, et al. The functional status and perceived quality of life in long-term survivors of out-of-hospital cardiac arrest. *Acta Anaesthesiol Scand*. 2007; **51**(2): 206-9.
127. Jennett B, Bond M. Assessment of outcome after severe brain damage. *Lancet*. 1975; **1**(7905): 480-4.
128. Rankin J. Cerebral vascular accidents in patients over the age of 60. II. Prognosis. *Scott Med J*. 1957; **2**(5): 200-15.
129. Haywood K, Whitehead L, Nadkarni VM, Achana F, Beesems S, Böttiger BW, et al. COSCA (Core Outcome Set for Cardiac Arrest) in Adults: An Advisory Statement From the International Liaison Committee on Resuscitation. *Resuscitation*. 2018; **127**: 147-63.
130. Banks JL, Marotta CA. Outcomes validity and reliability of the modified Rankin scale: implications for stroke clinical trials: a literature review and synthesis. *Stroke*. 2007; **38**(3): 1091-6.
131. Raina KD, Callaway C, Rittenberger JC, Holm MB. Neurological and functional status following cardiac arrest: method and tool utility. *Resuscitation*. 2008; **79**(2): 249-56.
132. Case N, Coppler PJ, Mettenburg J, Ratay C, Tam J, Faiver L, et al. Time-dependent association of grey-white ratio on early brain CT predicting outcomes after cardiac arrest at hospital discharge. *Resuscitation*. 2025; **206**: 110440.
133. AM C. Representation of a Function by Its Line Integrals, with some Radiological Applications. *Journal of Applied Physics*. 1963; **34**: 2722-7.
134. AM C. Representation of a Function by Its Line Integrals, with some Radiological Applications. II. *Journal of Applied Physics*. 1964; **35**: 2908-13.
135. Hounsfield GN. Computerized transverse axial scanning (tomography): Part I. Description of system. *British Journal of Radiology*. 1973; **46**: 1016-22.
136. McCollough CH RP. Milestones in CT: Past, Present, and Future. *Radiology*. 2023; Oct; **309**(1).
137. Hsieh J, Flohr T. Computed tomography recent history and future perspectives. *J Med Imaging (Bellingham)*. 2021; **8**(5): 052109.
138. Romans LE. *Computed Tomography for Technologists*. 2 ed: Wolters Kluwer; 2019.
139. Seeram E. *Computed Tomography: Physical Principles and Recent Technical Advances*. *J Med Imaging Radiat Sci*. 2010; **41**(2): 87-109.

140. Weinstein MA, Duchesneau, MacIntyre WJ. White and gray matter of the brain differentiated by computed tomography. *Radiology*. 1977; **122**: 699-702.
141. Zatz LM. Basic principles of computed tomography scanning. Technical aspects of computed tomography. St. Louis, MO: Mosby; 1981. pp. 3853–76.
142. Oh JH, Choi SP, Wee JH, Park JH. Inter-scanner variability in Hounsfield unit measured by CT of the brain and effect on gray-to-white matter ratio. *Am J Emerg Med*. 2019; **37**(4): 680-4.
143. J. M. Core Radiology - A visual approach to diagnostic imaging. 9th ed. Great Britain: Cambridge University Press; 2019.
144. Barrett JF, Keat N. Artifacts in CT: recognition and avoidance. *Radiographics*. 2004; **24**(6): 1679-91.
145. Triche BL, Nelson JT, Jr., McGill NS, Porter KK, Sanyal R, Tessler FN, et al. Recognizing and Minimizing Artifacts at CT, MRI, US, and Molecular Imaging. *Radiographics*. 2019; **39**(4): 1017-8.
146. Torbey MT, Selim M, Knorr J, Bigelow C, Recht L. Quantitative analysis of the loss of distinction between gray and white matter in comatose patients after cardiac arrest. *Stroke*. 2000; **31**(9): 2163-7.
147. Streitberger KJ, Endisch C, Ploner CJ, Stevens R, Scheel M, Kenda M, et al. Timing of brain computed tomography and accuracy of outcome prediction after cardiac arrest. *Resuscitation*. 2019; **145**: 8-14.
148. Wang GN, Zhang ZM, Chen W, Xu XQ, Zhang JS. Timing of brain computed tomography for predicting neurological prognosis in comatose cardiac arrest survivors: a retrospective observational study. *World J Emerg Med*. 2022; **13**(5): 349-54.
149. In YN, Lee IH, Park JS, Kim DM, You Y, Min JH, et al. Delayed head CT in out-of-hospital cardiac arrest survivors: Does this improve predictive performance of neurological outcome? *Resuscitation*. 2022; **172**: 1-8.
150. Spiegel SM, Fox AJ, Vinuela F, Pelz DM. Increased density of tentorium and falx: a false positive CT sign of subarachnoid hemorrhage. *Can Assoc Radiol J*. 1986; **37**(4): 243-7.
151. Avrahami E, Katz R, Rabin A, Friedman V. CT diagnosis of non-traumatic subarachnoid haemorrhage in patients with brain edema. *Eur J Radiol*. 1998; **28**(3): 222-5.
152. Lee BK, Kim YJ, Ryoo SM, Kim SJ, Lee DH, Jeung KW, et al. "Pseudo-subarachnoid hemorrhage sign" on early brain computed tomography in out-of-hospital cardiac arrest survivors receiving targeted temperature management. *J Crit Care*. 2017; **40**: 36-40.
153. Yuzawa H, Higano S, Mugikura S, Umetsu A, Murata T, Nakagawa A, et al. Pseudo-subarachnoid hemorrhage found in patients with postresuscitation encephalopathy: characteristics of CT findings and clinical importance. *AJNR Am J Neuroradiol*. 2008; **29**(8): 1544-9.
154. Kavanagh EC. The reversal sign. *Radiology*. 2007; **245**(3): 914-5.

155. Kjos BO, Brant-Zawadzki M, Young RG. Early CT findings of global central nervous system hypoperfusion. *AJR Am J Roentgenol.* 1983; **141**(6): 1227-32.
156. Han BK, Towbin RB, De Courten-Myers G, McLaurin RL, Ball WS, Jr. Reversal sign on CT: effect of anoxic/ischemic cerebral injury in children. *AJNR Am J Neuroradiol.* 1989; **10**(6): 1191-8.
157. Baby N, Gilvaz P, Kuriakose AM. White Cerebellum Sign: A Poor Prognostic Sign. *Pediatr Neurol.* 2019; **101**: 86-7.
158. Beekman R, Maciel CB, Ormseth CH, Zhou SE, Galluzzo D, Miyares LC, et al. Early head CT in post-cardiac arrest patients: A helpful tool or contributor to self-fulfilling prophecy? *Resuscitation.* 2021; **165**: 68-76.
159. Moseby-Knappe M, Pellis T, Dragancea I, Friberg H, Nielsen N, Horn J, et al. Head computed tomography for prognostication of poor outcome in comatose patients after cardiac arrest and targeted temperature management. *Resuscitation.* 2017; **119**: 89-94.
160. Caraganis A, Mulder M, Kempainen RR, Brown RZ, Oswood M, Hoffman B, et al. Interobserver Variability in the Recognition of Hypoxic-Ischemic Brain Injury on Computed Tomography Soon After Out-of-Hospital Cardiac Arrest. *Neurocrit Care.* 2020; **33**(2): 414-21.
161. Ahn SH, Savarraj JP, Pervez M, Jones W, Park J, Jeon SB, et al. The Subarachnoid Hemorrhage Early Brain Edema Score Predicts Delayed Cerebral Ischemia and Clinical Outcomes. *Neurosurgery.* 2018; **83**(1): 137-45.
162. Said M, Gümüş M, Herten A, Dinger TF, Chihi M, Darkwah Oppong M, et al. Subarachnoid Hemorrhage Early Brain Edema Score (SEBES) as a radiographic marker of clinically relevant intracranial hypertension and unfavorable outcome after subarachnoid hemorrhage. *Eur J Neurol.* 2021; **28**(12): 4051-9.
163. Barber PA, Demchuk AM, Zhang J, Buchan AM. Validity and reliability of a quantitative computed tomography score in predicting outcome of hyperacute stroke before thrombolytic therapy. ASPECTS Study Group. Alberta Stroke Programme Early CT Score. *Lancet.* 2000; **355**(9216): 1670-4.
164. Puetz V, Sylaja PN, Coutts SB, Hill MD, Dzialowski I, Mueller P, et al. Extent of hypoattenuation on CT angiography source images predicts functional outcome in patients with basilar artery occlusion. *Stroke.* 2008; **39**(9): 2485-90.
165. Puetz V, Dzialowski I, Hill MD, Demchuk AM. The Alberta Stroke Program Early CT Score in clinical practice: what have we learned? *Int J Stroke.* 2009; **4**(5):354-64.
166. Schröder J, Thomalla G. A Critical Review of Alberta Stroke Program Early CT Score for Evaluation of Acute Stroke Imaging. *Front Neurol.* 2016; **7**: 245.
167. Sugimori H, Kanna T, Yamashita K, Kuwashiro T, Yoshiura T, Zaitzu A, et al. Early findings on brain computed tomography and the prognosis of post-cardiac arrest syndrome: application of the score for stroke patients. *Resuscitation.* 2012; **83**(7): 848-54.
168. Lee KS, Lee SE, Choi JY, Gho YR, Chae MK, Park EJ, et al. Useful Computed Tomography Score for Estimation of Early Neurologic Outcome in Post-Cardiac Arrest Patients With Therapeutic Hypothermia. *Circ J.* 2017; **81**(11): 1628-35.

169. Sandroni C, D'Arrigo S, Cacciola S, Hoedemaekers CWE, Westhall E, Kamps MJA, et al. Prediction of good neurological outcome in comatose survivors of cardiac arrest: a systematic review. *Intensive Care Med.* 2022; **48**(4): 389-413.
170. Inamasu J, Miyatake S, Suzuki M, Nakatsukasa M, Tomioka H, Honda M, et al. Early CT signs in out-of-hospital cardiac arrest survivors: Temporal profile and prognostic significance. *Resuscitation.* 2010; **81**(5): 534-8.
171. Yamamura H, Kaga S, Kaneda K, Yamamoto T, Mizobata Y. Head Computed Tomographic measurement as an early predictor of outcome in hypoxic-ischemic brain damage patients treated with hypothermia therapy. *Scand J Trauma Resusc Emerg Med.* 2013; **21**: 37.
172. Wu O, Batista LM, Lima FO, Vangel MG, Furie KL, Greer DM. Predicting clinical outcome in comatose cardiac arrest patients using early noncontrast computed tomography. *Stroke.* 2011; **42**(4): 985-92.
173. Panchal AR, Bartos JA, Cabañas JG, Donnino MW, Drennan IR, Hirsch KG, et al. Part 3: Adult Basic and Advanced Life Support: 2020 American Heart Association Guidelines for Cardiopulmonary Resuscitation and Emergency Cardiovascular Care. *Circulation.* 2020; **142**(16_suppl_2): S366-s468.
174. Metter RB, Rittenberger JC, Guyette FX, Callaway CW. Association between a quantitative CT scan measure of brain edema and outcome after cardiac arrest. *Resuscitation.* 2011; **82**(9): 1180-5.
175. Kirsch K, Heymel S, Günther A, Vahl K, Schmidt T, Michalski D, et al. Prognostication of neurologic outcome using gray-white-matter-ratio in comatose patients after cardiac arrest. *BMC Neurol.* 2021; **21**(1): 456.
176. Gentsch A, Storm C, Leithner C, Schroeder T, Ploner CJ, Hamm B, et al. Outcome prediction in patients after cardiac arrest: a simplified method for determination of gray-white matter ratio in cranial computed tomography. *Clin Neuroradiol.* 2015; **25**(1): 49-54.
177. Scheel M, Storm C, Gentsch A, Nee J, Luckenbach F, Ploner CJ, et al. The prognostic value of gray-white-matter ratio in cardiac arrest patients treated with hypothermia. *Scand J Trauma Resusc Emerg Med.* 2013; **21**: 23.
178. Choi SP, Park HK, Park KN, Kim YM, Ahn KJ, Choi KH, et al. The density ratio of grey to white matter on computed tomography as an early predictor of vegetative state or death after cardiac arrest. *Emerg Med J.* 2008; **25**(10): 666-9.
179. Cristia C, Ho ML, Levy S, Andersen LW, Perman SM, Giberson T, et al. The association between a quantitative computed tomography (CT) measurement of cerebral edema and outcomes in post-cardiac arrest-a validation study. *Resuscitation.* 2014; **85**(10): 1348-53.
180. Scarpino M, Lanzo G, Lolli F, Carrai R, Moretti M, Spalletti M, et al. Neurophysiological and neuroradiological multimodal approach for early poor outcome prediction after cardiac arrest. *Resuscitation.* 2018; **129**: 114-20.
181. Lee BK, Jeung KW, Song KH, Jung YH, Choi WJ, Kim SH, et al. Prognostic values of gray matter to white matter ratios on early brain computed tomography in adult comatose patients after out-of-hospital cardiac arrest of cardiac etiology. *Resuscitation.* 2015; **96**: 46-52.

182. Wang GN, Chen XF, Lv JR, Sun NN, Xu XQ, Zhang JS. The prognostic value of gray-white matter ratio on brain computed tomography in adult comatose cardiac arrest survivors. *J Chin Med Assoc.* 2018; **81**(7): 599-604.
183. Zhou F, Wang H, Jian M, Wang Z, He Y, Duan H, et al. Gray-White Matter Ratio at the Level of the Basal Ganglia as a Predictor of Neurologic Outcomes in Cardiac Arrest Survivors: A Literature Review. *Front Med (Lausanne).* 2022; **9**: 847089.
184. Akdogan AI, Sahin H, Pekcevik Y, Uluer H. Utility of brain parenchyma density measurement and computed tomography perfusion imaging in predicting brain death. *Pol J Radiol.* 2020; **85**: e636-e42.
185. Kenda M, Scheel M, Kemmling A, Aalberts N, Guettler C, Streitberger KJ, et al. Automated Assessment of Brain CT After Cardiac Arrest-An Observational Derivation/Validation Cohort Study. *Crit Care Med.* 2021; **49**(12): e1212-e22.
186. Hanning U, Sporns PB, Lebiecz P, Niederstadt T, Zoubi T, Schmidt R, et al. Automated assessment of early hypoxic brain edema in non-enhanced CT predicts outcome in patients after cardiac arrest. *Resuscitation.* 2016; **104**: 91-4.
187. Kemmling A, Wersching H, Berger K, Knecht S, Groden C, Nölte I. Decomposing the Hounsfield unit: probabilistic segmentation of brain tissue in computed tomography. *Clin Neuroradiol.* 2012; **22**(1): 79-91.
188. Tsai H, Chi CY, Wang LW, Su YJ, Chen YF, Tsai MS, et al. Outcome prediction of cardiac arrest with automatically computed gray-white matter ratio on computed tomography images. *Crit Care.* 2024; **28**(1): 118.
189. Kenda M, Lang M, Nee J, Hinrichs C, Dell'Orco A, Salih F, et al. Regional Brain Net Water Uptake in Computed Tomography after Cardiac Arrest - A Novel Biomarker for Neuroprognostication. *Resuscitation.* 2024; **200**: 110243.
190. You YH, Park JS, Yoo IS, Min JH, Jeong WJ, Cho YC, et al. Usefulness of a quantitative analysis of the cerebrospinal fluid volume proportion in brain computed tomography for predicting neurological prognosis in cardiac arrest survivors who undergo target temperature management. *J Crit Care.* 2019; **51**: 170-4.
191. Dhar R, Chen Y, Hamzehloo A, Kumar A, Heitsch L, He J, et al. Reduction in Cerebrospinal Fluid Volume as an Early Quantitative Biomarker of Cerebral Edema After Ischemic Stroke. *Stroke.* 2020; **51**(2): 462-7.
192. Mansour A, Fuhrman JD, Ammar FE, Loggini A, Davis J, Lazaridis C, et al. Machine Learning for Early Detection of Hypoxic-Ischemic Brain Injury After Cardiac Arrest. *Neurocrit Care.* 2022; **36**(3): 974-82.
193. Liu C, Elmer J, Arefan D, Pease M, Wu S. Interpretable machine learning model for imaging-based outcome prediction after cardiac arrest. *Resuscitation.* 2023; **191**: 109894.
194. Molinski NS, Kenda M, Leithner C, Nee J, Storm C, Scheel M, et al. Deep learning-enabled detection of hypoxic-ischemic encephalopathy after cardiac arrest in CT scans: a comparative study of 2D and 3D approaches. *Front Neurosci.* 2024; **18**: 1245791.
195. Mokri B. The Monroe-Kellie hypothesis: applications in CSF volume depletion. *Neurology.* 2001; **56**(12): 1746-8.
196. Selhorst JB, Chen Y. The optic nerve. *Semin Neurol.* 2009; **29**(1): 29-35.

197. Lee SH, Kim HS, Yun SJ. Optic nerve sheath diameter measurement for predicting raised intracranial pressure in adult patients with severe traumatic brain injury: A meta-analysis. *J Crit Care*. 2020; **56**: 182-7.
198. Kang C, Min JH, Park JS, You Y, Yoo I, Cho YC, et al. Relationship between optic nerve sheath diameter measured by magnetic resonance imaging, intracranial pressure, and neurological outcome in cardiac arrest survivors who underwent targeted temperature management. *Resuscitation*. 2019; **145**: 43-9.
199. Chae MK, Ko E, Lee JH, Lee TR, Yoon H, Hwang SY, et al. Better prognostic value with combined optic nerve sheath diameter and grey-to-white matter ratio on initial brain computed tomography in post-cardiac arrest patients. *Resuscitation*. 2016; **104**: 40-5.
200. Shankar J, Alcock S, Wiens E, Ayroso M, Park J, Singh N, et al. Computed tomography perfusion assessment of poor neurological outcome in comatose cardiac arrest patients (CANCCAP): a prospective study. *Crit Care*. 2025; **29**(1): 211.
201. Stein T, Lang F, Rau S, Reiser M, Russe MF, Schürmann T, et al. Photon-counting detector CT of the brain reduces variability of Hounsfield units and has a mean offset compared with energy-integrating detector CT. *AJNR Am J Neuroradiol*. 2025 Jul.
202. Callaway CW. Neuroprognostication postcardiac arrest: translating probabilities to individuals. *Curr Opin Crit Care*. 2018;24(3):158-64.
203. Nielsen N, Wetterslev J, al-Subaie N, Andersson B, Bro-Jeppesen J, Bishop G, et al. Target Temperature Management after out-of-hospital cardiac arrest--a randomized, parallel-group, assessor-blinded clinical trial--rationale and design. *Am Heart J*. 2012; **163**(4): 541-8.
204. Dankiewicz J, Cronberg T, Lilja G, Jakobsen JC, Bělohávek J, Callaway C, et al. Targeted hypothermia versus targeted Normothermia after out-of-hospital cardiac arrest (TTM2): A randomized clinical trial-Rationale and design. *Am Heart J*. 2019; **217**: 23-31.
205. Genske U, Jahnke P. Human Observer Net: A Platform Tool for Human Observer Studies of Image Data. *Radiology*. 2022; **303**(3): 524-30.
206. Kirkwood BR SJ. Medical statistics-2nd edition. Malden, Massachusetts, USA: Blackwell Publishing company; 2003.
207. Zweig MH. ROC plots display test accuracy, but are still limited by the study design. *Clin Chem*. 1993; **39**(6): 1345-6.
208. McHugh ML. Interrater reliability: the kappa statistic. *Biochem Med (Zagreb)*. 2012; **22**(3): 276-82.
209. Benchoufi M, Matzner-Lober E, Molinari N, Jannot AS, Soyer P. Interobserver agreement issues in radiology. *Diagn Interv Imaging*. 2020; **101**(10):639-41.
210. Giavarina D. Understanding Bland Altman analysis. *Biochem Med (Zagreb)*. 2015; **25**(2): 141-51.
211. Bland JM, Altman DG. Statistical methods for assessing agreement between two methods of clinical measurement. *Lancet*. 1986; **1**(8476): 307-10.

212. Sandroni C, Cavallaro F, Callaway CW, Sanna T, D'Arrigo S, Kuiper M, et al. Predictors of poor neurological outcome in adult comatose survivors of cardiac arrest: a systematic review and meta-analysis. Part 1: patients not treated with therapeutic hypothermia. *Resuscitation*. 2013; **84**(10): 1310-23.
213. Sandroni C, Cavallaro F, Callaway CW, D'Arrigo S, Sanna T, Kuiper MA, et al. Predictors of poor neurological outcome in adult comatose survivors of cardiac arrest: a systematic review and meta-analysis. Part 2: Patients treated with therapeutic hypothermia. *Resuscitation*. 2013; **84**(10): 1324-38.
214. Elmer J, Coppler PJ, Ratay C, Steinberg A, DiFiore-Sprouse S, Case N, et al. Recovery Potential in Patients After Cardiac Arrest Who Die After Limitations or Withdrawal of Life Support. *JAMA Netw Open*. 2025; **8**(3):e251714.
215. Elmer J, Kurz MC, Coppler PJ, Steinberg A, DeMasi S, De-Arteaga M, et al. Time to Awakening and Self-Fulfilling Prophecies After Cardiac Arrest. *Crit Care Med*. 2023; **51**(4): 503-12.
216. Ryoo SM, Jeon SB, Sohn CH, Ahn S, Han C, Lee BK, et al. Predicting Outcome With Diffusion-Weighted Imaging in Cardiac Arrest Patients Receiving Hypothermia Therapy: Multicenter Retrospective Cohort Study. *Crit Care Med*. 2015;**43**(11): 2370-7.
217. Moseby-Knappe M, Westhall E, Backman S, Mattsson-Carlgrén N, Dragancea I, Lybeck A, et al. Performance of a guideline-recommended algorithm for prognostication of poor neurological outcome after cardiac arrest. *Intensive Care Med*. 2020; **46**(10): 852-62.
218. Estraneo A, Moretta P, Loreto V, Lanzillo B, Cozzolino A, Saltalamacchia A, et al. Predictors of recovery of responsiveness in prolonged anoxic vegetative state. *Neurology*. 2013; **80**(5): 464-70.
219. Scarpino M, Lolli F, Lanzo G, Carrai R, Spalletti M, Valzania F, et al. Neurophysiology and neuroimaging accurately predict poor neurological outcome within 24 hours after cardiac arrest: The ProNeCA prospective multicentre prognostication study. *Resuscitation*. 2019; **143**: 115-23.
220. Strauss K, et. al. Size specific dose estimates in pediatric and adult body CT examinations. AAPM Task Group 2014. 2011.
221. McCollough C, Bakalyar DM, Bostani M, Brady S, Boedeker K, Boone JM, et. al. Use of Water Equivalent Diameter for Calculating Patient Size and Size-Specific Dose Estimates (SSDE) in CT: The Report of AAPM Task Group 220. AAPM Rep. 2014; **2014**: 6-23.
222. Human Experimentation: Code of Ethics of the World Medical Association (Declaration of Helsinki). *Can Med Assoc J*. 1964; **91**(11): 619.
223. Gillon R. Medical ethics: four principles plus attention to scope. *Bmj*. 1994; **309**(6948): 184-8.
224. Hong JY, Lee DH, Oh JH, Lee SH, Choi YH, Kim SH, et al. Grey-white matter ratio measured using early unenhanced brain computed tomography shows no correlation with neurological outcomes in patients undergoing targeted temperature management after cardiac arrest. *Resuscitation*. 2019; **140**: 161-9.

- 225. Adriaansens KO, Jewbali LSD, Lemkes JS, Spoormans EM, Meuwissen M, Blans MJ, et al. Routine reporting of grey-white matter differentiation in early brain computed tomography in comatose patients after cardiac arrest: A substudy of the COACT trial. *Resuscitation*. 2022; **175**: 13-8.
- 226. Fisher R, Bernett MJ, Paternoster R, Karabon P, Devlin W, Swor R. Utility of Abnormal Head Computed Tomography in Predicting Outcome in Out-of-Hospital Cardiac Arrest Victims. *Ther Hypothermia Temp Manag*. 2021; **11**(3): 164-9.
- 227. Coppler PJ, Flickinger KL, Darby JM, Doshi A, Guyette FX, Faro J, et al. Early risk stratification for progression to death by neurological criteria following out-of-hospital cardiac arrest. *Resuscitation*. 2022; **179**: 248-55.
- 228. Michinaga S, Koyama Y. Pathogenesis of brain edema and investigation into anti-edema drugs. *Int J Mol Sci*. 2015; **16**(5): 9949-75.
- 229. Oh JH, Choi SP, Zhu JH, Kim SH, Park KN, Youn CS, et al. Differences in the gray-to-white matter ratio according to different computed tomography scanners for outcome prediction in post-cardiac arrest patients receiving target temperature management. *PLoS One*. 2021; **16**(10): e0258480.

